

RECEIVED: January 3, 2017

REVISED: March 22, 2017

ACCEPTED: May 24, 2017

PUBLISHED: June 1, 2017

Adinkras from ordered quartets of BC_4 Coxeter group elements and regarding 1,358,954,496 matrix elements of the Gadget

S. James Gates, Jr.,^{a,b} Forrest Guyton,^c Siddhartha Harmalkar,^a David S. Kessler,^a Vadim Korotkikh^a and Victor A. Meszaros^a

^aCenter for String and Particle Theory, Department of Physics, University of Maryland, 4150 Campus Dr., College Park, MD 20472, U.S.A.

^bDepartment of Physics, Brown University, Box 1843, 182 Hope Street, Barus & Holley 545, Providence, RI 02912, U.S.A.

^cPhysics, Applied Physics, and Astronomy, Rensselaer Polytechnic Institute, Jonsson Rowland Science Center, Room 1C25, 110 Eighth Street, Troy, NY 12180, U.S.A.

E-mail: gatess@wam.umd.edu, guytof@rpi.edu, sharmalk@umd.edu, 3.14159.david@gmail.com, va.korotki@gmail.com, victorameszaros@gmail.com

ABSTRACT: We examine values of the Adinkra Holonomy-induced Gadget representation space metric over *all* possible four-color, four-open node, and four-closed node adinkras. Of the 1,358,954,496 gadget matrix elements, only 226,492,416 are non-vanishing and take on one of three values: $-1/3$, $1/3$, or 1 and thus a subspace isomorphic to a description of a body-centered tetrahedral molecule emerges.

KEYWORDS: Field Theories in Lower Dimensions, Space-Time Symmetries, Superspaces

ARXIV EPRINT: [1701.00304](https://arxiv.org/abs/1701.00304)

Contents

1	Introduction	2
2	Calculating the Gadget with ordered quartets	6
2.1	The ℓ and $\tilde{\ell}$ coefficients basis	7
2.2	The results	8
3	Visual graph of adinkra Gadget values over the “small BC_4 library”	10
4	Computing 4D Gadget values	11
5	The Coxeter group BC_4 & the “small BC_4 library”	17
5.1	Illustrative discussion	19
6	Expanding by including complements for the Coxeter group BC_4 quartets	23
7	Expanding to ordered Coxeter group BC_4 quartets	24
8	A counting intermezzo	27
9	The codes	27
9.1	Program, libraries.py	27
9.2	C++ code to calculate gadget values given $\ell/\tilde{\ell}$ coefficients	28
9.3	MATLAB program	30
9.4	Mathematica-Gadget Code.nb	31
10	Conclusion	33
A	Multiplications of $\{\mathcal{V}_{(4)}\}$ by permutation group of order four elements	34
B	“Fiducial” Boolean Factors	36
C	Adinkra ℓ & $\tilde{\ell}$ values over the “small BC_4 library”	38
D	Adinkra Gadget values over the “small BC_4 library”	42
E	Cycle labelling conventions	52

1 Introduction

Over the course of some number of years [1–4], one of the authors (SJG) of this current work noted a series of what appeared to be “curious” hints that the very representation space of spacetime supersymmetry, even without consideration of dynamics, might contain an exquisite yet hidden mathematical structure. This suggested that whatever this hidden structure might be, it warranted careful study. This direction has at this point finally begun to yield a trove of unexpected connections to deep mathematical structures... Riemann surfaces and algebraic geometry, among others. This can be seen in two very illuminating recent works.

The works “Geometrization of N-extended 1-dimensional supersymmetry algebras (I & II)” [5] and [6] conclusively describe the not generally appreciated nor previously recognized connections between spacetime supersymmetry representations, as described by adinkra graphs, and a raft of mathematical structures that include:

- (a.) Grothendieck’s “dessin d’enfant,”
- (b.) Belyi pairs,
- (c.) Cimasoni-Reshetikhin dimer models on Riemann surfaces,
- (d.) Donagi-Witten parabolic structure/ramified coverings of super Riemann surface,
- (e.) Morse divisors,
- (f.) Fuchsian uniformization, and
- (g.) elliptic curves.

Built on the observation of the ubiquitous appearance of an algebraic structure (eventually given the name of “Garden Algebras”) [1–4], that seem to universally exist in all linear realizations of spacetime supersymmetry, a type of graph [7] (thus permitting use of graph theory techniques [8]) was proposed in order to study the properties of “Garden Algebras” in a more general manner. These graphs were christened as “adinkras” and come extraordinarily close, if not achieving, the goal of providing a coordinate-independent description of one dimensional spacetime supersymmetry representations.

The introduction of adinkra graphs was an important milestone in the effort that was envisioned as in the inaugural works [1, 2] in this direction. The importance of achieving such coordinate-independent descriptions of spacetime supersymmetry algebras was especially emphasized in the response to a presentation given by SJG at the 2006 workshop on “Affine Hecke algebras, the Langlands Program, Conformal Field Theory and Matrix Models” at the Centre International de Rencontres Mathématiques (CIRM) in Luminy/France.

Independent researchers have also utilized concepts that arose from the study of adinkras. For example, the concept of “the root superfield” [9] has found applications such as the construction of new models and the classification of N-extended supersymmetric quantum mechanical systems in the research of [10–16]. The program has also created links

to purely mathematical discussions such as combinatorics [17], Coxeter Groups [18, 19], and Klein’s Vierergruppe [20, 21], and spectral geometry [22]. The adinkra concept has generated at least one publication purely in the mathematical literature [23] and uncovered other surprising structures [24, 25].

The complete specification of adinkras at the level of a rigorous mathematical formulation has led to an enhanced level of understanding of the relationships between decorated cubical cohomology and the *very* surprising role of coding theory [26–28] as it apparently controls the definitions and structure of adinkras with more than four colors that define the irreducible representations of spacetime supersymmetry.

The works of Doran, Iga, Kostiuik, Landweber, and Mendez-Diez [5, 6] have now erected a sturdy and broad causeway to increase and deepen a mathematical representation theory of spacetime supersymmetry in a way that has never before existed. In spite of this major advance, however, there remain numbers of puzzles.

One of these is, how does higher dimensional spacetime Lorentz symmetry manifest itself in the context of adinkra graphs?

Several works have taken steps toward investigating this problem. It was conjectured [4] there must exist some sort of “holography” that connects one dimensional adinkras to higher dimensional superfield theories. We currently have renamed this concept “SUSY holography” to distinguish it from other concepts that use the word “holography.” This viewpoint was strengthened in later work [9]. An obvious consequent possibility from such a viewpoint is it might be possible to start solely with an adinkra and perform the process of “dimensional extension” to reconstruct a higher dimensional supermultiplet. One example, where looking at an adinkra-based structures were related to higher dimensional ones occurred in relation to 4D $\mathcal{N} = 2$ supermultiplets [30, 31].

The first concrete examples [32, 33] of how to accomplish this outcome of connecting adinkras to 4D, $\mathcal{N} = 1$ supermultiplets used calculations which showed by successively raising adinkra nodes from a valise configuration, one could examine when a Lorentz covariant (in the context of 4D Minkowski space) interpretation was consistent. These papers provide a demonstration of proof of concept most certainly. However, the steps of systematically lifting nodes is computationally expensive. Thus, we will not take this route.

Another approach [34], somewhat related, was taken with respect to the simpler problem of providing a dimensional extension of adinkras into the construction of 2D Minkowski space supersymmetric representations. In particular, this work uncovered the “no two-color ambidextrous bow-tie” rule which governs the lifting of the adinkra into a 2D Minkowski space supermultiplet. A “two-color ambidextrous bow-tie” is a structure that can be directly calculated in terms of closed four-cycles within the context of a valise adinkra once 2D helicity labels are adding to the links in an adinkra. If this obstruction occurs, the lifting of a node will remove it and the resulting adinkra can then be extended to the higher dimension. Next, an approach [35] was also created as an alternate efficient calculation for solving the problem of providing a dimensional extension of adinkras into the construction of 2D Minkowski space supersymmetric representations. This approach is based on the underlying coding theory structures [26–28] that were discovered within the structure of all adinkras.

In facing the problem of reconstructing 4D simple supermultiplets from adinkras, unlike the successful paths shown for the analogous problem in 2D, another path has been pursued also [36–42]. This alternate path is based on the fact that closed four-cycles for four color valise adinkras possess naturally an $SO(4)$ symmetry. Since $SO(4)$ can be decomposed into $SU(2) \otimes SU(2)$, and since the covering algebra of the 4D Dirac matrices is also $SO(4)$, these explorations have endeavored to explore a variant of the concept of “spin from isospin” [43]. As adinkras naturally carry isospin, it is indicated to ask if this property can be used in a way to make 4D Lorentz symmetry an emergent symmetry arising from adinkras with at least four colors.

It is the purpose of this paper to continue to explore the possibility that 4D Lorentz symmetry *is an emergent symmetry* arising from the isospin symmetry of adinkras with at least four colors. The outline of this paper is given below.

In sections 2 and 3, we present the new results of this work. These results support the concept of “SUSY holography” by showing the “angles” [38–42] between any two adinkras constructed from ordered quartets of BC_4 elements take on exactly and *only* the same values as the “angles” [40] between any of the 4D, $\mathcal{N} = 1$ supermultiplets with minimal numbers of bosons and fermions. The presentation in section 3 is made in terms of a visual/graphical representation.

In section 4 in comparison to our previous work [40], we find there is one additional value of the 4D “angles” between supermultiplets when one expands the space of supermultiplet representations to include the axial vector and axial tensor supermultiplets. We note that certain “parity flipped versions” may be added to the list of representation studied in our previous work and we expand the values of the 4D Gadget matrix to include the calculations related to these additional supermultiplets.

The approach to deriving our main results was a bifurcated one. The first part of our analysis and code-based exploration only covered the case of a small subset of the adinkras. This subset consisted only of the adinkras described in detail in [44] as in this case there was a previously established “library” of SUSY pairings between “Boolean Factors” and permutation elements from BC_4 .

Section 5 describes our previous construction of adinkras with four colors, four open-nodes, and four closed nodes based on the elements of Coxeter Group BC_4 [44]. Here we *do not* consider the role of ordered quartets. This results in the possibility of writing 1,536 adinkras that are potentially “usefully inequivalent” [45]. We also concentrate on the role of a subset of the elements of the permutation that sets the stage of separating the twenty-four elements of the permutation group into a group of “corrals” containing four elements each. We discuss the relation of reduced versions of the 4D $\mathcal{N} = 2$ chiral and twisted chiral [46, 47] supermultiplets and show in this example that it is the distinct corrals that appear to play the dominant role in determining the “usefully inequivalent.”

Section 6 goes to the consideration of looking at the effects of considering the role of “twisting” quartets by introducing relative sign factors among the components within quartets of the “small BC_4 library” that results strictly from taking a single representation of the elements of BC_4 and using them to construct supersymmetric quartets that satisfy the “Garden Algebra” conditions. This material has *exactly* appeared previously in [42] and the reader familiar with this discussion can skip this.

Also as was *explicitly* discussed [42], given a complete BC_4 description of an adinkra, one can construct “complements” of any adinkra. These also include “anti-podal” representations where one representation can be obtained from the other by simply re-defining either *all* of closed nodes (or open nodes) by a minus sign. So we can reduce this number by a factor of two since “anti-podal” representations where one representation can be obtained from the other by simply re-defining either *all* closed nodes (or open nodes) by a minus sign are included.

In section 7, we describe the expansion of our previous construction of adinkras with four colors, four open-nodes, and four closed nodes based on the elements of Coxeter Group BC_4 [44]. Whereas before we *did not* consider the role of ordered quartets, in this work we *do* consider such quartets. This is also another source for the expansion in the number of adinkras to consider. Without removing “anti-podal” representations this results in the possibility of writing 36,864 adinkras that are potentially “usefully inequivalent.”

In the short discussion of section 8, we review the counting arguments that show how the 384 elements in the BC_4 Coxeter group at first naively leads to a total of ninety six quartets, but that by considering the effects of sign flips and expanded to ordered quartets this number increases almost a hundred-fold.

The work of section 9 includes the description of the codes that were created to attack the problem of calculating the “angles” between the adinkra with four colors, four open-nodes, and four closed nodes. There were actually four different codes created independently that support the work undertaken in section 4. These were created using C++, *Mathematica*TM, MATLAB, and Python. We report the results of the calculations with regards to the results related to the discussion in section 4.

This same section next turns to the main task of describing what was undertaken in computing the “angles” between all 36,864 adinkras based on ordered quartets of BC_4 elements. This was done by once more creating an entirely independent code using the 3.5 version of Python together with the Numpy module for Python which allows for the matrix calculations. After running for 1.86 hours calculating all the entries in a $36,864 \times 36,864$ matrix, the only values found were those given in section 2.

The final section includes a discussion of our conclusions and a number of appendices are included to provide details about all the computations. Appendix A consists of a set of multiplication tables showing the action of the multiplication of element of the permutation group on a quartet of permutations denoted by $\{\mathcal{V}_{(4)}\}$, which is a realization of the the Vierergruppe over the 2×2 identity and first Pauli matrix. Appendix B has appeared in some of previous work, and contains the assignment of “Boolean Factors” with quartets of permutations that are required to construct supersymmetry representations. Appendix C is drawn from previous work and reports the values of the “ ℓ and $\tilde{\ell}$ ” parameters associated with permutation factor and Boolean Factors. The final appendix D reports on the outcome of the evaluation of the values of the Gadget function over a 96×96 matrix over the domain of the “small BC_4 library” (the latter is defined in this work also).

Any party seeking to obtain the codes described in this work can contact any of the authors in order to receive the code of interest.

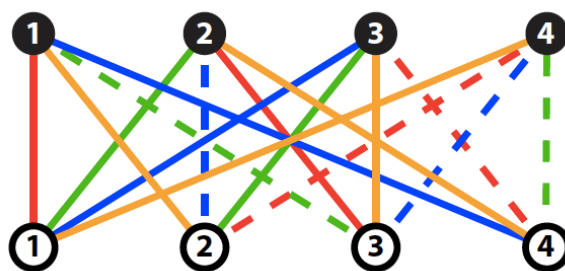


Figure 1. A “valise” adinkra.

2 Calculating the Gadget with ordered quartets

An example of an image given the name of an “adinkra graph” [7] and mathematically defined in subsequent works [24–29] is shown in figure 1.

Every N -color adinkra representation (\mathcal{R}) leads, via a set of Feynman-like rules, to sets of matrices denoted by $L_I^{(\mathcal{R})}$ and $R_I^{(\mathcal{R})}$ which satisfy the “Garden Algebra” conditions,

$$\begin{aligned} (L_I^{(\mathcal{R})})_{i\hat{j}} (R_J^{(\mathcal{R})})_{j\hat{k}} + (L_J^{(\mathcal{R})})_{i\hat{j}} (R_I^{(\mathcal{R})})_{j\hat{k}} &= 2 \delta_{IJ} \delta_{i\hat{k}}, \\ (R_J^{(\mathcal{R})})_{i\hat{j}} (L_I^{(\mathcal{R})})_{j\hat{k}} + (R_I^{(\mathcal{R})})_{i\hat{j}} (L_J^{(\mathcal{R})})_{j\hat{k}} &= 2 \delta_{IJ} \delta_{i\hat{k}}, \\ (R_I^{(\mathcal{R})})_{j\hat{k}} \delta_{ik} &= (L_I^{(\mathcal{R})})_{i\hat{k}} \delta_{j\hat{k}}. \end{aligned} \tag{2.1}$$

The “color-link rainbow to matrix” assignments associated with figure 1 correspond to “red = L_1 ,” “green = L_2 ,” “blue = L_3 ,” and “orange = L_4 ” and the explicit forms of the L-matrices associated with figure 1 are given by

$$\begin{aligned} (L_1)_{i\hat{k}} &= \begin{bmatrix} 1 & 0 & 0 & 0 \\ 0 & 0 & 0 & -1 \\ 0 & 1 & 0 & 0 \\ 0 & 0 & -1 & 0 \end{bmatrix}, & (L_2)_{i\hat{k}} &= \begin{bmatrix} 0 & 1 & 0 & 0 \\ 0 & 0 & 1 & 0 \\ -1 & 0 & 0 & 0 \\ 0 & 0 & 0 & -1 \end{bmatrix}, \\ (L_3)_{i\hat{k}} &= \begin{bmatrix} 0 & 0 & 1 & 0 \\ 0 & -1 & 0 & 0 \\ 0 & 0 & 0 & -1 \\ 1 & 0 & 0 & 0 \end{bmatrix}, & (L_4)_{i\hat{k}} &= \begin{bmatrix} 0 & 0 & 0 & 1 \\ 1 & 0 & 0 & 0 \\ 0 & 0 & 1 & 0 \\ 0 & 1 & 0 & 0 \end{bmatrix}. \end{aligned} \tag{2.2}$$

A set of L-matrices and R-matrices for a specified adinkra representation (\mathcal{R}) , can be used to define two additional sets of matrices. We have given the name of “bosonic holeraumy matrices” and “fermionic holeraumy matrices,” respectively, to the sets denoted by $V_{IJ}^{(\mathcal{R})}$ and $\tilde{V}_{IJ}^{(\mathcal{R})}$ [36–40] and defined via the equations

$$\begin{aligned} (L_I^{(\mathcal{R})})_{i\hat{j}} (R_J^{(\mathcal{R})})_{j\hat{k}} - (L_J^{(\mathcal{R})})_{i\hat{j}} (R_I^{(\mathcal{R})})_{j\hat{k}} &= i 2 (V_{IJ}^{(\mathcal{R})})_{i\hat{k}}, \\ (R_I^{(\mathcal{R})})_{i\hat{j}} (L_J^{(\mathcal{R})})_{j\hat{k}} - (R_J^{(\mathcal{R})})_{i\hat{j}} (L_I^{(\mathcal{R})})_{j\hat{k}} &= i 2 (\tilde{V}_{IJ}^{(\mathcal{R})})_{i\hat{k}}. \end{aligned} \tag{2.3}$$

Given two adinkras denoted by (\mathcal{R}) and (\mathcal{R}') (which possess N colors, and d open nodes) along with their associated fermionic holoraummy matrices $\tilde{\mathbf{V}}_{\mathbf{IJ}}^{(\mathcal{R})}$ and $\tilde{\mathbf{V}}_{\mathbf{IJ}}^{(\mathcal{R}')}$ we can form a scalar, “the gadget value” between two representations (\mathcal{R}) and (\mathcal{R}') defined by

$$\mathcal{G}[(\mathcal{R}), (\mathcal{R}')] = \left[\frac{1}{N(N-1)d_{\min}(N)} \right] \sum_{\mathbf{I}, \mathbf{J}} \text{Tr} \left[\tilde{\mathbf{V}}_{\mathbf{IJ}}^{(\mathcal{R})} \tilde{\mathbf{V}}_{\mathbf{IJ}}^{(\mathcal{R}')} \right], \quad (2.4)$$

where

$$d_{\min}(N) = \begin{cases} 2^{\frac{N-1}{2}}, & N \equiv 1, 7 \pmod{8} \\ 2^{\frac{N}{2}}, & N \equiv 2, 4, 6 \pmod{8} \\ 2^{\frac{N+1}{2}}, & N \equiv 3, 5 \pmod{8} \\ 2^{\frac{N-2}{2}}, & N \equiv 8 \pmod{8} \end{cases} \quad (2.5)$$

and we exclude the case of $N = 0$ (i.e. no supersymmetry) in these expressions. For every adinkra [7, 8] based on the Coxeter Group BC_4 , the L-matrices and R-matrices [1, 2] must have four colors ($\mathbf{I} = 1, \dots, 4$), four open nodes ($i = 1, \dots, 4$), and four closed nodes ($\hat{k} = 1, \dots, 4$).

2.1 The ℓ and $\tilde{\ell}$ coefficients basis

Since we will only be looking at adinkras and associated quantities related to BC_4 , there is one special feature related to the fact that for such adinkras, the holoraummy matrices are necessarily related to $\text{SO}(4)$. Due to this, the holoraummy matrices may be expanded in the “ α - β basis where six matrices defined by

$$\begin{aligned} \alpha^{\hat{1}} &= \sigma^2 \otimes \sigma^1, & \alpha^{\hat{2}} &= \mathbf{I}_{2 \times 2} \otimes \sigma^2, & \alpha^{\hat{3}} &= \sigma^2 \otimes \sigma^3, \\ \beta^{\hat{1}} &= \sigma^1 \otimes \sigma^2, & \beta^{\hat{2}} &= \sigma^2 \otimes \mathbf{I}_{2 \times 2}, & \beta^{\hat{3}} &= \sigma^3 \otimes \sigma^2, \end{aligned} \quad (2.6)$$

can be chosen as a basis over which to expand $(\tilde{\mathbf{V}}_{\mathbf{IJ}}^{(\mathcal{R})})_{i^{\hat{k}}}$ as

$$\tilde{\mathbf{V}}_{\mathbf{IJ}}^{(\mathcal{R})} = \left[\ell_{\mathbf{IJ}}^{(\mathcal{R})\hat{1}} \alpha^{\hat{1}} + \ell_{\mathbf{IJ}}^{(\mathcal{R})\hat{2}} \alpha^{\hat{2}} + \ell_{\mathbf{IJ}}^{(\mathcal{R})\hat{3}} \alpha^{\hat{3}} \right] + \left[\tilde{\ell}_{\mathbf{IJ}}^{(\mathcal{R})\hat{1}} \beta^{\hat{1}} + \tilde{\ell}_{\mathbf{IJ}}^{(\mathcal{R})\hat{2}} \beta^{\hat{2}} + \tilde{\ell}_{\mathbf{IJ}}^{(\mathcal{R})\hat{3}} \beta^{\hat{3}} \right], \quad (2.7)$$

written in terms of the thirty-six coefficients $\ell_{\mathbf{IJ}}^{(\mathcal{R})\hat{1}}, \ell_{\mathbf{IJ}}^{(\mathcal{R})\hat{2}}, \ell_{\mathbf{IJ}}^{(\mathcal{R})\hat{3}}, \tilde{\ell}_{\mathbf{IJ}}^{(\mathcal{R})\hat{1}}, \tilde{\ell}_{\mathbf{IJ}}^{(\mathcal{R})\hat{2}},$ and $\tilde{\ell}_{\mathbf{IJ}}^{(\mathcal{R})\hat{3}}$.

Using this approach, the values of the “gadget,” expressed in terms of the ℓ and $\tilde{\ell}$ coefficients, are defined by

$$\begin{aligned} \mathcal{G}[(\mathcal{R}), (\mathcal{R}')]_{\ell} &\equiv \frac{1}{6} \sum_{\hat{a}} \left[\ell_{12}^{(\mathcal{R})\hat{a}} \ell_{12}^{(\mathcal{R}')\hat{a}} + \ell_{13}^{(\mathcal{R})\hat{a}} \ell_{13}^{(\mathcal{R}')\hat{a}} + \ell_{14}^{(\mathcal{R})\hat{a}} \ell_{14}^{(\mathcal{R}')\hat{a}} + \right. \\ &\quad \left. \ell_{23}^{(\mathcal{R})\hat{a}} \ell_{23}^{(\mathcal{R}')\hat{a}} + \ell_{24}^{(\mathcal{R})\hat{a}} \ell_{24}^{(\mathcal{R}')\hat{a}} + \ell_{34}^{(\mathcal{R})\hat{a}} \ell_{34}^{(\mathcal{R}')\hat{a}} \right] + \\ &\quad \frac{1}{6} \sum_{\hat{a}} \left[\tilde{\ell}_{12}^{(\mathcal{R})\hat{a}} \tilde{\ell}_{12}^{(\mathcal{R}')\hat{a}} + \tilde{\ell}_{13}^{(\mathcal{R})\hat{a}} \tilde{\ell}_{13}^{(\mathcal{R}')\hat{a}} + \tilde{\ell}_{14}^{(\mathcal{R})\hat{a}} \tilde{\ell}_{14}^{(\mathcal{R}')\hat{a}} + \right. \\ &\quad \left. \tilde{\ell}_{23}^{(\mathcal{R})\hat{a}} \tilde{\ell}_{23}^{(\mathcal{R}')\hat{a}} + \tilde{\ell}_{24}^{(\mathcal{R})\hat{a}} \tilde{\ell}_{24}^{(\mathcal{R}')\hat{a}} + \tilde{\ell}_{34}^{(\mathcal{R})\hat{a}} \tilde{\ell}_{34}^{(\mathcal{R}')\hat{a}} \right], \end{aligned} \quad (2.8)$$

and necessarily

$$\cos \{ \theta [(\mathcal{R}), (\mathcal{R}')]_{\ell} \} = \frac{\mathcal{G}[(\mathcal{R}), (\mathcal{R}')]_{\ell}}{\sqrt{\mathcal{G}[(\mathcal{R}), (\mathcal{R})]_{\ell}} \sqrt{\mathcal{G}[(\mathcal{R}'), (\mathcal{R}')]_{\ell}}}. \quad (2.9)$$

The existence of the ℓ and $\tilde{\ell}$ coefficients also means that for each BC_4 adinkra representation (\mathcal{R}) there is a vector in an associated thirty-six dimensional vector space defined by all the values of the coefficients. If we denote the elements in this space by the symbol $\vec{\gamma}_{\ell\tilde{\ell}}(\mathcal{R})$ we can lexicographically order the I, J , and \hat{a} indices according to

$$\vec{\gamma}_{\ell\tilde{\ell}}(\mathcal{R}) = \left(\ell_{12}^{(\mathcal{R})\hat{1}}, \ell_{12}^{(\mathcal{R})\hat{2}}, \ell_{12}^{(\mathcal{R})\hat{3}}, \ell_{23}^{(\mathcal{R})\hat{1}}, \ell_{23}^{(\mathcal{R})\hat{2}}, \ell_{23}^{(\mathcal{R})\hat{3}}, \dots, \tilde{\ell}_{34}^{(\mathcal{R})\hat{1}}, \tilde{\ell}_{34}^{(\mathcal{R})\hat{2}}, \tilde{\ell}_{34}^{(\mathcal{R})\hat{3}} \right), \quad (2.10)$$

to create a convention for the definition of the components of the vector. The Gadget acts as the “dot product” on this space. Alternately, we can regard the components of $\vec{\gamma}_{\ell\tilde{\ell}}(\mathcal{R})$ as forming the components of a rank one tensor $\gamma_{\ell\tilde{\ell}}^{A^*}(\mathcal{R})$ where the index A^* enumerates the components in (2.10) in the order shown. Also given $\gamma_{\ell\tilde{\ell}}^{A^*_1}(\mathcal{R}_1), \dots, \gamma_{\ell\tilde{\ell}}^{A^*_p}(\mathcal{R}_p)$ corresponding to representations $(\mathcal{R}_1), \dots, (\mathcal{R}_p)$, we can form a p -th order simplex via the definition

$$Y^{A^*_1 \dots A^*_p}(\mathcal{R}_1, \dots, \mathcal{R}_p) = \gamma_{\ell\tilde{\ell}}^{A^*_1}(\mathcal{R}_1) \wedge \gamma_{\ell\tilde{\ell}}^{A^*_2}(\mathcal{R}_2) \dots \wedge \gamma_{\ell\tilde{\ell}}^{A^*_p}(\mathcal{R}_p). \quad (2.11)$$

2.2 The results

In the work of [42], there was presented and released a list of the values of the ℓ and $\tilde{\ell}$ parameters, though the calculations of these occurred contemporaneously with work of [44]. On the basis of this “library” (that we will subsequently call the “small BC_4 library,” algorithms and codes, to be discussed later, were written in order to calculate the values of the quadratic forms (2.8) on the $\tilde{\ell}$ and ℓ adinkra parameter spaces. However, for the current work, codes were also developed to carry out the calculation directly that follow from the expression in (2.4). The results of these calculation provide the foundation for the statements made subsequently.

One may regard the Gadget, \mathcal{G} , as a mapping that assigns the value of a real number to a pairs of adinkras. In this sense the Gadget acts as a metric on the space of adinkras. Each adinkra may be associated with a representation label $(\mathcal{R}_1), (\mathcal{R}_2), \dots, (\mathcal{R}_T)$ where T is a integer. In the case of adinkras based on ordered quartets of elements of BC_4 , the value of T is 36,864. We can now report the main result of this current study.

The values of the Gadget over all the adinkras based on ordered quartets of elements of BC_4 may be regarded as a square matrix with the rank of the matrix being 36,864. Thus, the task of calculating all $(36,864) \times (36,864) = 1,358,954,496$ values of the matrix elements seems impossible. However, with the aid of modern computational capacities, this task has been completed.

The Adinkra “Gadget” Representation Matrix (AGRM) over the 36,864 ordered-pair BC_4 -based adinkras is very sparse. Just over 83% of the entries, or 1,132,462,080, are zero. Among the remaining non-vanishing entries only three numbers appear: $\pm 1/3$, and 1. The frequencies of appearance with which these three numbers together with 0 appear are shown in table 1.

The sum of the counts add up to 1,358,954,496 which means one of our programs calculated every single entry in the AGRM. It is clear that the independent values that appear and the multiplicities of their appearance in table 1 can be written in the form of

Gadget Value	Count
- 1/3	127,401,984
0	1,132,462,080
1/3	84,934,656
1	14,155,776

Table 1. Frequency of appearance of AGRM elements.

a polynomial

$$\mathcal{P}_{\mathcal{G}}(y) = 1,132,462,080y \left[127,401,984 \left(y + \frac{1}{3} \right) \right] \left[84,934,656 \left(y - \frac{1}{3} \right) \right] [14,155,776(y - 1)] \tag{2.12}$$

where the roots of the polynomial correspond to the non-vanishing entries.

The normalization given in (2.4) is such that for all these representations (\mathcal{R}) satisfy the condition

$$\mathcal{G}[(\mathcal{R}), (\mathcal{R})] = 1 . \tag{2.13}$$

Thus, it is possible for any two adinkra (\mathcal{R}) and (\mathcal{R}') to define an angle $\theta[(\mathcal{R}), (\mathcal{R}')]$ between them via the equation

$$\cos \{ \theta[(\mathcal{R}), (\mathcal{R}')] \} = \frac{\mathcal{G}[(\mathcal{R}), (\mathcal{R}')] }{\sqrt{\mathcal{G}[(\mathcal{R}), (\mathcal{R})]} \sqrt{\mathcal{G}[(\mathcal{R}'), (\mathcal{R}')]}} . \tag{2.14}$$

and this may be applied to adinkras based on ordered quartets of elements of BC_4 .

Since the Gadget values only take on the four values shown in the table, the corresponding angles are: $\arccos(-1/3)$, $\pi/2$, $\arccos(1/3)$, and 0. The result in (2.13) implies we can regard the 36,864 adinkras as defining an equivalent number of unit vectors. Next the angles defined via (2.14) informs us that these unit vectors only meet at the angles of $\arccos(-1/3)$, $\pi/2$, $\arccos(1/3)$, and 0. The fact that $14,155,776 - 36,864 = 14,118,912$ implies that among the 36,864 associated unit vectors many are colinear to one another. The angle $\arccos(-1/3)$ has been noted for some time in our past research papers [36–40]. In fact, with the exception of the angle of $\arccos(1/3)$ all the other angles have been found in our previous calculations. We will discuss in a later section this exception.

The presence of the angle $\arccos(-1/3)$ is amusing from the view of tetrahedral geometry. In figure 2, there appears a regular tetrahedron inscribed within a sphere. Referring to the labelling of the vertices shown in the figure, $\angle ACD$ has the value of $\arccos(1/2)$ while the angles $\angle AOD$, $\angle AOC$, and $\angle AOB$ all have the same value of $\arccos(-1/3)$.

As it will prove useful in a later section, let us observe the points on the sphere that lie respectively along the line segments \overline{OA} , \overline{OB} , \overline{OC} , and \overline{OD} , have the coordinates given by $(0, 0, 1)$, $\left(-\frac{\sqrt{2}}{3}, -\frac{\sqrt{6}}{3}, -\frac{1}{3}\right)$, $\left(\frac{2\sqrt{2}}{3}, 0, -\frac{1}{3}\right)$, and $\left(-\frac{\sqrt{2}}{3}, \frac{\sqrt{6}}{3}, -\frac{1}{3}\right)$ in the same order. Each of these (considered as vectors) has length one, and a dot product between any pair is equal to $-1/3$. It should be noted the condition in (2.13) implies these all must be unit vectors.

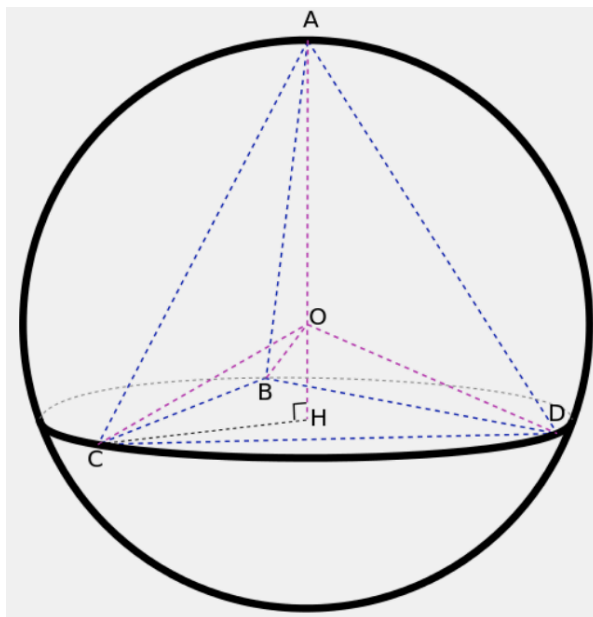


Figure 2. The adinkra representations with angle $\arccos(-1/3)$ are equidistant from each other within the considered 3D space in the metric defined by the gadget.

3 Visual graph of adinkra Gadget values over the “small BC_4 library”

Any attempt to present the results that describe the entries in a $36,864 \times 36,864$ symmetrical matrix obviously presents some challenges. In fact, we shall not even attempt this. We will provide copies of all our codes to any interested party upon request.

However as a “peek” into one tiny (96×96) sector of the total 1.3+ billion results, we will here describe the results for the “small BC_4 library” described in detail in a later section. One very accessible way to present this data is in the form of an array, but where the entries in the array are colored squares that play the role of pixels. As there are only four values found in the entirety of the range of our calculations, we only need pixels of four colors. We make the numerical assignments between the calculated gadget values and the colors according to: red = $-1/3$, white = 0, black = $+1/3$, and green = 1. When this assignment is done, we find the image¹ in figure 3 over the 96×96 entries of the small BC_4 library. The image in figure 3 possesses no black “pixels” as the value of $+1/3$ does not occur in the context of the small library. However, it might be an interesting problem in computer visualization to extend this graphical presentation beyond the small library.

Let us also note that the lack of appearance of the black pixels seems correlated with the method by which the small library was constructed. Its construction began from the dimensional reduction of supermultiplets in four dimensions which were then extended using signed permutation elements to conjugate elements of this original set.

¹The image in figure 3 is a scalable pdf file in the native format of this document which implies it can be magnified as desired to obtain greater detail.

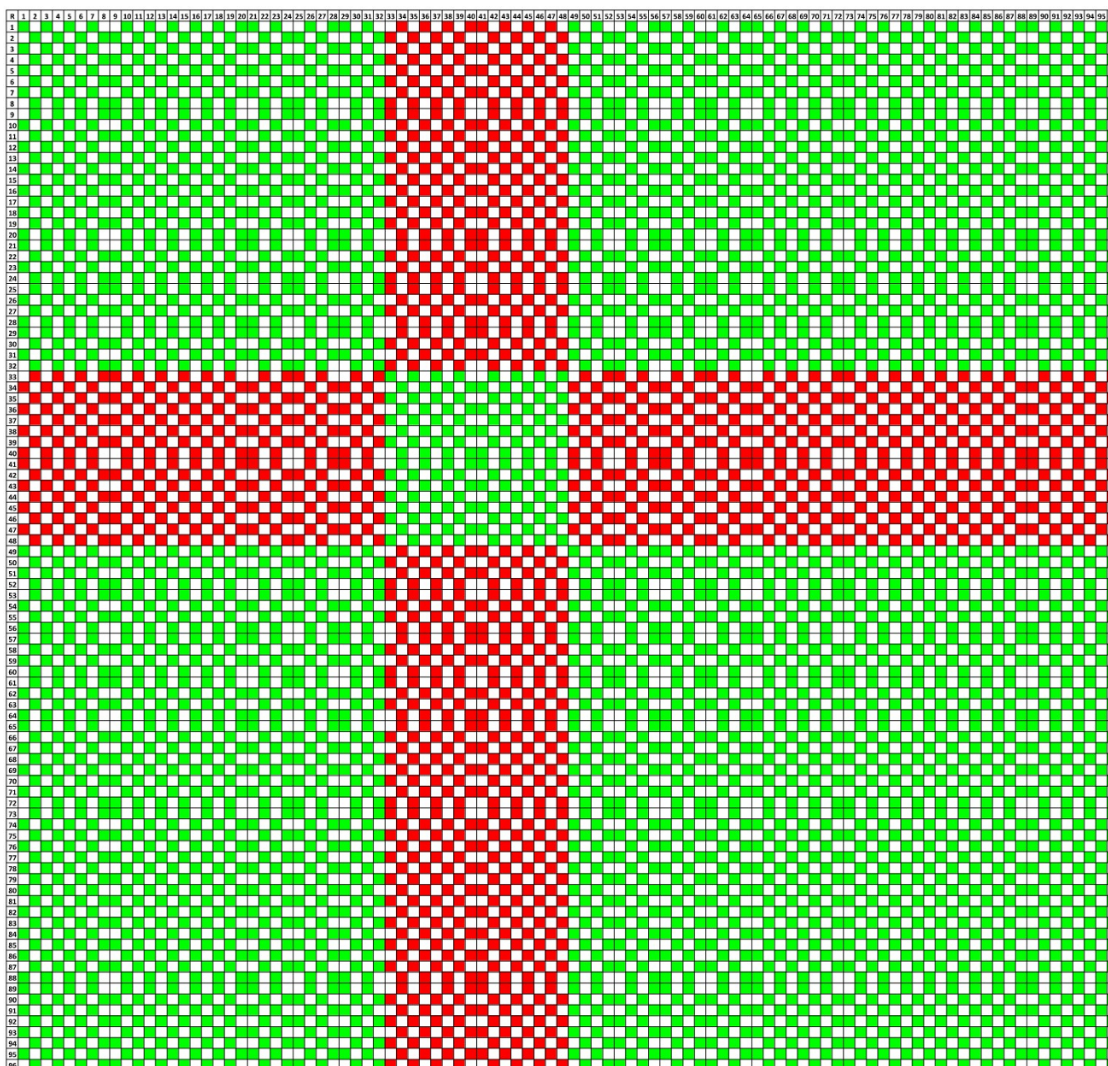


Figure 3. Graphical representation of the values in the adinkra Gadget representation matrix.

4 Computing 4D Gadget values

We have proposed [40] that the analog of the adinkra Gadget exists in the form of a supermultiplet Gadget denoted by $\hat{\mathcal{G}}$. Unlike the adinkra Gadget, the supermultiplet Gadget is defined by calculations *solely* involving supermultiplets in higher dimensions. As such its arguments, denoted by $(\hat{\mathcal{R}})$, and $(\hat{\mathcal{R}}')$, refer to higher dimensional supermultiplets.² Like the adinkra Gadget \mathcal{G} , the supermultiplet Gadget $\hat{\mathcal{G}}$ assigns a real number to the pair of supermultiplets denoted by $(\hat{\mathcal{R}})$, and $(\hat{\mathcal{R}}')$.

²We use the symbol “ $\hat{}$ ” in order to distinguish when a representation and associated Gadget are related to adinkras or to supermultiplets. Those related to adinkra representations and associated Gadgets appear without the “hat,” while those associated with supermultiplets representations and associated Gadgets appear with the “hat”.

The most general expression for a four dimensional ‘‘Gadget’’ defined in previous work [40], for minimal $\mathcal{N} = 1$ supermultiplets that is Lorentz covariant is given by

$$\begin{aligned} \widehat{\mathcal{G}}[(\widehat{\mathcal{R}}), (\widehat{\mathcal{R}}')] &= m_1 [\mathbf{H}^{\mu(\widehat{\mathcal{R}})}]_{abc}{}^d [\mathbf{H}_{\mu}{}^{(\widehat{\mathcal{R}}')}]^{ab}{}_d{}^c \\ &+ m_2 (\gamma^\alpha)_c{}^e [\mathbf{H}^{\mu(\widehat{\mathcal{R}})}]_{abe}{}^f (\gamma_\alpha)_f{}^d [\mathbf{H}_{\mu}{}^{(\widehat{\mathcal{R}}')}]^{ab}{}_d{}^c \\ &+ m_3 ([\gamma^\alpha, \gamma^\beta])_c{}^e [\mathbf{H}^{\mu(\widehat{\mathcal{R}})}]_{abe}{}^f ([\gamma_\alpha, \gamma_\beta])_f{}^d [\mathbf{H}_{\mu}{}^{(\widehat{\mathcal{R}}')}]^{ab}{}_d{}^c \\ &+ m_4 (\gamma^5 \gamma^\alpha)_c{}^e [\mathbf{H}^{\mu(\widehat{\mathcal{R}})}]_{abe}{}^f (\gamma^5 \gamma_\alpha)_f{}^d [\mathbf{H}_{\mu}{}^{(\widehat{\mathcal{R}}')}]^{ab}{}_d{}^c \\ &+ m_5 (\gamma^5)_c{}^e [\mathbf{H}^{\mu(\widehat{\mathcal{R}})}]_{abe}{}^f (\gamma^5)_f{}^d [\mathbf{H}_{\mu}{}^{(\widehat{\mathcal{R}}')}]^{ab}{}_d{}^c, \end{aligned} \quad (4.1)$$

in terms of constants $m_1, m_2, m_3, m_4,$ and m_5 . The expressions in (4.1) define a mapping that assigns the value of a real number given by $\widehat{\mathcal{G}}$ to the two supermultiplet representations denoted by $(\widehat{\mathcal{R}})$ and, $(\widehat{\mathcal{R}}')$.

The constant rank four tensors $[\mathbf{H}^{\mu(\widehat{\mathcal{R}})}]_{abc}{}^d,$ and $[\mathbf{H}^{\mu(\widehat{\mathcal{R}}')}]^{ab}{}_d{}^c$ are called the ‘‘holoraummy’’ tensors for the supermultiplet representations $(\widehat{\mathcal{R}}),$ and $(\widehat{\mathcal{R}}'),$ respectively. The means for calculating the ‘‘holoraummy’’ tensors for the minimal supermultiplet representations was given previously [40] with results that were reported.

All 4D holoraummy tensors can be subjected to a transformation of the form

$$[\mathbf{H}^{\mu(\widehat{\mathcal{R}})}]_{abc}{}^d \rightarrow (\gamma^5)_c{}^e [\mathbf{H}^{\mu(\widehat{\mathcal{R}})}]_{abe}{}^f (\gamma^5)_f{}^d \quad (4.2)$$

which is equivalent to a ‘‘parity-swap’’ for all the bosonic fields in each supermultiplets. Accordingly, all scalars are interchanged with pseudo-scalars and vice-versa, all vectors are interchanged with axial-vectors and vice-versa, etc.

Since the chiral supermultiplet has equal numbers of bosons of opposite parity, its holoraummy tensor is unchanged by the transformation in (4.2). This is not the case for the latter two supermultiplets. The transformation in (4.2) replaces the vector in the vector supermultiplet by an axial vector and similarly replaces the tensor in the tensor supermultiplet by an axial tensor, thus leading to new holoraummy tensors that follow.

$$\begin{aligned} [\mathbf{H}^{\mu(AVS)}]_{abc}{}^d &= (\gamma^5)_c{}^e [\mathbf{H}^{\mu(VS)}]_{abe}{}^f (\gamma^5)_f{}^d, \\ [\mathbf{H}^{\mu(ATS)}]_{abc}{}^d &= (\gamma^5)_c{}^e [\mathbf{H}^{\mu(TS)}]_{abe}{}^f (\gamma^5)_f{}^d. \end{aligned} \quad (4.3)$$

Including the two new representation implies all can be expressed as in a single formula by writing³

$$\begin{aligned} [\mathbf{H}^{\mu(\mathcal{P}(\mathcal{R}), \mathcal{Q}(\mathcal{R}), \mathcal{I}(\mathcal{R}), \mathcal{S}(\mathcal{R}))}]_{abc}{}^d &= -i2 \left[\mathcal{P}(\mathcal{R}) C_{ab} (\gamma^\mu)_c{}^d + \mathcal{Q}(\mathcal{R}) (\gamma^5)_{ab} (\gamma^5 \gamma^\mu)_c{}^d \right. \\ &+ \mathcal{I}(\mathcal{R}) (\gamma^5 \gamma^\mu)_{ab} (\gamma^5)_c{}^d \\ &+ \left. \frac{1}{2} \mathcal{S}(\mathcal{R}) (\gamma^5 \gamma^\nu)_{ab} (\gamma^5 [\gamma_\nu, \gamma^\mu])_c{}^d \right], \end{aligned} \quad (4.4)$$

where the representation labels in this formula takes on the range of values given by $(CS), (VS), (TS), (AVS),$ and $(ATS).$ The integers $\mathcal{P}(\mathcal{R}), \mathcal{Q}(\mathcal{R}), \mathcal{I}(\mathcal{R}),$ and $\mathcal{S}(\mathcal{R})$ are correlated

³Here we have changed slightly the conventions used in [40].

with the representation labels according to the results shown in equations in (4.5).

$$\begin{aligned}
 0 &= p_{(CS)} = q_{(CS)} = r_{(CS)}, & 1 &= s_{(CS)}, \\
 1 &= p_{(VS)} = q_{(VS)} = r_{(VS)}, & 0 &= s_{(VS)}, \\
 1 &= -p_{(TS)} = q_{(TS)} = -r_{(TS)}, & 0 &= s_{(TS)}, \\
 1 &= -p_{(AVS)} = -q_{(AVS)} = r_{(AVS)}, & 0 &= s_{(AVS)}, \\
 1 &= p_{(ATS)} = -q_{(ATS)} = -r_{(ATS)}, & 0 &= s_{(ATS)}.
 \end{aligned} \tag{4.5}$$

When the result in (4.4) is substituted into (4.1), it yields

$$\begin{aligned}
 \widehat{\mathcal{G}}[(\widehat{\mathcal{R}}), (\widehat{\mathcal{R}}')] &= 256 \left\{ p_{(\mathcal{R})} p_{(\mathcal{R}')} (-m_1 + 2m_2 + 2m_4 + m_5) + \right. \\
 &\quad q_{(\mathcal{R})} q_{(\mathcal{R}')} (m_1 + 2m_2 + 2m_4 - m_5) + \\
 &\quad r_{(\mathcal{R})} r_{(\mathcal{R}')} (m_1 - 4m_2 - 48m_3 + 4m_4 + m_5) + \\
 &\quad \left. 3 s_{(\mathcal{R})} s_{(\mathcal{R}')} (-m_1 - 16m_3 - m_5) \right\}.
 \end{aligned} \tag{4.6}$$

Let us now observe that there are five undetermined constants m_1, \dots, m_5 on the four lines of the equation in (4.6). We are therefore free to impose the following *four* conditions on these constants,

$$\begin{aligned}
 \frac{1}{768} &= -m_1 + 2m_2 + 2m_4 + m_5, \\
 \frac{1}{768} &= m_1 + 2m_2 + 2m_4 - m_5, \\
 \frac{1}{768} &= m_1 - 4m_2 - 48m_3 + 4m_4 + m_5, \\
 \frac{1}{768} &= -m_1 - 16m_3 - m_5,
 \end{aligned} \tag{4.7}$$

which possesses the solution

$$m_1 = -m_4 = m_5 = - \left[\frac{1}{1,536} + 8m_3 \right], \quad m_2 = -8m_3, \tag{4.8}$$

and further implies the result for the 4D, Lorentz covariant Gadget can be written as⁴

$$\begin{aligned}
 \widehat{\mathcal{G}}[(\widehat{\mathcal{R}}), (\widehat{\mathcal{R}}')] &= -\frac{1}{1,536} \left\{ [\mathbf{H}^{\mu(\widehat{\mathcal{R}})}]_{abc}{}^d [\mathbf{H}_{\mu}^{(\widehat{\mathcal{R}}')}]^{ab}{}^c \right. \\
 &\quad - (\gamma^5 \gamma^\alpha)_c{}^e [\mathbf{H}^{\mu(\widehat{\mathcal{R}})}]_{abe}{}^f (\gamma^5 \gamma_\alpha)_f{}^d [\mathbf{H}_{\mu}^{(\widehat{\mathcal{R}}')}]^{ab}{}^c \\
 &\quad \left. + (\gamma^5)_c{}^e [\mathbf{H}^{\mu(\widehat{\mathcal{R}})}]_{abe}{}^f (\gamma^5)_f{}^d [\mathbf{H}_{\mu}^{(\widehat{\mathcal{R}}')}]^{ab}{}^c \right\},
 \end{aligned} \tag{4.9}$$

for $m_3 = 0$ or alternately as

$$\begin{aligned}
 \widehat{\mathcal{G}}[(\widehat{\mathcal{R}}), (\widehat{\mathcal{R}}')] &= \frac{1}{1,536} \left\{ (\gamma^\alpha)_c{}^e [\mathbf{H}^{\mu(\widehat{\mathcal{R}})}]_{abe}{}^f (\gamma_\alpha)_f{}^d [\mathbf{H}_{\mu}^{(\widehat{\mathcal{R}}')}]^{ab}{}^c \right. \\
 &\quad \left. - \frac{1}{8} ([\gamma^\alpha, \gamma^\beta])_c{}^e [\mathbf{H}^{\mu(\widehat{\mathcal{R}})}]_{abe}{}^f ([\gamma_\alpha, \gamma_\beta])_f{}^d [\mathbf{H}_{\mu}^{(\widehat{\mathcal{R}}')}]^{ab}{}^c \right\},
 \end{aligned} \tag{4.10}$$

for $8m_3 = -1/1,536$. Now independent of m_1, \dots, m_5 due to the four conditions in (4.7), the expression in (4.6) becomes

$$\widehat{\mathcal{G}}[(\widehat{\mathcal{R}}), (\widehat{\mathcal{R}}')] = \frac{1}{3} \left[p_{(\mathcal{R})} p_{(\mathcal{R}')} + q_{(\mathcal{R})} q_{(\mathcal{R}')} + r_{(\mathcal{R})} r_{(\mathcal{R}')} + 3 s_{(\mathcal{R})} s_{(\mathcal{R}')} \right]. \tag{4.11}$$

⁴These results correct the previously reported ones in [40].

It follows, from the allowed values of $p_{(\mathcal{R})}$, $q_{(\mathcal{R})}$, $r_{(\mathcal{R})}$, and $s_{(\mathcal{R})}$ in (4.5), the supermultiplet matrix analogous to the AGRM over these representations takes the form

$$\widehat{\mathcal{G}}[(\widehat{\mathcal{R}}), (\widehat{\mathcal{R}}')] = \begin{bmatrix} 1 & 0 & 0 & 0 & 0 \\ 0 & 1 & -\frac{1}{3} & -\frac{1}{3} & -\frac{1}{3} \\ 0 & -\frac{1}{3} & 1 & -\frac{1}{3} & -\frac{1}{3} \\ 0 & -\frac{1}{3} & -\frac{1}{3} & 1 & -\frac{1}{3} \\ 0 & -\frac{1}{3} & -\frac{1}{3} & -\frac{1}{3} & 1 \end{bmatrix}. \quad (4.12)$$

This matrix has been obtained previously, but purely in the context of solely 1D arguments [39]. Here we have also proven this result is obtained strictly on the basis of 4D supermultiplet calculations.

Given the values of the supermultiplet Gadget representation matrix above, we can define a set of angles between the supermultiplets via the equation,

$$\cos \left\{ \theta[(\widehat{\mathcal{R}}), (\widehat{\mathcal{R}}')] \right\} = \frac{\widehat{\mathcal{G}}[(\widehat{\mathcal{R}}), (\widehat{\mathcal{R}}')]}{\sqrt{\widehat{\mathcal{G}}[(\widehat{\mathcal{R}}), (\widehat{\mathcal{R}})]} \sqrt{\widehat{\mathcal{G}}[(\widehat{\mathcal{R}}'), (\widehat{\mathcal{R}}')]}} , \quad (4.13)$$

and the angles thus found correspond to $\arccos(-1/3)$, $\pi/2$, and 0 via calculation directly in 4D, $\mathcal{N} = 1$ supersymmetry. The supermultiplet Gadget in (4.11) allows us to map:

- (a.) the vector supermultiplet into the point on the sphere along the line segment \overline{OA} ,
- (b.) the axial-vector supermultiplet into the point on the sphere along the line segment \overline{OB} ,
- (c.) the axial-tensor supermultiplet into the point on the sphere the along line segment \overline{OC} , and
- (d.) the tensor supermultiplet into the point on the sphere along the line segment \overline{OD} ,

in the image shown in figure 2. This is a “weight space like” diagram showing these minimal 4D, $\mathcal{N} = 1$ supermultiplets while the chiral supermultiplet lies in a direction orthogonal to this three dimensional subspace. With this interpretation, the formulae in (4.4) and (4.11) define a space of minimal 4D, $\mathcal{N} = 1$ representations together with its metric. The coordinates of points for each superfield representation in the space are provided by the values of $p_{(\mathcal{R})}$, $q_{(\mathcal{R})}$, $r_{(\mathcal{R})}$, and $s_{(\mathcal{R})}$. So the the vector supermultiplet, the axial-vector supermultiplet, the axial-tensor supermultiplet, and the tensor supermultiplet all reside in the $s_{(\mathcal{R})} = 0$ three dimensional subspace.

Let us delve more deeply into this point. The quantity $(p_{(\mathcal{R})}, q_{(\mathcal{R})}, r_{(\mathcal{R})}, s_{(\mathcal{R})})$ defines a vector in four-dimensional space. For this space the expression in (4.11) defines a metric or inner product. The results already presented in the section imply the following components of such a vector associated with each representation label.

The components shown in table 2 indicate that the vectors associated with each of the representation labels are unit vectors with regard to the metric defined in (4.11). This same metric implies that the vector associated with (CS) is orthogonal to the vectors associated

$(\widehat{\mathcal{R}})$	$p(\mathcal{R})$	$q(\mathcal{R})$	$r(\mathcal{R})$	$s(\mathcal{R})$
(CS)	0	0	0	1
(VS)	1	1	1	0
(AVS)	-1	-1	1	0
(ATS)	1	-1	-1	0
(TS)	-1	1	-1	0

Table 2. Components for the (CS), (VS), (AVS) (ATS), and (TS) supermultiplets.

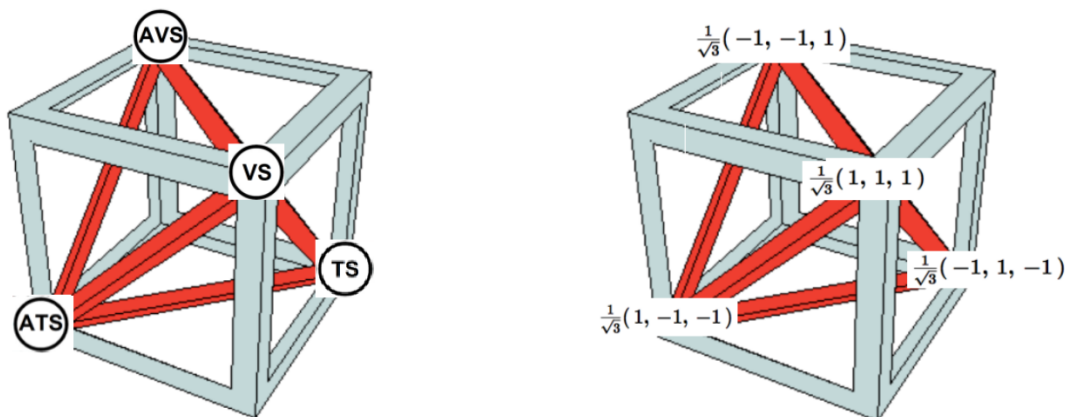


Figure 4. Cubically inscribed tetrahedron with supermultiplets and their re-scaled $p(\mathcal{R})$, $q(\mathcal{R})$, and $r(\mathcal{R})$ coordinates at intersecting vertices.

with the four remaining representations. These remaining representations all ‘live’ in a three dimensional subspace which is shown in figure 4.

We note the diagonal entries in the matrix shown in (4.12) imply that the distance defined by the metric in (4.11) from the center of the cube to any of its vertices must be equal to one.

The vector associated with the (CS) representation is not shown in this diagram as it is not contained within this three dimensional-subspace. We have re-scaled the $p(\mathcal{R})$, $q(\mathcal{R})$, and $r(\mathcal{R})$ components so that the standard Euclidean metric implies that the vectors drawn from the center of the cube to any vertex containing a supermultiplet vectors has length one.

It is now a simple matter to show the three dimensional rotation matrix \mathbf{R} (satisfying $\mathbf{R}\mathbf{R}^T = \mathbf{R}^T\mathbf{R} = \mathbf{I}$, where the superscript T stands for transposed) described by⁵

$$\mathbf{R} = \begin{bmatrix} -\frac{\sqrt{6}}{6} & \frac{\sqrt{6}}{3} & -\frac{\sqrt{6}}{6} \\ \frac{\sqrt{2}}{2} & 0 & -\frac{\sqrt{2}}{2} \\ \frac{\sqrt{3}}{3} & \frac{\sqrt{3}}{3} & \frac{\sqrt{3}}{3} \end{bmatrix} \tag{4.14}$$

transforms the red tetrahedron (defined *solely* from superfield considerations above) to align it with the tetrahedron shown at the end of section 2 (defined *solely* from adinkra

⁵This matrix should not be confused with one of the R-matrices that appear in (2.1).

considerations). We write the four vectors from the point O to the points of intersection indicated below figure 2 in the forms

$$\vec{A}_1 = \begin{bmatrix} 0 \\ 0 \\ 1 \end{bmatrix}, \quad \vec{A}_2 = \begin{bmatrix} -\frac{\sqrt{2}}{3} \\ -\frac{\sqrt{6}}{3} \\ -\frac{1}{3} \end{bmatrix}, \quad \vec{A}_3 = \begin{bmatrix} \frac{2\sqrt{2}}{3} \\ 0 \\ -\frac{1}{3} \end{bmatrix}, \quad \vec{A}_4 = \begin{bmatrix} -\frac{\sqrt{2}}{3} \\ \frac{\sqrt{6}}{3} \\ -\frac{1}{3} \end{bmatrix}, \quad (4.15)$$

and in a similar manner we denote four more vectors by the equations

$$\vec{B}_1 = \frac{1}{\sqrt{3}} \begin{bmatrix} 1 \\ 1 \\ 1 \end{bmatrix}, \quad \vec{B}_2 = \frac{1}{\sqrt{3}} \begin{bmatrix} -1 \\ -1 \\ 1 \end{bmatrix}, \quad \vec{B}_3 = \frac{1}{\sqrt{3}} \begin{bmatrix} -1 \\ 1 \\ -1 \end{bmatrix}, \quad \vec{B}_4 = \frac{1}{\sqrt{3}} \begin{bmatrix} 1 \\ -1 \\ -1 \end{bmatrix}, \quad (4.16)$$

having been obtained from the coordinates of the intersecting points that appear on the right hand side of figure 4. Next one can note

$$\mathbf{R} \vec{B}_1 = \vec{A}_1, \quad \mathbf{R} \vec{B}_2 = \vec{A}_2, \quad \mathbf{R} \vec{B}_3 = \vec{A}_3, \quad \mathbf{R} \vec{B}_4 = \vec{A}_4, \quad (4.17)$$

which implies the alignment of the tetrahedron in figure 2 and the tetrahedron in figure 4.

Let us close this section with two amusing idylls, with the second one possibly hinting at tantalizing additional developments.

A first one is the observation that the presence of the sphere, the cube, and the tetrahedron (with the latter two being among the five platonic solids [48]) implies 4D, $\mathcal{N} = 1$ space-time supersymmetry representation theory contains in a hidden manner a structure with some similarity to Kepler’s “Mysterium Cosmographicum” [49].

The second comment relates to results by Nekrasov [50, 52–56]. In the first of these, it is noted that the tetrahedral angle $\arccos(-1/3)$ can be uncovered by looking at Yang-Mills gauge theories in various dimensions in the presence of a supergravity background. In relation to summing up instantons for 4D, $\mathcal{N} = 2$ theories he observed that, “the theory is subject to a special supergravity background, which softly breaks super-Poincare symmetry yet deforms some of the supercharges in such a way that they anti-commute onto spacetime rotations instead of translations. The supersymmetric field configurations then become (for gauge groups the products of unitary groups) enumerated by sequences of Young diagrams, i.e. two dimensional arrangements of squares.

One can then study higher dimensional theories, e.g. maximal super-Yang-Mills in 6 or 7 dimensions (which should be defined quantum mechanically using D6 branes in IIA string theory) and then the instanton counting becomes the study of three dimensional Young diagrams aka the plane partitions. These can be visualized by projecting them onto a two-plane along the (1,1,1) axis, where the plane partitions look like the tessellations of the plane by three types of rombi.”

It is this final step that leads to the appearance of the angle $\arccos(-1/3)$ as seen in adinkra gadget values.

In the work of [56], there is also one other tantalizing similarity between some of Nekrasov’s discussions and the structure uncovered in the work of [44]. In the former,

there is defined a function ε that maps the set of 2-element subsets of the partitions of four objects to \mathbf{Z}_2 . The 2-element subsets, which Nekrasov denoted by

$$\underline{6} = \binom{4}{2} = \{12, 13, 14, 23, 24, 34\} \tag{4.18}$$

correspond to the six distinct sets shown in the Venn diagram in figure 5. Furthermore, the work in [44] explicitly seems to note a realization of Nekrasov’s ε -map. When the 2-element subsets are represented by permutation matrices, the ε -map corresponds to a construction based on matrix transposition seen in [44].

5 The Coxeter group BC_4 & the “small BC_4 library”

We define elements of the Coxeter Group BC_4 [18, 19] by consider the set of all real 4×4 matrices that arise as a bilinear product of the form [44]

$$\mathbf{L} = \mathbf{S} \cdot \mathbf{P} \tag{5.1}$$

The real 4×4 diagonal matrix \mathbf{S} is the “Boolean Factor” [44] and squares to the identity. The matrix \mathbf{P} is a representation of a permutation of 4 objects. There are $2^d d! = 2^4 \times 4! = 384$ ways to choose the factors which is the dimension of the Coxeter group BC_4 . More explicitly this expression can be written as

$$(\mathbf{L}_I^{(\mathcal{R})})_i^{\hat{k}} = [\mathbf{S}^{(I)(\mathcal{R})}]_i^{\hat{\ell}} [\mathcal{P}_{(I)}^{(\mathcal{R})}]_{\hat{\ell}}^{\hat{k}}, \quad \text{for each fixed } I = 1, 2, 3, 4 \text{ on the l.h.s. .} \tag{5.2}$$

This notation anticipates distinct adinkra representations exist and are denoted by “a representation label” (\mathcal{R}) that takes on values from one to some integer, T.

Our experience in the work of [44] gave a very valuable lesson... there is an smaller algebraic structure, the Vierergruppe,

$$\{\mathcal{V}\} = \{(), (12)(34), (13)(24), (14)(23)\}, \tag{5.3}$$

whose role is critical. The Vierergruppe elements above are written using cycle notation to indicate the distinct permutations and can be used in partitioning the permutation elements. These partitions allow all 24 permutation elements to be gathered into six “corrals” which then provide a basis for constructing adinkras. Since the elements of $\{\mathcal{V}\}$ can also be represented as 4×4 matrices as well, we can alternately express them in the form of outer products of the 2×2 identity matrix $\mathbf{I}_{2 \times 2}$ and the first Pauli matrix σ^1 ,

$$\{\mathcal{V}_{(4)}\} = \{ \mathbf{I}_{2 \times 2} \otimes \mathbf{I}_{2 \times 2}, \mathbf{I}_{2 \times 2} \otimes \sigma^1, \sigma^1 \otimes \mathbf{I}_{2 \times 2}, \sigma^1 \otimes \sigma^1 \}. \tag{5.4}$$

Written in this form, we are able to connect this expression back to the first works [1, 2] that launched our efforts.

Using either notation, one can show that for unordered quartets, the equations

$$\begin{aligned}
 (12) \{\mathcal{V}_{(4)}\} &= (34) \{\mathcal{V}_{(4)}\} = (1324) \{\mathcal{V}_{(4)}\} = (1423) \{\mathcal{V}_{(4)}\}, \\
 (13) \{\mathcal{V}_{(4)}\} &= (24) \{\mathcal{V}_{(4)}\} = (1234) \{\mathcal{V}_{(4)}\} = (1432) \{\mathcal{V}_{(4)}\}, \\
 (14) \{\mathcal{V}_{(4)}\} &= (23) \{\mathcal{V}_{(4)}\} = (1243) \{\mathcal{V}_{(4)}\} = (1342) \{\mathcal{V}_{(4)}\}, \\
 (123) \{\mathcal{V}_{(4)}\} &= (134) \{\mathcal{V}_{(4)}\} = (142) \{\mathcal{V}_{(4)}\} = (243) \{\mathcal{V}_{(4)}\}, \\
 (124) \{\mathcal{V}_{(4)}\} &= (132) \{\mathcal{V}_{(4)}\} = (143) \{\mathcal{V}_{(4)}\} = (234) \{\mathcal{V}_{(4)}\}.
 \end{aligned} \tag{5.5}$$

$$\begin{aligned}
 \{\mathcal{V}_{(4)}\} (12) &= \{\mathcal{V}_{(4)}\} (34) = \{\mathcal{V}_{(4)}\} (1324) = \{\mathcal{V}_{(4)}\} (1423), \\
 \{\mathcal{V}_{(4)}\} (13) &= \{\mathcal{V}_{(4)}\} (24) = \{\mathcal{V}_{(4)}\} (1234) = \{\mathcal{V}_{(4)}\} (1432), \\
 \{\mathcal{V}_{(4)}\} (14) &= \{\mathcal{V}_{(4)}\} (23) = \{\mathcal{V}_{(4)}\} (1243) = \{\mathcal{V}_{(4)}\} (1342), \\
 \{\mathcal{V}_{(4)}\} (123) &= \{\mathcal{V}_{(4)}\} (134) = \{\mathcal{V}_{(4)}\} (142) = \{\mathcal{V}_{(4)}\} (243), \\
 \{\mathcal{V}_{(4)}\} (124) &= \{\mathcal{V}_{(4)}\} (132) = \{\mathcal{V}_{(4)}\} (143) = \{\mathcal{V}_{(4)}\} (234).
 \end{aligned} \tag{5.6}$$

of (5.5) and (5.6) are satisfied. These define five ‘‘corrals’’ of the permutation operators. The set defined by $\{\mathcal{V}_{(4)}\}$ provides a sixth such corral.

In order to precede with explicit calculations, it is necessary to choose ‘‘fiducial set’’ quartets⁶ where explicit choices are made for which quartets of permutation matrices are given a specific designation and what is the order of the permutations in each designation. Using the conventions of [44] we assign the following definitions of these ‘fiducial set’ quartets.

$$\begin{array}{cccc}
 \mathbf{L}_1 & \mathbf{L}_2 & \mathbf{L}_3 & \mathbf{L}_4 \\
 \{\mathcal{P}_{[1]}\} &= \{(243), (123), (134), (142)\}, \\
 \{\mathcal{P}_{[2]}\} &= \{(234), (124), (132), (143)\}, \\
 \{\mathcal{P}_{[3]}\} &= \{(1243), (23), (14), (1342)\}, \\
 \{\mathcal{P}_{[4]}\} &= \{(1432), (24), (1234), (13)\}, \\
 \{\mathcal{P}_{[5]}\} &= \{(1324), (1423), (12), (34)\}, \\
 \{\mathcal{P}_{[6]}\} &= \{(13)(24), (14)(23), (), (12)(34)\}.
 \end{array} \tag{5.7}$$

In fact, if one computes the cycles that are associated with the adinkra shown in figure 1, the cycles that arise from such deductions are precisely the cycles shown for $\{\mathcal{P}_{[1]}\}$ and in the same order. The meaning of the results shown in (5.7) is that one can obtain the L-matrices shown at the top once appropriate Boolean Factors are attached to the permutations in each corral.

We collectively express the permutations subsets as $\{\mathcal{P}_{[\Lambda]}\}$, with the index $[\Lambda]$ taking on values [1] through [6]. These are cosets involving the Vierergruppe and this allows a partitioning of \mathbf{BC}_4 (since it contains S_4) into six distinct subsets or ‘‘corrals,’’ that contain four permutations in unordered quartets as shown in figure 5. All of the 384 elements associated with figure 1. now reside inside 96 quartets which are equally distributed among all six partitions (i.e. 16 quartets per corral).

⁶The ‘‘fiducial set’’ is simply a historical artifact of our path of discovery on this subject has taken.

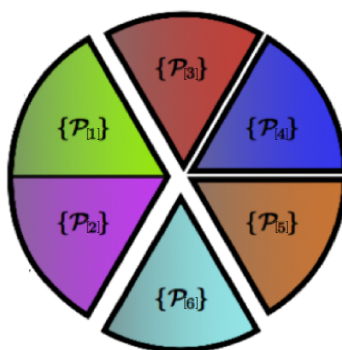


Figure 5. $\{Z_2 \times Z_2\}$ partitioning of S_4 .

We now turn to the assignments of the “Boolean Factors” to the permutation elements. In order to do this, we first observe there exists 16 sets of “Boolean Factors” that can be assigned to each of the permutation partition factors and faithfully represent BC_4 .

Each “Boolean Factor” is equivalent to a real diagonal matrix that squares to the identity. In the work of [44], a convention was created whereby each of the “Boolean Factors” could be unambiguously specified by a single real natural number. Applying this convention to the “Boolean Factor” shown (5.8)

$$\begin{aligned}
 \mathcal{S}_1 &= \mathbf{I}_{2 \times 2} \otimes \mathbf{I}_{2 \times 2} , \\
 \mathcal{S}_2 &= \mathbf{I}_{2 \times 2} \otimes \sigma^3 , \\
 \mathcal{S}_3 &= \sigma^3 \otimes \mathbf{I}_{2 \times 2} , \\
 \mathcal{S}_4 &= \sigma^3 \otimes \sigma^3 ,
 \end{aligned}
 \tag{5.8}$$

we see these are mapped into the efficient notation as $(0)_b$, $(10)_b$, $(12)_b$, and $(6)_b$, respectively.

In appendix B, the Boolean Factors appropriate to the fiducial choice of the quartets of permutations set out in eq. (5.7) are listed. As an example for how to use the list, it is instructive to construct an example in an explicit manner. As noted in the list, there are 16 appropriate choices of Boolean Factors for each of the fiducial permutation quartets in (5.7).

5.1 Illustrative discussion

In order to show how all this formalism works, let us “derive” a set of L-matrices by making the choice $\mathbf{L}(\mathcal{S}_{\mathcal{P}_1[12]} \cdot \mathcal{P}_{[1]})$.⁷ From the list in appendix B, we find the Boolean Factor quartet and from eq. (5.7) we have the permutation element quartet. So we need to calculate the “dot product” indicated by,

$$\begin{aligned}
 \mathbf{L}(\mathcal{S}_{\mathcal{P}_1[12]} \cdot \mathcal{P}_{[1]}) &= (\{(10)_b, (12)_b, (6)_b, (0)_b\} \cdot \{(243), (123), (134), (142)\}) \\
 &= \{(10)_b(243), (12)_b(123), (6)_b(134), (0)_b(142)\} ,
 \end{aligned}
 \tag{5.9}$$

⁷The assignment of signed permutations and their association with the so-called “chiral,” “tensor,” and “vector” sets of L-matrices is incorrectly stated in the works of [41, 42] and are corrected in (5.10), (5.12), and (5.14) here.

which implies

$$\begin{aligned}
 \mathbf{L}_1(\mathcal{S}_{\mathcal{P}_1[12]} \cdot \mathcal{P}_{[1]}) &= \begin{bmatrix} 1 & 0 & 0 & 0 \\ 0 & 0 & 0 & -1 \\ 0 & 1 & 0 & 0 \\ 0 & 0 & -1 & 0 \end{bmatrix}, & \mathbf{L}_2(\mathcal{S}_{\mathcal{P}_1[12]} \cdot \mathcal{P}_{[1]}) &= \begin{bmatrix} 0 & 1 & 0 & 0 \\ 0 & 0 & 1 & 0 \\ -1 & 0 & 0 & 0 \\ 0 & 0 & 0 & -1 \end{bmatrix}, \\
 \mathbf{L}_3(\mathcal{S}_{\mathcal{P}_1[12]} \cdot \mathcal{P}_{[1]}) &= \begin{bmatrix} 0 & 0 & 1 & 0 \\ 0 & -1 & 0 & 0 \\ 0 & 0 & 0 & -1 \\ 1 & 0 & 0 & 0 \end{bmatrix}, & \mathbf{L}_4(\mathcal{S}_{\mathcal{P}_1[12]} \cdot \mathcal{P}_{[1]}) &= \begin{bmatrix} 0 & 0 & 0 & 1 \\ 1 & 0 & 0 & 0 \\ 0 & 0 & 1 & 0 \\ 0 & 1 & 0 & 0 \end{bmatrix}. \quad (5.10)
 \end{aligned}$$

These are precisely the L-matrices associated with the adinkra shown in figure 1. For other choices of the Boolean Factor $\mathcal{S}_{\mathcal{P}_1[\alpha]}$, it is possible to generate other representations of the L-matrices associated with the $\mathcal{P}_{[1]}$ element.

Another set of such matrices can be constructed from $\mathbf{L}(\mathcal{S}_{\mathcal{P}_2[15]} \cdot \mathcal{P}_{[2]})$ which implies

$$\begin{aligned}
 \mathbf{L}(\mathcal{S}_{\mathcal{P}_2[15]} \cdot \mathcal{P}_{[2]}) &= (\{14\}_b, (4)_b, (8)_b, (2)_b) \cdot \{(234), (124), (132), (143)\} \\
 &= \{(14)_b(124), (4)_b(124), (8)_b(132), (2)_b(143)\}, \quad (5.11)
 \end{aligned}$$

and this yields

$$\begin{aligned}
 \mathbf{L}_1(\mathcal{S}_{\mathcal{P}_2[15]} \cdot \mathcal{P}_{[2]}) &= \begin{bmatrix} 1 & 0 & 0 & 0 \\ 0 & 0 & -1 & 0 \\ 0 & 0 & 0 & -1 \\ 0 & -1 & 0 & 0 \end{bmatrix}, & \mathbf{L}_2(\mathcal{S}_{\mathcal{P}_2[15]} \cdot \mathcal{P}_{[2]}) &= \begin{bmatrix} 0 & 1 & 0 & 0 \\ 0 & 0 & 0 & 1 \\ 0 & 0 & -1 & 0 \\ 1 & 0 & 0 & 0 \end{bmatrix}, \\
 \mathbf{L}_3(\mathcal{S}_{\mathcal{P}_2[15]} \cdot \mathcal{P}_{[2]}) &= \begin{bmatrix} 0 & 0 & 1 & 0 \\ 1 & 0 & 0 & 0 \\ 0 & 1 & 0 & 0 \\ 0 & 0 & 0 & -1 \end{bmatrix}, & \mathbf{L}_4(\mathcal{S}_{\mathcal{P}_2[15]} \cdot \mathcal{P}_{[2]}) &= \begin{bmatrix} 0 & 0 & 0 & 1 \\ 0 & -1 & 0 & 0 \\ 1 & 0 & 0 & 0 \\ 0 & 0 & 1 & 0 \end{bmatrix}. \quad (5.12)
 \end{aligned}$$

A third set of such matrices can be constructed from $\mathbf{L}(\mathcal{S}_{\mathcal{P}_3[12]} \cdot \mathcal{P}_{[3]})$ which implies

$$\begin{aligned}
 \mathbf{L}(\mathcal{S}_{\mathcal{P}_3[12]} \cdot \mathcal{P}_{[3]}) &= (\{10\}_b, (12)_b, (0)_b, (6)_b) \cdot \{(1243), (23), (14), (1342)\} \\
 &= \{(10)_b(1243), (12)_b(23), (0)_b(14), (6)_b(1342)\}, \quad (5.13)
 \end{aligned}$$

and this yields

$$\begin{aligned}
 \mathbf{L}_1(\mathcal{S}_{\mathcal{P}_3[12]} \cdot \mathcal{P}_{[3]}) &= \begin{bmatrix} 0 & 1 & 0 & 0 \\ 0 & 0 & 0 & -1 \\ 1 & 0 & 0 & 0 \\ 0 & 0 & -1 & 0 \end{bmatrix}, & \mathbf{L}_2(\mathcal{S}_{\mathcal{P}_3[12]} \cdot \mathcal{P}_{[3]}) &= \begin{bmatrix} 1 & 0 & 0 & 0 \\ 0 & 0 & 1 & 0 \\ 0 & -1 & 0 & 0 \\ 0 & 0 & 0 & -1 \end{bmatrix}, \\
 \mathbf{L}_3(\mathcal{S}_{\mathcal{P}_3[12]} \cdot \mathcal{P}_{[3]}) &= \begin{bmatrix} 0 & 0 & 0 & 1 \\ 0 & 1 & 0 & 0 \\ 0 & 0 & 1 & 0 \\ 1 & 0 & 0 & 0 \end{bmatrix}, & \mathbf{L}_4(\mathcal{S}_{\mathcal{P}_3[12]} \cdot \mathcal{P}_{[3]}) &= \begin{bmatrix} 0 & 0 & 1 & 0 \\ -1 & 0 & 0 & 0 \\ 0 & 0 & 0 & -1 \\ 0 & 1 & 0 & 0 \end{bmatrix}. \quad (5.14)
 \end{aligned}$$

Representation	$\ell_{12}^{\widehat{2}}$	$\ell_{13}^{\widehat{3}}$	$\ell_{14}^{\widehat{1}}$	$\ell_{23}^{\widehat{1}}$	$\ell_{24}^{\widehat{3}}$	$\ell_{34}^{\widehat{2}}$	$\widetilde{\ell}_{12}^{\widehat{3}}$	$\widetilde{\ell}_{13}^{\widehat{2}}$	$\widetilde{\ell}_{14}^{\widehat{1}}$	$\widetilde{\ell}_{23}^{\widehat{1}}$	$\widetilde{\ell}_{24}^{\widehat{2}}$	$\widetilde{\ell}_{34}^{\widehat{3}}$
$(\mathcal{S}_{\mathcal{P}_1}[12] \cdot \mathcal{P}_{[1]})$	1	1	1	1	-1	1	0	0	0	0	0	0
$(\mathcal{S}_{\mathcal{P}_2}[15] \cdot \mathcal{P}_{[2]})$	0	0	0	0	0	0	1	1	1	-1	1	-1
$(\mathcal{S}_{\mathcal{P}_3}[12] \cdot \mathcal{P}_{[3]})$	0	0	0	0	0	0	-1	1	-1	1	1	1

Table 3. A selection of ℓ and $\widetilde{\ell}$ values for the three fiducial adinkras.

The matrices that appear in (5.10), (5.12), and (5.14) are, respectively, the ones we have traditionally referred to as the “chiral,” “tensor,” and “vector” supermultiplets L-matrices [9] as we initially derived these by application of a reduction process to the corresponding usual 4D, $\mathcal{N} = 1$ supermultiplets.

For each of the cases, we can next calculate the fermionic holoraumy matrices. We find,

$$\begin{aligned}
 \widetilde{V}_{12}(\mathcal{S}_{\mathcal{P}_1}[12] \cdot \mathcal{P}_{[1]}) &= +\widetilde{V}_{34}(\mathcal{S}_{\mathcal{P}_1}[12] \cdot \mathcal{P}_{[1]}) = +\alpha^2, \\
 \widetilde{V}_{13}(\mathcal{S}_{\mathcal{P}_1}[12] \cdot \mathcal{P}_{[1]}) &= -\widetilde{V}_{24}(\mathcal{S}_{\mathcal{P}_1}[12] \cdot \mathcal{P}_{[1]}) = +\alpha^3, \\
 \widetilde{V}_{14}(\mathcal{S}_{\mathcal{P}_1}[12] \cdot \mathcal{P}_{[1]}) &= +\widetilde{V}_{23}(\mathcal{S}_{\mathcal{P}_1}[12] \cdot \mathcal{P}_{[1]}) = +\alpha^1,
 \end{aligned} \tag{5.15}$$

for the chiral supermultiplet fermionic holoraumy matrices,

$$\begin{aligned}
 \widetilde{V}_{12}(\mathcal{S}_{\mathcal{P}_2}[15] \cdot \mathcal{P}_{[2]}) &= -\widetilde{V}_{34}(\mathcal{S}_{\mathcal{P}_2}[15] \cdot \mathcal{P}_{[2]}) = +\beta^3, \\
 \widetilde{V}_{13}(\mathcal{S}_{\mathcal{P}_2}[15] \cdot \mathcal{P}_{[2]}) &= +\widetilde{V}_{24}(\mathcal{S}_{\mathcal{P}_2}[15] \cdot \mathcal{P}_{[2]}) = +\beta^2, \\
 \widetilde{V}_{14}(\mathcal{S}_{\mathcal{P}_2}[15] \cdot \mathcal{P}_{[2]}) &= -\widetilde{V}_{23}(\mathcal{S}_{\mathcal{P}_2}[15] \cdot \mathcal{P}_{[2]}) = +\beta^1,
 \end{aligned} \tag{5.16}$$

for the tensor supermultiplet fermionic holoraumy matrices, and

$$\begin{aligned}
 \widetilde{V}_{12}(\mathcal{S}_{\mathcal{P}_3}[12] \cdot \mathcal{P}_{[3]}) &= -\widetilde{V}_{34}(\mathcal{S}_{\mathcal{P}_3}[12] \cdot \mathcal{P}_{[3]}) = -\beta^3, \\
 \widetilde{V}_{13}(\mathcal{S}_{\mathcal{P}_3}[12] \cdot \mathcal{P}_{[3]}) &= +\widetilde{V}_{24}(\mathcal{S}_{\mathcal{P}_3}[12] \cdot \mathcal{P}_{[3]}) = +\beta^2, \\
 \widetilde{V}_{14}(\mathcal{S}_{\mathcal{P}_3}[12] \cdot \mathcal{P}_{[3]}) &= -\widetilde{V}_{23}(\mathcal{S}_{\mathcal{P}_3}[12] \cdot \mathcal{P}_{[3]}) = -\beta^1,
 \end{aligned} \tag{5.17}$$

for the vector supermultiplet fermionic holoraumy matrices. These results may be used in the formula that appears in (2.4) to replicate the 3×3 matrix in the upper left-hand corner of (4.12) when evaluated over the L-matrices in (5.10), (5.12), and (5.14) respectively and taken in this order.

The results in (5.17) can also be used in conjunction with the three Fiducial Adinkra formulae in (2.6), (2.7) and (2.8) to show that only some of the non-vanishing values of ℓ 's and $\widetilde{\ell}$'s associated with (5.10), (5.12), and (5.14) and these are show in the table 3 (all values not shown are equal to zero also).

The calculation of the Gadget values between these representations can be easily carried out by regarding the rows containing either entries of $1/3$, 0 , or 1 as components of vectors and calculating their dot products followed by multiplying these dot products by

1/6. This yields

$$\begin{aligned}
 \mathcal{G}[(\mathcal{S}_{\mathcal{P}_1}[12] \cdot \mathcal{P}_{[1]}), (\mathcal{S}_{\mathcal{P}_1}[12] \cdot \mathcal{P}_{[1]})] &= \frac{1}{6} \{ 1 + 1 + 1 + 1 + (-1)^2 + 1 + 0 + 0 + \\
 &\quad 0 + 0 + 0 + 0 \} = 1, \\
 \mathcal{G}[(\mathcal{S}_{\mathcal{P}_1}[12] \cdot \mathcal{P}_{[1]}), (\mathcal{S}_{\mathcal{P}_2}[15] \cdot \mathcal{P}_{[2]})] &= \frac{1}{6} \{ 0 + 0 + 0 + 0 + 0 + 0 + 0 + 0 + \\
 &\quad 0 + 0 + 0 + 0 \} = 0, \\
 \mathcal{G}[(\mathcal{S}_{\mathcal{P}_2}[15] \cdot \mathcal{P}_{[2]}), (\mathcal{S}_{\mathcal{P}_3}[12] \cdot \mathcal{P}_{[3]})] &= \frac{1}{6} \{ 0 + 0 + 0 + 0 + 0 + 0 + (-1) + (1) + \\
 &\quad (-1) + (-1) + (1) + (-1) \} = -\frac{1}{3}, \quad (5.18)
 \end{aligned}$$

as three examples.

The connection to the concept of “useful inequivalence” [45] comes from reduction from 4D considerations to 2D considerations. The 4D, $\mathcal{N} = 1$ chiral supermultiplet can be reduced to become the 2D, $\mathcal{N} = 2$ chiral supermultiplet which also yields the matrices in (5.10). The 4D, $\mathcal{N} = 1$ vector supermultiplet can be reduced to become the 2D, $\mathcal{N} = 2$ twisted chiral supermultiplet [47] which, in a similar manner, yields the matrices in (5.12). When one examines the Boolean Factors that appear in (5.9) and (5.11), it can be seen that both use the same quartet of Boolean Factors, though the order is different.

For the skeptical reader, let us dwell on this matter for a bit. To our knowledge, the initiation of the topic of usefully inequivalent supermultiplets in the physics literature can be traced back to the work in [46], where one of the current authors (SJG) gave the first prescription for extracting the 2D, $\mathcal{N} = 2$ “twisted chiral supermultiplet” via dimensional reduction. In a follow-up work [47], the significance and even the name “twisted chiral supermultiplet,” was introduced. But of even greater importance it was shown that in 2D, $\mathcal{N} = 2$ non-linear sigma models with *both* chiral and twisted chiral supermultiplets the geometry of the associated target space manifolds are non-Riemannian and contain torsion. This latter result is impossible within the context of sigma-models constructed *solely* from chiral supermultiplets or only twisted chiral supermultiplets alone. In fact prior to the work of [46], it was thought that all non-linear sigma-models with 2D, $\mathcal{N} = 2$ must possess a target space geometry that is Riemannian. So the work in [47] established in the physics literature, the principle of “useful inequivalence” between SUSY representations precisely by showing how this matters at the level of building actions.

The next portion of the cornerstone for our statements can be seen through the calculations in appendix B and appendix C of the work seen in [39]. This work carefully performed an analysis of the earlier work in [46] with regard to its implication for adinkras. It was explicitly rederived that the reduction of 4D, $\mathcal{N} = 1$ vector supermultiplet in [46] leads the 2D, $\mathcal{N} = 2$ twisted chiral supermultiplet in the Majorana conventions that we use to derive adinkras. Subsequently, a reduction of both the 2D, $\mathcal{N} = 2$ chiral and twisted chiral supermultiplets were shown to lead to adinkras that lie in different corrals.

Thus, the distinction of the L-matrices related to the 2D, $\mathcal{N} = 2$ chiral supermultiplet and those related 2D, $\mathcal{N} = 2$ twisted chiral supermultiplet is that the permutation quartets utilized are very different as each arises from distinct partitions of S_4 . To our knowledge, this insight into the mathematical origins of the distinctions between 2D, $\mathcal{N} = 2$ chiral and twisted chiral supermultiplets is a unique observation arising from the use of adinkras.

We thus have an example to prove that the different corrals used to construct different supermultiplets are directly related to the possibility of “useful inequivalence.” Though we are able to make this observation, we do not know the breadth to which this relationship is realized. This is a topic for future study.

6 Expanding by including complements for the Coxeter group BC_4 quartets

At this stage, we have distributed all of the elements of BC_4 among the partitions. This, however, does not saturate the number of adinkras that were found by the code enabled search. There are more quartets whose existence is due to “complement flips.” In order to define “complement flips,” it is first convenient to define “complement pairs” of “Boolean Factors.’ Given a “Boolean Factor” $(\#)_b$, its complement is given by $(15 - \#)_b$. In order to illustrate this, a few examples suffice. The contents of this section have appeared previously [42], however, for the sake of the convenience of the reader, we include these here.

As we have already described, it takes a quartet of “Boolean Factor” to construct a representation of the Garden Algebra. We now make an observation.

If a specified “Boolean Factor” quartet (together with a permutation partition) satisfies the Garden Algebra, then replacing any of the “Boolean Factors” by their complements leads to another “Boolean Factor” quartet that satisfies the Garden Algebra.

Let us illustrate the import of this by examining the “Boolean Factor” quartet $\{(0)_b, (6)_b, (12)_b, (10)_b\}$ and all of its “Boolean Factor” quartet complements shown below.

$$\begin{aligned}
 & \{(0)_b, (6)_b, (12)_b, (10)_b\} : \\
 & \{(0)_b, (6)_b, (12)_b, (5)_b\}, \{(0)_b, (6)_b, (3)_b, (5)_b\}, \{(0)_b, (6)_b, (3)_b, (10)_b\} , \\
 & \{(0)_b, (9)_b, (12)_b, (5)_b\}, \{(0)_b, (9)_b, (3)_b, (5)_b\}, \{(0)_b, (9)_b, (3)_b, (10)_b\} , \\
 & \{(0)_b, (9)_b, (12)_b, (10)_b\}, \{(15)_b, (9)_b, (12)_b, (5)_b\}, \{(15)_b, (9)_b, (3)_b, (5)_b\} , \\
 & \{(15)_b, (9)_b, (3)_b, (10)_b\}, \{(15)_b, (9)_b, (12)_b, (10)_b\}, \{(15)_b, (9)_b, (12)_b, (5)_b\} , \\
 & \{(15)_b, (6)_b, (3)_b, (5)_b\}, \{(15)_b, (6)_b, (3)_b, (10)_b\}, \{(15)_b, (6)_b, (12)_b, (10)_b\} . \tag{6.1}
 \end{aligned}$$

On the first line of this expression we have the specified “Boolean Factor” quartet and under this we list all of its “Boolean Factor” quartet complements.

For the first listed complement, only the fourth “Boolean Factor” entry or the “fourth color” was replaced by its complement. This is what is meant by a single “color flip.” For the second listed complement, the third and fourth “Boolean Factor” entries or the “third color” and “fourth color” were replaced by their complements. This is what is meant by “flipping” two colors. For the third listed complement, only the third “Boolean Factor” entry or the “third color” was replaced by its complement. This is again a “flipping” of one color.

Concentrating now once more only on the “Boolean Factor” quartet $\{(0)_b, (6)_b, (12)_b, (10)_b\}$, we can see among the complements one is related to it in a special manner. The complement “Boolean Factor” quartet $\{(15)_b, (9)_b, (3)_b, (5)_b\}$ has all four of its colors flipped with respect to the initial “Boolean Factor” quartet. Thus we call $\{(0)_b, (6)_b, (12)_b, (10)_b\}$

and $\{(15)_b, (9)_b, (3)_b, (5)_b\}$ antipodal “Boolean Factor” quartet pairs. Among the sixteen “Boolean Factor” quartets shown in (6.1) eight such pairs occur. Thus, for each value of α , one must specify which of the complements is used to construct and L-matrix. For this purpose, we use an index β_a which takes on eight values.

Given two quartets $(L_I^{(\mathcal{R})})_{i^{\hat{j}}}$ and $(L_I^{(\mathcal{R}')})_{i^{\hat{j}}}$ where the elements in the second set are related to the first by replacing at least one “Boolean Factor” by its complement, there exist a 4×4 “Boolean Factor” matrix denoted by $[\mathcal{A}(\mathcal{R}, \mathcal{R}')]_{I^J}$ which acts on the color space of the links (i.e. the indices of the I, J, \dots type) such that

$$(L_I^{(\mathcal{R})})_{i^{\hat{j}}} = [\mathcal{A}(\mathcal{R}, \mathcal{R}')]_{I^J} (L_J^{(\mathcal{R}')})_{i^{\hat{j}}} , \quad (6.2)$$

and as a consequence of (6.2) we see

$$(R_I^{(\mathcal{R})})_{\hat{j}^i} = [\mathcal{A}(\mathcal{R}, \mathcal{R}')]_{I^J} (R_J^{(\mathcal{R}')})_{\hat{j}^i} . \quad (6.3)$$

It should also be noted that the definition of the complements imply that the representations \mathcal{R}' and \mathcal{R} that appear in (6.2) and (6.3) must belong to the same partition sector shown in diagram shown in figure 2. The equations in (2.3), (6.2) and (6.3) imply

$$\begin{aligned} \ell_{IJ}^{(\mathcal{R})\hat{a}} &= [\mathcal{A}(\mathcal{R}, \mathcal{R}')]_{I^K} [\mathcal{A}(\mathcal{R}, \mathcal{R}')]_{J^L} \ell_{KL}^{(\mathcal{R}')\hat{a}} \\ \tilde{\ell}_{IJ}^{(\mathcal{R})\hat{a}} &= [\mathcal{A}(\mathcal{R}, \mathcal{R}')]_{I^K} [\mathcal{A}(\mathcal{R}, \mathcal{R}')]_{J^L} \tilde{\ell}_{KL}^{(\mathcal{R}')\hat{a}} . \end{aligned} \quad (6.4)$$

Let us observe the distinction between the Boolean quartet factors that appear in (B.1)–(B.6) and all of their complements is not intrinsic, but is an artifact of the choices made to discuss this aspect of the construction. It may be possible to provide a more symmetrical treatment of the (B.1)–(B.6) and all of their complements. However, we have not been able to create such a formulation.

Now the meaning of the “representation label,” first written in (2.1), can be explicitly discussed. Each value of \mathcal{R} corresponds to a specification of the pairs of indices $(\Lambda, \alpha|\beta_a)$. This implies there are $6 \times 16 \times 8 = 6 \times 128 = 768$ quartets which satisfy the Garden Algebra conditions. Notice that $1,536/762 = 2$ which shows the algorithmic counting did not remove antipodal “Boolean Factor” quartets.

Let us observe that the Λ in the paragraph denotes to which partition the element resides, the α label denotes which of the Boolean Factors identified in the work of [44], and finally $\alpha|\beta_a$ denotes the complementary Boolean Factors listed in appendix B. The order in which the Boolean Factor appears within each quartet matters and the $\alpha|\beta_a$ label indicates the order from the results listed in this appendix.

Finally, let us note all discussions in this section are totally disconnected from considerations of four dimensional supersymmetry representations. We have simply enunciated the rich mathematical structure imposed on the Coxeter Group BC_4 when analyzed through the lens of the “Garden Algebra” $\mathcal{GR}(4,4)$.

7 Expanding to ordered Coxeter group BC_4 quartets

The discussion in the preceding sections (and all our previous works) only considered the quartets without consideration of the order in which the permutations appeared with the

quartets. In this subsequent discussion we will explore which feature are modified when consideration of ordered quartets is undertaken. There are more quartets whose existence is due to “color flips.” In order to define “color flips,” let us make note of the previous assumptions used through the analysis so far.

However, what these multiplication tables imply is the existence of thirty permutation operators $\mathbf{\Pi}_1, \dots, \mathbf{\Pi}_{30}$ defined to act on the quartet entries such that

$$\begin{aligned}
 (12) \{\mathcal{V}_{(4)}\} &= \mathbf{\Pi}_1[(34) \{\mathcal{V}_{(4)}\}] = \mathbf{\Pi}_2[(1324) \{\mathcal{V}_{(4)}\}] = \mathbf{\Pi}_3[(1423) \{\mathcal{V}_{(4)}\}], \\
 (13) \{\mathcal{V}_{(4)}\} &= \mathbf{\Pi}_4[(24) \{\mathcal{V}_{(4)}\}] = \mathbf{\Pi}_5[(1234) \{\mathcal{V}_{(4)}\}] = \mathbf{\Pi}_6[(1432) \{\mathcal{V}_{(4)}\}], \\
 (14) \{\mathcal{V}_{(4)}\} &= \mathbf{\Pi}_7[(23) \{\mathcal{V}_{(4)}\}] = \mathbf{\Pi}_8[(1243) \{\mathcal{V}_{(4)}\}] = \mathbf{\Pi}_9[(1342) \{\mathcal{V}_{(4)}\}], \\
 (123) \{\mathcal{V}_{(4)}\} &= \mathbf{\Pi}_{10}[(134) \{\mathcal{V}_{(4)}\}] = \mathbf{\Pi}_{11}[(142) \{\mathcal{V}_{(4)}\}] = \mathbf{\Pi}_{12}[(243) \{\mathcal{V}_{(4)}\}], \\
 (124) \{\mathcal{V}_{(4)}\} &= \mathbf{\Pi}_{13}[(132) \{\mathcal{V}_{(4)}\}] = \mathbf{\Pi}_{14}[(143) \{\mathcal{V}_{(4)}\}] = \mathbf{\Pi}_{15}[(234) \{\mathcal{V}_{(4)}\}]. \quad (7.1)
 \end{aligned}$$

$$\begin{aligned}
 \{\mathcal{V}_{(4)}\} (12) &= \mathbf{\Pi}_{16}[\{\mathcal{V}_{(4)}\} (34)] = \mathbf{\Pi}_{17}[\{\mathcal{V}_{(4)}\} (1324)] = \mathbf{\Pi}_{18}[\{\mathcal{V}_{(4)}\} (1423)], \\
 \{\mathcal{V}_{(4)}\} (13) &= \mathbf{\Pi}_{19}[\{\mathcal{V}_{(4)}\} (24)] = \mathbf{\Pi}_{20}[\{\mathcal{V}_{(4)}\} (1234)] = \mathbf{\Pi}_{21}[\{\mathcal{V}_{(4)}\} (1432)], \\
 \{\mathcal{V}_{(4)}\} (14) &= \mathbf{\Pi}_{22}[\{\mathcal{V}_{(4)}\} (23)] = \mathbf{\Pi}_{23}[\{\mathcal{V}_{(4)}\} (1243)] = \mathbf{\Pi}_{23}[\{\mathcal{V}_{(4)}\} (1342)], \\
 \{\mathcal{V}_{(4)}\} (123) &= \mathbf{\Pi}_{25}[\{\mathcal{V}_{(4)}\} (134)] = \mathbf{\Pi}_{26}[\{\mathcal{V}_{(4)}\} (142)] = \mathbf{\Pi}_{27}[\{\mathcal{V}_{(4)}\} (243)], \\
 \{\mathcal{V}_{(4)}\} (124) &= \mathbf{\Pi}_{28}[\{\mathcal{V}_{(4)}\} (132)] = \mathbf{\Pi}_{29}[\{\mathcal{V}_{(4)}\} (143)] = \mathbf{\Pi}_{30}[\{\mathcal{V}_{(4)}\} (234)]. \quad (7.2)
 \end{aligned}$$

It is instructive to illustrate the action of the $\mathbf{\Pi}$ -operators. As they are permutations also, cycle notation can be used to denote them. The $\mathbf{\Pi}$ -operator $(\mathbf{34})_q$ can be apply to the quartet set $\{\mathcal{V}_{(4)}\}$ where we find

$$\begin{aligned}
 (\mathbf{34})_q \{\mathcal{V}_{(4)}\} &= (\mathbf{34})_q \{(), (12)(34), (13)(24), (14)(23)\} \\
 &= \{(), (12)(34), (14)(23), (13)(24)\}. \quad (7.3)
 \end{aligned}$$

As there is no need to find the explicit forms of all the $\mathbf{\Pi}$ -operators, we dispense with further discussion on this. The important point about these equations is that they show even if ordered quartets of elements are considered, the notion of the six⁸ “corrals” continues to have a mathematically well defined meaning.

In light of the results for the Gadget matrix elements reported in section 2, we believe working out one explicit example will demonstrate both the use of complements as well as the use of the $\mathbf{\Pi}$ -operator.s⁹ Let us arbitrarily pick the $\{\mathcal{P}_{[3]}\}$ corral as well as the fifteenth of the appropriate Boolean Factors in (B.3) so that we have

$$\begin{array}{cccc}
 \mathbf{L}_1 & \mathbf{L}_2 & \mathbf{L}_3 & \mathbf{L}_4 \\
 \{\mathcal{P}_{[3]}\} &= \{(1243), (23), (14), (1342)\}, & & (7.4)
 \end{array}$$

and as well

$$\mathbf{S}_{\mathcal{P}_3}[15] = \{(14)_b, (2)_b, (8)_b, (4)_b\}. \quad (7.5)$$

⁸We continue to include the corral defined by $\{\mathcal{V}_{(4)}\}$ itself.

⁹We here acknowledge conversations with K. Iga who first gave arguments on the importance of this case.

Thus we are led to

$$\begin{aligned} \mathbf{L}(\mathcal{S}_{\mathcal{P}_3[15]} \cdot \mathcal{P}_{[3]}) &= (\{(14)_b, (2)_b, (8)_b, (4)_b\} \cdot \{(1243), (23), (14), (1342)\}) \\ &= \{(14)_b(1243), (2)_b(23), (8)_b(14), (4)_b(1342)\}, \end{aligned} \quad (7.6)$$

and we can apply the Π -operator that interchanges the final two entries of the quartet. We can also use cycle-notation to indicate this to obtain

$$\mathbf{L}[(\mathbf{34})_q(\mathcal{S}_{\mathcal{P}_3[15]} \cdot \mathcal{P}_{[3]})] = \{(14)_b(1243), (2)_b(23), (4)_b(1342), (8)_b(14)\}. \quad (7.7)$$

Finally we apply the complement flip $(2 \leftrightarrow 13)_b$ that switches $(2)_b$ with $(13)_b$ to obtain

$$\mathbf{L}[(2 \leftrightarrow 13)_b(\mathbf{34})_q(\mathcal{S}_{\mathcal{P}_3[15]} \cdot \mathcal{P}_{[3]})] = \{(14)_b(1243), (13)_b(23), (4)_b(1342), (8)_b(14)\}, \quad (7.8)$$

and as a way to write a more compact notation we introduce with $(13)_b$ to obtain

$$\widehat{\mathbf{L}}[(\mathcal{S}_{\mathcal{P}_3[15]} \cdot \mathcal{P}_{[3]})] \equiv \mathbf{L}[(2 \leftrightarrow 13)_b(\mathbf{34})_q(\mathcal{S}_{\mathcal{P}_3[15]} \cdot \mathcal{P}_{[3]})], \quad (7.9)$$

and this yields

$$\begin{aligned} \widehat{\mathbf{L}}_1(\mathcal{S}_{\mathcal{P}_3[15]} \cdot \mathcal{P}_{[3]}) &= \begin{bmatrix} 0 & 1 & 0 & 0 \\ 0 & 0 & 0 & -1 \\ -1 & 0 & 0 & 0 \\ 0 & 0 & -1 & 0 \end{bmatrix}, & \widehat{\mathbf{L}}_2(\mathcal{S}_{\mathcal{P}_3[15]} \cdot \mathcal{P}_{[3]}) &= \begin{bmatrix} -1 & 0 & 0 & 0 \\ 0 & 0 & 1 & 0 \\ 0 & -1 & 0 & 0 \\ 0 & 0 & 0 & -1 \end{bmatrix}, \\ \widehat{\mathbf{L}}_3(\mathcal{S}_{\mathcal{P}_3[15]} \cdot \mathcal{P}_{[3]}) &= \begin{bmatrix} 0 & 0 & 1 & 0 \\ 1 & 0 & 0 & 0 \\ 0 & 0 & 0 & -1 \\ 0 & 1 & 0 & 0 \end{bmatrix}, & \widehat{\mathbf{L}}_4(\mathcal{S}_{\mathcal{P}_3[15]} \cdot \mathcal{P}_{[3]}) &= \begin{bmatrix} 0 & 0 & 0 & 1 \\ 0 & 1 & 0 & 0 \\ 0 & 0 & 1 & 0 \\ -1 & 0 & 0 & 0 \end{bmatrix}. \end{aligned} \quad (7.10)$$

These lead to fermionic holonomy matrices based on the $\widehat{\mathbf{L}}$ function to be given by

$$\begin{aligned} \widetilde{\mathbf{V}}_{12}[\widehat{\mathbf{L}}(\mathcal{S}_{\mathcal{P}_1[15]} \cdot \mathcal{P}_{[1]})] &= +\widetilde{\mathbf{V}}_{34}[\widehat{\mathbf{L}}(\mathcal{S}_{\mathcal{P}_1[15]} \cdot \mathcal{P}_{[1]})] = \alpha^2, \\ \widetilde{\mathbf{V}}_{13}[\widehat{\mathbf{L}}(\mathcal{S}_{\mathcal{P}_1[15]} \cdot \mathcal{P}_{[1]})] &= -\widetilde{\mathbf{V}}_{24}[\widehat{\mathbf{L}}(\mathcal{S}_{\mathcal{P}_1[15]} \cdot \mathcal{P}_{[1]})] = \alpha^1, \\ \widetilde{\mathbf{V}}_{14}[\widehat{\mathbf{L}}(\mathcal{S}_{\mathcal{P}_1[15]} \cdot \mathcal{P}_{[1]})] &= +\widetilde{\mathbf{V}}_{23}[\widehat{\mathbf{L}}(\mathcal{S}_{\mathcal{P}_1[15]} \cdot \mathcal{P}_{[1]})] = -\alpha^3. \end{aligned} \quad (7.11)$$

Using the formula in (2.4) and picking the two representations to be $(\mathcal{R}) = (\mathcal{S}_{\mathcal{P}_1[12]} \cdot \mathcal{P}_{[1]})$ and $(\mathcal{R}') = \widehat{\mathbf{L}}(\mathcal{S}_{\mathcal{P}_1[15]} \cdot \mathcal{P}_{[3]})$ leads to

$$\begin{aligned} \mathcal{G}[(\mathcal{R}), (\mathcal{R}')] &= \frac{1}{24} \text{Tr} \left[\widetilde{\mathbf{V}}_{12}(\mathcal{S}_{\mathcal{P}_1[12]} \cdot \mathcal{P}_{[1]}) \widetilde{\mathbf{V}}_{12}[\widehat{\mathbf{L}}(\mathcal{S}_{\mathcal{P}_1[15]} \cdot \mathcal{P}_{[1]})] \right. \\ &\quad + \widetilde{\mathbf{V}}_{34}(\mathcal{S}_{\mathcal{P}_1[12]} \cdot \mathcal{P}_{[1]}) \widetilde{\mathbf{V}}_{34}[\widehat{\mathbf{L}}(\mathcal{S}_{\mathcal{P}_1[15]} \cdot \mathcal{P}_{[1]})] \\ &\quad + \widetilde{\mathbf{V}}_{13}(\mathcal{S}_{\mathcal{P}_1[12]} \cdot \mathcal{P}_{[1]}) \widetilde{\mathbf{V}}_{13}[\widehat{\mathbf{L}}(\mathcal{S}_{\mathcal{P}_1[15]} \cdot \mathcal{P}_{[1]})] \\ &\quad + \widetilde{\mathbf{V}}_{24}(\mathcal{S}_{\mathcal{P}_1[12]} \cdot \mathcal{P}_{[1]}) \widetilde{\mathbf{V}}_{24}[\widehat{\mathbf{L}}(\mathcal{S}_{\mathcal{P}_1[15]} \cdot \mathcal{P}_{[1]})] \\ &\quad + \widetilde{\mathbf{V}}_{14}(\mathcal{S}_{\mathcal{P}_1[12]} \cdot \mathcal{P}_{[1]}) \widetilde{\mathbf{V}}_{14}[\widehat{\mathbf{L}}(\mathcal{S}_{\mathcal{P}_1[15]} \cdot \mathcal{P}_{[1]})] \\ &\quad \left. + \widetilde{\mathbf{V}}_{23}(\mathcal{S}_{\mathcal{P}_1[12]} \cdot \mathcal{P}_{[1]}) \widetilde{\mathbf{V}}_{23}[\widehat{\mathbf{L}}(\mathcal{S}_{\mathcal{P}_1[15]} \cdot \mathcal{P}_{[1]})] \right] \\ &= \frac{1}{24} \text{Tr} \left[\alpha^2 \alpha^2 + \alpha^2 \alpha^2 + \alpha^3 \alpha^1 + \alpha^3 \alpha^1 - \alpha^1 \alpha^3 - \alpha^1 \alpha^3 \right] \\ &= \frac{1}{24} [4 + 4 + 0 + 0 - 0 - 0] = \frac{1}{3}, \end{aligned} \quad (7.12)$$

which is one of the allowed values over the $36,864 \times 36,864$ matrix elements. One can trace back through the calculation that it is the insertion of the Π -operator in the quartet that is responsible for the appearances of the traces $\text{Tr} [\alpha^1 \alpha^3]$ on the penultimate line in this calculation.

8 A counting intermezzo

It is useful here to step back and do a bit of counting to clearly see the magnitude of the task of calculating every matrix element that arises (2.4) or (2.8) from all possible choices of the adinkra representations (\mathcal{R}) and (\mathcal{R}').

```

BC4 Contains 384 Elements
leads to 96 unordered quartets
leads to 2,304 ordered quartets
Diadem Separation Divides By Six
leads to 16 unordered quartets/corral
leads to 384 ordered quartets/corral
Complements Multiply By Sixteen
leads to 256 unordered quartets/corral
leads to 6,144 ordered quartets/corral
Total Summing Over All Corrals
1,536 total unordered quartets
36,864 total ordered quartets
=====
36,864 x 36,864 = 1,358,954,496
Sym[36,864 x 36,864] = 679,495,680

```

So the task of calculating (2.4) or (2.8) corresponds to calculating 1,358,954,496 matrix elements or given the fact that the Gadget is symmetrical 679,495,680 matrix elements.

Before the era of modern computing technology, to carry out such a multitude of calculations was simply impossible. In the next section, the codes that were developed to tackle this problem are described. The approach was to develop four different codes, using different languages, to attack the problem over the “small BC_4 library.” As these were each developed independently, we relied on the consensus of final results to de-bug any errors that may have occurred. This was successfully done to carry out the evaluation of the 9,216 matrix elements of the 96×96 Gadget values over the “small BC_4 library” of representations. These results were graphically shown in figure 3 and are analytically reported in the tables of appendix D.

9 The codes

9.1 Program, libraries.py

The Program, libraries.py, First uses the numpy library to create 2 5D nested arrays `lib` and `libtil` to store the values of $\ell_{nm}^{(i)j}$ and $\tilde{\ell}_{nm}^{(i)j}$ respectively.

When the Latex document containing the libraries is properly formatted(in the style of the file provided), the program will iterate though all the libraries \mathcal{P}_k in the file and store all ℓ and $\tilde{\ell}$ values into `lib[k][i][n][m][j]` and `libtil[k][i][n][m][j]`.

The main loop then iterates though all ℓ values in all dictionaries and calculates all the gadgets, $\mathcal{G}[\mathcal{R}, \mathcal{R}']$, using the function `gadget(r,rprime,lr,lrprime)` it takes as input the following parameters. `r`: the \mathcal{R} value. `rprime`: the \mathcal{R}' value. `lr`: the library number for the \mathcal{R} value(k) and `lrprime` the library number for the \mathcal{R}' value and uses them to compute the gadget.

After finishing the gadget calculations other contributors completed other pieces of software using a different format of for displacing the gadget, using `r` and `rprime` values ranging all the way up to 96 instead of ranging to 16 and being associated a dictionary number. As a sanity check it became necessary to confirm all programs produced the same gadget values. This was done in a section of code commented out prior to publication in this program. In order to allow other contributors to do the same the method of printing the gadget values to a file was adapted to list gadgets calculated with `r` and `rprime` values ranging up to 96. In order to accomplish this with the existing `gadget` function the following loop was utilized in the main function.

```

hori=1
verti=1
for vertc in range(1,97):
    for horc in range(1,97):
        f.write(str(gadget(vertc-(verti-1)*16,horc-(hori-1)*16,verti,hori))+",")
        if(horc%16==0):
            hori+=1
        hori=1
        if(vertc%16==0):
            verti+=1
        f.write("\n")

```

The values of the gadget are then written to the file object `f` which will write to a csv spreadsheet file.

Additional Documentation is provided in the comments embedded into `libraries.py`.

9.2 C++ code to calculate gadget values given $\ell/\tilde{\ell}$ coefficients

This code takes an input file ‘data.txt’ containing the ℓ and $\tilde{\ell}$ coefficients which the gadget may be calculated with by summing over the coefficients related to a specific pair (\mathcal{R}), (\mathcal{R}') of adinkras that are related by the gadget value. The code will then output a 96×96 array of gadget values into ‘results.txt.’ In order to do this calculation, the code makes use of the fact that many of the ℓ and $\tilde{\ell}$ values are 0 and has a look up function to either return 0 or the $\ell/\tilde{\ell}$ value that is provided in the ‘data.txt’ input file.

```

#include <ios t ream>
#include <f s t ream>
#include <s t r ing>

using namespace std;

int neg(int n) {if(n == 0) return 1; else return 0;}

```

```

        // "negates" integer values as if they were booleans
int lookup(int r, int l, int a, int arr[96][7])
//Returns the desired l-value to be used in the gadget calculation
{
    if(l == 0) //L12
    {
        if (a != 2) return 0;
        else return neg(arr[r][0])*arr[r][1];
    }
    else if (l == 1) //L13
    {
        if(a != 3) return 0;
        else return neg(arr[r][0])*arr[r][2];
    }
    else if(l == 2) //L14
    {
        if (a != 1) return 0;
        else return neg(arr[r][0])*arr[r][3];
    }
    else if(l == 3) //L23
    {
        if (a != 1) return 0;
        else return neg(arr[r][0])*arr[r][4];
    }
    else if(l == 4) //L24
    {
        if (a != 3) return 0;
        else return neg(arr[r][0])*arr[r][5];
    }
    else if(l == 5) //L34
    {
        if(a != 2) return 0;
        else return neg(arr[r][0])*arr[r][6];
    }
    else if(l == 6) //~L12
    {
        if(a != 3) return 0;
        else return arr[r][0]*arr[r][1];
    }
    else if(l == 7) //~L13
    {
        if(a != 2) return 0;
        else return arr[r][0]*arr[r][2];
    }
    else if(l == 8) //~L14
    {
        if(a != 1) return 0;
        else return arr[r][0]*arr[r][3];
    }
    else if(l == 9) //~L23
    {
        if(a != 1) return 0;
        else return arr[r][0]*arr[r][4];
    }
    else if(l == 10) //~L24
    {
        if(a != 2) return 0;
        else return arr[r][0]*arr[r][5];
    }
    else if(l == 11) //~L34

```

```

    {
        if(a != 3) return 0;
        else return arr[r][0]*arr[r][6];
    }
}

double g(int n, int m, int arr[96][7])
{
    // This method will return the correct value for the G function with r = n, and r' = m
    double result = 0;
    for(int a = 1; a <= 3; a++) for(int l = 0; l < 12; l++)
        result += lookup(n, l, a, arr)*lookup(m, l, a, arr);
    return result/6;
}

void read(std::fstream& data, int arr[96][7])
{
    // This method will read data into the arr in the proper format
    for(int i = 0; i < 96; i++) for(int j = 0; j < 7; j++) data << arr[i][j];
}

int main()
{
    // This method will calculate the gadget values and put them in "results.txt"
    string line;
    int n, m;
    int arr[96][7];
    std::fstream data("data.txt");
    std::fstream results("results.txt");
    if(data.is_open())
    {
        read(data, arr);
        data.close();
    } else cout << "error: unable to open data file";
    if(results.is_open())
    {
        for(n=0;n<96;n++) {for(m=0;m<96;m++) results << g(n,m,arr) << "\t"; results << "\n";}
        cout << "Calculated gadgets";
    }
    else cout << "error: unable to open results file";
    return 0;
}

```

9.3 MATLAB program

The MATLAB program for calculating values of the Gadget from the “small” BC_4 library is composed of two elements: the function “GFunction.m” and the script “GadgetCalculationCode.m”. The Excel file “Computational Project Data Full.xlsm”, which contains the BC_4 library arranged properly for the code, is also required.

The function “GFunction.m” performs the operation described in equation (2.8). It takes as input the two indexes (\mathcal{R}) and (\mathcal{R}'), as well as two data arrays labeled L1 and L2 which contain the ℓ and $\tilde{\ell}$ library elements respectively. It outputs the value of the Gadget element indexed by (\mathcal{R}) and (\mathcal{R}'). In explaining this code’s calculation process, it is best to begin with the result in (2.8).

The calculation is considerably simplified by taking advantage of a helpful property of the “small” BC_4 library. For all values of index (\mathcal{R}) within the set of a single given value of index IJ , there is only a single value of index \hat{a} with nonzero library elements. For example, for $IJ = 1$ (representing subscript 12), all nonzero ℓ values have index $\hat{a} = 2$, while all nonzero $\tilde{\ell}$ values have index $\hat{a} = 3$. Similar patterns are observed to hold for all six index IJ values within this library.

Taking advantage of this property, the data sets L1 and L2 contain only the library values with the appropriate \hat{a} index for each corresponding IJ value. This allowed all library elements necessary for calculating elements of G to be described by only two indexes. In the L1 and L2 arrays, superscript index (\mathcal{R}) is contained in the row number of each cell, and subscript index IJ is contained in the column number. With these arrays, the Gadget calculation is reduced to only a single summation over the “hatted a ” values.

This is the form of the equation utilized by “GFunction.m” in calculating the Gadget element for given (\mathcal{R}) and (\mathcal{R}') . In order to carry out this calculation, the function first establishes a 6-element vector named “subGadget”. The IJ^{th} entry of subGadget is then determined by performing $l_{IJ}^{(\mathcal{R})} * l_{IJ}^{(\mathcal{R}')} + \tilde{l}_{IJ}^{(\mathcal{R})} * \tilde{l}_{IJ}^{(\mathcal{R}')}$, as IJ is looped from 1 through 6. Lastly, all six elements of subGadget are summed up, and the sum is multiplied by $1/6$ to produce the Gadget element. This is the standard procedure for summing over an index in MATLAB.

The script “GadgetCalculationCode.m” runs the function “GFunction.m” for all $96*96$ combinations of (\mathcal{R}) and (\mathcal{R}') , to produce the Gadget matrix. It begins by defining L1 and L2 using data imported from the Excel file “Computational Project Data Full.xlsm”. It next establishes a $96 * 96$ matrix named “Result”. Each element $((\mathcal{R}), (\mathcal{R}'))$ of matrix “Result” is determined by running “GFunction.m” with (\mathcal{R}) and (\mathcal{R}') as input. To reduce computation time, following the calculation of each $((\mathcal{R}), (\mathcal{R}'))$ element, the corresponding element at coordinate $((\mathcal{R}'), (\mathcal{R}))$ is subsequently filled in with the same value. This is permitted, as the Gadget matrix is symmetric over switching (\mathcal{R}) and (\mathcal{R}') .

At the end of the computation, the matrix “Result” is the Gadget matrix, fully calculated for the “small” BC_4 library. Additionally, the script counts the number of times each that the values 1, 0, and $-1/3$ are found in the Gadget. The Gadget matrix and the three value counts are saved as variables in the MATLAB workspace each time the script is run, where they can be easily retrieved and exported to Excel or similar data visualization programs.

9.4 Mathematica-Gadget Code.nb

The purpose of this Mathematica code is to calculate all values of the Gadget, as defined in (2.8), given the ℓ and $\tilde{\ell}$ values of the, “small” BC_4 library in appendix B. Gadget Code.nb is broken up into 9 distinct annotated sections each performing a set of steps toward achieving this goal.

The code begins by clearing all associations. In order for Mathematica to store the ℓ and $\tilde{\ell}$ values from the library in appendix B, a data structure consisting of a multi-dimensional array is first constructed. It will hold all the index information pertaining to the ℓ and $\tilde{\ell}$ coefficients, as well as their values. Each ℓ and $\tilde{\ell}$ coefficient has 4 indices

associated with it, (\mathcal{R}) , \hat{a} , I and J . Depending on the values of these 4 indices an ℓ and $\tilde{\ell}$ will equal either 1, -1, or 0. The ℓ s and $\tilde{\ell}$ s which equal 0 are not shown in the appendix B library. Two arrays of dimension $6 \times 3 \times 96 \times 1$ are constructed to support all ℓ and $\tilde{\ell}$ coefficients. The ℓ s are mapped to variable L1 as a function of n , a , and $r1$ as part of one array, and the $\tilde{\ell}$ s are mapped to variable L2 as a function of n , a , and $r2$ as part of the another array. The \hat{a} index maps to the variable a , with values 1 through 3. The (\mathcal{R}) index maps to the variables $r1$ and $r2$, with values 1 through 96, $r1$ being associated with the L1 matrix and $r2$ being associated with the L2 matrix. In the appendix B library each of the ℓ and $\tilde{\ell}$ values are grouped into 6 \mathbf{P} permutation sets of (\mathcal{R}) 1 to 16, in this code (\mathcal{R}) is counted from 1 to 96, simplifying encoding which \mathbf{P} set the ℓ or $\tilde{\ell}$ coefficient is associated with. Additionally, to further simplify things, because I and J appear in the same 6 pairs 12, 13, 14, 23, 24, 34, the code interprets IJ as one variable, n , with values 1 through 6. Each ℓ or $\tilde{\ell}$ is represented in its corresponding L1 or L2 array such that the first 3 dimensions of the multi-dimensional array encode its n , a , $r1$ or $r2$ index values respectively. The goal is to be able to call for example, the 1st,2nd,30th entry in the L1, ℓ coefficient, array and return back an integer value, 1, -1, or 0, equaling that particular ℓ coefficient, given each of its specific indices as encoded by the multi-dimensional array structure. This allows Mathematica to have access to all the ℓ and $\tilde{\ell}$ values and perform the proper Gadget sum.

With the data structure now established, the data from the library must be imported into the code. In order to do this an Excel document, Data Record Structure.xlsx, was used. In this Excel document are color coded tables for each ℓ and $\tilde{\ell}$ value from the library. The tables group the values by their \mathbf{P} set and corresponding indices, as defined above. Each ℓ and $\tilde{\ell}$ value from the library was added to the Excel sheet manually, and the tables were double checked to make sure the correct values were properly located. After all library values were inserted into the tables, Excel was used to automatically add the additional 0 value ℓ and $\tilde{\ell}$ coefficients which were missing from the library but are required in this data structure. The ℓ and $\tilde{\ell}$ values were then combined into a single (\mathcal{R}) 1 to 96 group, and divided into two 2 dimensional arrays separating the tilded and non-tilded coefficients. These arrays were then copied over to 2 separate files, L1s.csv, and L2s.csv. In these .csv files the transpose of the arrays were taken and every set of three rows, associated with coefficient values that have the same IJ index, or n index in the code, were placed one after the other to the right as columns. The data from the library was now in a format with an identical structure to the one mentioned in the previous paragraph. Using Mathematica's import function these .csv files, for the ℓ and $\tilde{\ell}$ coefficients, are now imported as $6 \times 3 \times 96 \times 1$ arrays.

In the third section of the code these $6 \times 3 \times 96 \times 1$ arrays of data are defined to have the functional structure described in section 1 using Mathematica's "part" structural function. Now using the second equation on page 15, the Gadget as a function $G[(\mathcal{R}), (\mathcal{R}')]$, (\mathcal{R}) and (\mathcal{R}') from 1 to 96, is defined as 1/6-th the sum of the products of the L1 and L2 array coefficients, with n from 1 to 6, and a from 1 to 3. A test value for the Gadget of $(\mathcal{R}) = 1$ and $(\mathcal{R}') = 34$ is checked to make sure the result is reasonable. Then in order to calculate all 96×96 Gadget values for the "small" BC_4 case, using the Array function in Mathematica,

the Gadget function is mapped onto a 96 by 96 matrix where each $i^{th} j^{th}$ element is the corresponding $G(i^{th}, j^{th})$ Gadget value. The Gadget Matrix has been determined! The result is quickly checked to make sure it is a symmetric matrix and exported as a .mat file.

In order to better present the result, as seen in appendix A, the 96×96 Gadget Matrix is partitioned into a $6 \times 6 \times 16 \times 16$ multi-dimensional matrix, where each of the 36 nested 16×16 matrices correspond to the P-Matrices of the Gadget Matrix Solution. A check is done and it is determined that the P Matrices themselves are symmetric. This is no surprise as the Gadget Matrix solution itself was symmetric. Given the symmetry of the P-Matrices only 21 of the 36 total, the Upper Triangular result of the Matrices in the P-Matrix array, need be presented in order to give the full result as is seen in appendix A. In the last section of code some interesting values of the Gadget Matrix are calculated, revealing the 3 unique elements of the Gadget Matrix, how many of each there are, and how many there are as a fraction of the total number of values.

10 Conclusion

Among the main results of this work are those that were shown in table 1 and summarized in the formula immediately below table 1. Therefore, we state our main result in the form of a mathematical conjecture.

Summary of the Minimal Four-Color Gadget Conjecture:

Let (\mathcal{R}) and (\mathcal{R}') denote any four color adinkra graphs associated with the Coxeter Group \mathbf{BC}_4 . To each such graph, there exist six associated matrices called “fermionic holonomy matrices” denoted by $\tilde{\mathbf{V}}_{\mathbf{IJ}}^{(\mathcal{R})}$ and computed from closed four-cycles in the specified graph. The adinkra Gadget values between all pairs of representations (\mathcal{R}) and (\mathcal{R}') , given by

$$\mathcal{G}[(\mathcal{R}), (\mathcal{R}')] = \left[\frac{1}{48} \right] \sum_{\mathbf{I}, \mathbf{J}} \text{Tr} \left[\tilde{\mathbf{V}}_{\mathbf{IJ}}^{(\mathcal{R})} \tilde{\mathbf{V}}_{\mathbf{IJ}}^{(\mathcal{R}')} \right],$$

defines a matrix over the space of representations such that the meromorphic “Summary of the Gadget” function

$$\mathcal{S}_{\mathcal{G}}(z) = \frac{1}{z^{p_1} \left(z + \frac{1}{3}\right)^{p_2} \left(z - \frac{1}{3}\right)^{p_3} (z - 1)^{p_4}},$$

$$p_1 = 1,132,462,080, \quad p_2 = 127,401,984,$$

$$p_3 = 84,934,656, \quad p_4 = 14,155,776,$$

has the following properties:

- (a.) the sum of the exponents equals to the square of 36,864, i.e. the rank of this matrix,*
- (b.) the poles of this function are the only non-vanishing entries that appear in this matrix, and*

(c.) *the exponent associated with each pole is the multiplicity with which the value of the pole appears in this matrix.*

We state this as a conjecture but recognizing the computations that underlie this paper constitute an exhaustive proof by construction, unless there is an error in either our reasoning or in our codes. Currently we know of no analytical way to go from the graph theoretic definition of adinkras with four colors, four open nodes, and four closed nodes to these results. We believe it would be an interesting mathematical challenge to create a theorem that replicates these results. Whether this “Summary of the Gadget” (i.e. $\mathcal{S}_G(z)$) function has a deeper mathematical significance is an open question. Should it be possible to create such a theorem, it potentially could extend the considerations of this work well beyond the class of adinkra graphs constructed on the foundation of BC_4 .

“Your work is going to fill a large part of your life, and the only way to be truly satisfied is to do what you believe is great work. And the only way to do great work is to love what you do. If you haven’t found it yet, keep looking. Don’t settle. As with all matters of the heart, you’ll know when you find it.”

- S. Jobs

Note added. An updated version of the Python code used for calculating all the ordered quartets/tetrads in the BC_4 Coxeter Group and for calculating the 1.3+ billion Gadget values can be obtained from the webpage below. <https://github.com/vkorotkikh/SUSY-BC4CG-36864-Adinkras-and-1.3billion-GadgetVals>.

Acknowledgments

We are grateful to recognize the contributions of Miles David Miller-Dickson, and Benedict A. Mondal for their efforts on the calculations in section four during the 2016 “Brown University Adinkra Math/Phys Hangout” (19–23 Dec. 2016).

This work was partially supported by the National Science Foundation grant PHY-1315155. Additional acknowledgment is given by F. Guyton, D.S. Kessler, S. Harmalkar, and V.A. Meszaros to the the University of Maryland Center for String & Particle Theory (CSPT), for their participation in the 2016 SSTPRS (Student Summer Theoretical Physics Research Session) program. S.J.G. acknowledges the generous support of the Provostial Visiting Professorship Program and the Department of Physics at Brown University for the very congenial and generous hospitality during the period of this work. This research was also supported in part by CSPT.

A Multiplications of $\{\mathcal{V}_{(4)}\}$ by permutation group of order four elements

In this appendix, we include tables that explicitly carry out the multiplication of the $\{\mathcal{V}_{(4)}\}$ subset by all of the elements of the permutation group of order four. The tables presented show the results for left multiplications and for right multiplications.

Cycle	()	(12)(34)	(13)(24)	(14)(23)
()	()	(12)(34)	(13)(24)	(14)(23)
(12)(34)	(12)(34)	()	(14)(23)	(13)(24)
(13)(24)	(13)(24)	(14)(23)	()	(12)(34)
(14)(23)	(14)(23)	(13)(24)	(12)(34)	()

Table 4. Multiplication of $\{\mathcal{V}_{(4)}\}$ by $\{\mathcal{V}_{(4)}\}$.

Cycle	()	(12)(34)	(13)(24)	(14)(23)
(12)	(12)	(34)	(1324)	(1423)
(13)	(13)	(1234)	(24)	(1432)
(14)	(14)	(1243)	(1342)	(23)
(23)	(23)	(1342)	(1243)	(14)
(24)	(24)	(1432)	(13)	(1234)
(34)	(34)	(12)	(1423)	(1324)

Table 5. Left multiplication of $\{\mathcal{V}_{(4)}\}$ by 2-cycles.

Cycle	()	(12)(34)	(13)(24)	(14)(23)
(123)	(123)	(134)	(243)	(142)
(124)	(124)	(143)	(132)	(234)
(132)	(132)	(234)	(124)	(143)
(134)	(134)	(123)	(142)	(243)
(142)	(142)	(243)	(134)	(123)
(143)	(143)	(124)	(234)	(132)
(234)	(234)	(132)	(143)	(124)
(243)	(243)	(142)	(123)	(134)

Table 6. Left multiplication of $\{\mathcal{V}_{(4)}\}$ by 3-cycles.

Cycle	()	(12)(34)	(13)(24)	(14)(23)
(1234)	(1234)	(13)	(1432)	(24)
(1243)	(1243)	(14)	(23)	(1342)
(1324)	(1324)	(1423)	(12)	(34)
(1342)	(1342)	(23)	(14)	(1243)
(1423)	(1423)	(1324)	(34)	(12)
(1432)	(1432)	(24)	(1234)	(13)

Table 7. Left multiplication of $\{\mathcal{V}_{(4)}\}$ by 4-cycles.

()	(12)(34)	(13)(24)	(14)(23)	Cycle
(12)	(34)	(1423)	(1324)	(12)
(13)	(1432)	(24)	(1234)	(13)
(14)	(1342)	(1243)	(23)	(14)
(23)	(1243)	(1342)	(14)	(23)
(24)	(1234)	(13)	(1432)	(24)
(34)	(12)	(1324)	(1423)	(34)

Table 8. Right multiplication of $\{\mathcal{V}_{(4)}\}$ by 2-cycles.

()	(12)(34)	(13)(24)	(14)(23)	Cycle
(123)	(243)	(142)	(134)	(123)
(124)	(234)	(143)	(132)	(124)
(132)	(143)	(234)	(124)	(132)
(134)	(142)	(243)	(123)	(134)
(142)	(134)	(123)	(243)	(142)
(143)	(132)	(124)	(234)	(143)
(234)	(124)	(132)	(143)	(234)
(243)	(123)	(134)	(142)	(243)

Table 9. Right multiplication of $\{\mathcal{V}_{(4)}\}$ by 3-cycles.

()	(12)(34)	(13)(24)	(14)(23)	Cycle
(1243)	(23)	(14)	(1342)	(1243)
(1234)	(24)	(1432)	(13)	(1234)
(1324)	(1423)	(34)	(12)	(1324)
(1342)	(14)	(23)	(1243)	(1342)
(1432)	(13)	(1234)	(24)	(1432)
(1423)	(1324)	(12)	(34)	(1423)

Table 10. Right multiplication of $\{\mathcal{V}_{(4)}\}$ by 4-cycles.

B “Fiducial” Boolean Factors

It suffices to specify the “Boolean Factors” in the same order as the permutation quartet factors appear in (5.7). Thus, for each of the six sectors we find

$$\begin{aligned}
 \mathcal{S}_{\mathcal{P}_1[\alpha]} : & \{(0)_b, (6)_b, (12)_b, (10)_b\}, \{(0)_b, (12)_b, (10)_b, (6)_b\}, \{(2)_b, (4)_b, (14)_b, (8)_b\}, \\
 & \{(2)_b, (14)_b, (8)_b, (4)_b\}, \{(4)_b, (2)_b, (8)_b, (14)_b\}, \{(4)_b, (8)_b, (14)_b, (2)_b\}, \\
 & \{(6)_b, (0)_b, (10)_b, (12)_b\}, \{(6)_b, (10)_b, (12)_b, (0)_b\}, \{(8)_b, (4)_b, (2)_b, (14)_b\}, \\
 & \{(8)_b, (14)_b, (4)_b, (2)_b\}, \{(10)_b, (6)_b, (0)_b, (12)_b\}, \{(10)_b, (12)_b, (6)_b, (0)_b\}, \\
 & \{(12)_b, (0)_b, (6)_b, (10)_b\}, \{(12)_b, (10)_b, (0)_b, (6)_b\}, \{(14)_b, (2)_b, (4)_b, (8)_b\}, \\
 & \{(14)_b, (8)_b, (2)_b, (4)_b\},
 \end{aligned}
 \tag{B.1}$$

$$\begin{aligned}
 \mathcal{S}_{\mathcal{P}_2}[\alpha] : & \{(0)_b, (10)_b, (6)_b, (12)_b\}, \{(0)_b, (12)_b, (10)_b, (6)_b\}, \{(2)_b, (8)_b, (4)_b, (14)_b\}, \\
 & \{(2)_b, (14)_b, (8)_b, (4)_b\}, \{(4)_b, (8)_b, (14)_b, (2)_b\}, \{(4)_b, (14)_b, (2)_b, (8)_b\}, \\
 & \{(6)_b, (10)_b, (12)_b, (0)_b\}, \{(6)_b, (12)_b, (0)_b, (10)_b\}, \{(8)_b, (2)_b, (14)_b, (4)_b\}, \\
 & \{(8)_b, (4)_b, (2)_b, (14)_b\}, \{(10)_b, (0)_b, (12)_b, (6)_b\}, \{(10)_b, (6)_b, (0)_b, (12)_b\}, \\
 & \{(12)_b, (0)_b, (6)_b, (10)_b\}, \{(12)_b, (6)_b, (10)_b, (0)_b\}, \{(14)_b, (2)_b, (4)_b, (8)_b\}, \\
 & \{(14)_b, (4)_b, (8)_b, (2)_b\},
 \end{aligned} \tag{B.2}$$

$$\begin{aligned}
 \mathcal{S}_{\mathcal{P}_3}[\alpha] : & \{(0)_b, (6)_b, (10)_b, (12)_b\}, \{(0)_b, (12)_b, (6)_b, (10)_b\}, \{(2)_b, (4)_b, (8)_b, (14)_b\}, \\
 & \{(2)_b, (14)_b, (4)_b, (8)_b\}, \{(4)_b, (2)_b, (14)_b, (8)_b\}, \{(4)_b, (8)_b, (2)_b, (14)_b\}, \\
 & \{(6)_b, (0)_b, (12)_b, (10)_b\}, \{(6)_b, (10)_b, (0)_b, (12)_b\}, \{(8)_b, (4)_b, (14)_b, (2)_b\}, \\
 & \{(8)_b, (14)_b, (2)_b, (4)_b\}, \{(10)_b, (6)_b, (12)_b, (0)_b\}, \{(10)_b, (12)_b, (0)_b, (6)_b\}, \\
 & \{(12)_b, (0)_b, (10)_b, (6)_b\}, \{(12)_b, (10)_b, (6)_b, (0)_b\}, \{(14)_b, (2)_b, (8)_b, (4)_b\}, \\
 & \{(14)_b, (8)_b, (4)_b, (2)_b\},
 \end{aligned} \tag{B.3}$$

$$\begin{aligned}
 \mathcal{S}_{\mathcal{P}_4}[\alpha] : & \{(0)_b, (10)_b, (12)_b, (6)_b\}, \{(0)_b, (12)_b, (6)_b, (10)_b\}, \{(2)_b, (8)_b, (14)_b, (4)_b\}, \\
 & \{(2)_b, (14)_b, (4)_b, (8)_b\}, \{(4)_b, (8)_b, (2)_b, (14)_b\}, \{(4)_b, (14)_b, (8)_b, (2)_b\}, \\
 & \{(6)_b, (10)_b, (0)_b, (12)_b\}, \{(6)_b, (12)_b, (10)_b, (0)_b\}, \{(8)_b, (2)_b, (4)_b, (14)_b\}, \\
 & \{(8)_b, (4)_b, (14)_b, (2)_b\}, \{(10)_b, (0)_b, (6)_b, (12)_b\}, \{(10)_b, (6)_b, (12)_b, (0)_b\}, \\
 & \{(12)_b, (0)_b, (10)_b, (6)_b\}, \{(12)_b, (6)_b, (0)_b, (10)_b\}, \{(14)_b, (2)_b, (8)_b, (4)_b\}, \\
 & \{(14)_b, (4)_b, (2)_b, (8)_b\},
 \end{aligned} \tag{B.4}$$

$$\begin{aligned}
 \mathcal{S}_{\mathcal{P}_5}[\alpha] : & \{(0)_b, (6)_b, (10)_b, (12)_b\}, \{(0)_b, (10)_b, (12)_b, (6)_b\}, \{(2)_b, (4)_b, (8)_b, (14)_b\}, \\
 & \{(2)_b, (8)_b, (14)_b, (4)_b\}, \{(4)_b, (2)_b, (14)_b, (8)_b\}, \{(4)_b, (14)_b, (8)_b, (2)_b\}, \\
 & \{(6)_b, (0)_b, (12)_b, (10)_b\}, \{(6)_b, (12)_b, (10)_b, (0)_b\}, \{(8)_b, (2)_b, (4)_b, (14)_b\}, \\
 & \{(8)_b, (14)_b, (2)_b, (4)_b\}, \{(10)_b, (0)_b, (6)_b, (12)_b\}, \{(10)_b, (12)_b, (0)_b, (6)_b\}, \\
 & \{(12)_b, (6)_b, (0)_b, (10)_b\}, \{(12)_b, (10)_b, (6)_b, (0)_b\}, \{(14)_b, (4)_b, (2)_b, (8)_b\}, \\
 & \{(14)_b, (8)_b, (4)_b, (2)_b\},
 \end{aligned} \tag{B.5}$$

$$\begin{aligned}
 \mathcal{S}_{\mathcal{P}_6}[\alpha] : & \{(0)_b, (6)_b, (12)_b, (10)_b\}, \{(0)_b, (10)_b, (6)_b, (12)_b\}, \{(2)_b, (4)_b, (14)_b, (8)_b\}, \\
 & \{(2)_b, (8)_b, (4)_b, (14)_b\}, \{(4)_b, (2)_b, (8)_b, (14)_b\}, \{(4)_b, (14)_b, (2)_b, (8)_b\}, \\
 & \{(6)_b, (0)_b, (10)_b, (12)_b\}, \{(6)_b, (12)_b, (0)_b, (10)_b\}, \{(8)_b, (2)_b, (14)_b, (4)_b\}, \\
 & \{(8)_b, (14)_b, (4)_b, (2)_b\}, \{(10)_b, (0)_b, (12)_b, (6)_b\}, \{(10)_b, (12)_b, (6)_b, (0)_b\}, \\
 & \{(12)_b, (6)_b, (10)_b, (0)_b\}, \{(12)_b, (10)_b, (0)_b, (6)_b\}, \{(14)_b, (4)_b, (8)_b, (2)_b\}, \\
 & \{(14)_b, (8)_b, (2)_b, (4)_b\} .
 \end{aligned} \tag{B.6}$$

The notation is designed to elicit the fact that for each choice of $\mathcal{P}_{[\Lambda]}$, with the subscript $[\Lambda]$ taking on values $[1], \dots, [6]$, there are sixteen possible choices of $\mathcal{S}_{\mathcal{P}_{[\Lambda]}}[\alpha]$ where the index α enumerates those choices taking on values $1, \dots, 16$.

C Adinkra ℓ & $\tilde{\ell}$ values over the “small BC_4 library”

In this appendix, for all of the elements of BC_4 , the explicit values of the ℓ , and $\tilde{\ell}$ coefficients which are related to each of the representation (\mathcal{R}) in the order shown in appendix C.

$\mathcal{P}_{[1]} :$	χ_o
$\ell_{12}^{(1)2} = 1$ $\ell_{13}^{(1)3} = 1$ $\ell_{14}^{(1)1} = 1$ $\ell_{23}^{(1)1} = 1$ $\ell_{24}^{(1)3} = -1$ $\ell_{34}^{(1)2} = 1$	1
$\tilde{\ell}_{12}^{(2)3} = 1$ $\tilde{\ell}_{13}^{(2)2} = 1$ $\tilde{\ell}_{14}^{(2)1} = 1$ $\tilde{\ell}_{23}^{(2)1} = -1$ $\tilde{\ell}_{24}^{(2)2} = 1$ $\tilde{\ell}_{34}^{(2)3} = -1$	-1
$\ell_{12}^{(3)2} = 1$ $\ell_{13}^{(3)3} = 1$ $\ell_{14}^{(3)1} = 1$ $\ell_{23}^{(3)1} = 1$ $\ell_{24}^{(3)3} = -1$ $\ell_{34}^{(3)2} = 1$	1
$\tilde{\ell}_{12}^{(4)3} = 1$ $\tilde{\ell}_{13}^{(4)2} = 1$ $\tilde{\ell}_{14}^{(4)1} = 1$ $\tilde{\ell}_{23}^{(4)1} = -1$ $\tilde{\ell}_{24}^{(4)2} = 1$ $\tilde{\ell}_{34}^{(4)3} = -1$	-1
$\ell_{12}^{(5)2} = 1$ $\ell_{13}^{(5)3} = 1$ $\ell_{14}^{(5)1} = 1$ $\ell_{23}^{(5)1} = 1$ $\ell_{24}^{(5)3} = -1$ $\ell_{34}^{(5)2} = 1$	1
$\tilde{\ell}_{12}^{(6)3} = 1$ $\tilde{\ell}_{13}^{(6)2} = 1$ $\tilde{\ell}_{14}^{(6)1} = 1$ $\tilde{\ell}_{23}^{(6)1} = -1$ $\tilde{\ell}_{24}^{(6)2} = 1$ $\tilde{\ell}_{34}^{(6)3} = -1$	-1
$\ell_{12}^{(7)2} = 1$ $\ell_{13}^{(7)3} = 1$ $\ell_{14}^{(7)1} = 1$ $\ell_{23}^{(7)1} = 1$ $\ell_{24}^{(7)3} = -1$ $\ell_{34}^{(7)2} = 1$	1
$\tilde{\ell}_{12}^{(8)3} = 1$ $\tilde{\ell}_{13}^{(8)2} = 1$ $\tilde{\ell}_{14}^{(8)1} = 1$ $\tilde{\ell}_{23}^{(8)1} = -1$ $\tilde{\ell}_{24}^{(8)2} = 1$ $\tilde{\ell}_{34}^{(8)3} = -1$	-1
$\tilde{\ell}_{12}^{(9)3} = 1$ $\tilde{\ell}_{13}^{(9)2} = 1$ $\tilde{\ell}_{14}^{(9)1} = 1$ $\tilde{\ell}_{23}^{(9)1} = -1$ $\tilde{\ell}_{24}^{(9)2} = 1$ $\tilde{\ell}_{34}^{(9)3} = -1$	-1
$\ell_{12}^{(10)2} = 1$ $\ell_{13}^{(10)3} = 1$ $\ell_{14}^{(10)1} = 1$ $\ell_{23}^{(10)1} = 1$ $\ell_{24}^{(10)3} = -1$ $\ell_{34}^{(10)2} = 1$	1
$\tilde{\ell}_{12}^{(11)3} = 1$ $\tilde{\ell}_{13}^{(11)2} = 1$ $\tilde{\ell}_{14}^{(11)1} = 1$ $\tilde{\ell}_{23}^{(11)1} = -1$ $\tilde{\ell}_{24}^{(11)2} = 1$ $\tilde{\ell}_{34}^{(11)3} = -1$	-1
$\ell_{12}^{(12)2} = 1$ $\ell_{13}^{(12)3} = 1$ $\ell_{14}^{(12)1} = 1$ $\ell_{23}^{(12)1} = 1$ $\ell_{24}^{(12)3} = -1$ $\ell_{34}^{(12)2} = 1$	1
$\tilde{\ell}_{12}^{(13)3} = 1$ $\tilde{\ell}_{13}^{(13)2} = 1$ $\tilde{\ell}_{14}^{(13)1} = 1$ $\tilde{\ell}_{23}^{(13)1} = -1$ $\tilde{\ell}_{24}^{(13)2} = 1$ $\tilde{\ell}_{34}^{(13)3} = -1$	-1
$\ell_{12}^{(14)2} = 1$ $\ell_{13}^{(14)3} = 1$ $\ell_{14}^{(14)1} = 1$ $\ell_{23}^{(14)1} = 1$ $\ell_{24}^{(14)3} = -1$ $\ell_{34}^{(14)2} = 1$	1
$\tilde{\ell}_{12}^{(15)3} = 1$ $\tilde{\ell}_{13}^{(15)2} = 1$ $\tilde{\ell}_{14}^{(15)1} = 1$ $\tilde{\ell}_{23}^{(15)1} = -1$ $\tilde{\ell}_{24}^{(15)2} = 1$ $\tilde{\ell}_{34}^{(15)3} = -1$	-1
$\ell_{12}^{(16)2} = 1$ $\ell_{13}^{(16)3} = 1$ $\ell_{14}^{(16)1} = 1$ $\ell_{23}^{(16)1} = 1$ $\ell_{24}^{(16)3} = -1$ $\ell_{34}^{(16)2} = 1$	1

Table 11. Non-vanishing ℓ , $\tilde{\ell}$, and χ_o values for representation $\mathcal{P}_{[1]}$.

$\mathcal{P}_{[2]} :$	χ_o					
$\tilde{\ell}_{12}^{(1)3} = 1$	$\tilde{\ell}_{13}^{(1)2} = 1$	$\tilde{\ell}_{14}^{(1)1} = 1$	$\tilde{\ell}_{23}^{(1)1} = -1$	$\tilde{\ell}_{24}^{(1)2} = 1$	$\tilde{\ell}_{34}^{(1)3} = -1$	-1
$\ell_{12}^{(2)2} = 1$	$\ell_{13}^{(2)3} = 1$	$\ell_{14}^{(2)1} = 1$	$\ell_{23}^{(2)1} = 1$	$\ell_{24}^{(2)3} = -1$	$\ell_{34}^{(2)2} = 1$	1
$\tilde{\ell}_{12}^{(3)3} = 1$	$\tilde{\ell}_{13}^{(3)2} = 1$	$\tilde{\ell}_{14}^{(3)1} = 1$	$\tilde{\ell}_{23}^{(3)1} = -1$	$\tilde{\ell}_{24}^{(3)2} = 1$	$\tilde{\ell}_{34}^{(3)3} = -1$	-1
$\ell_{12}^{(4)2} = 1$	$\ell_{13}^{(4)3} = 1$	$\ell_{14}^{(4)1} = 1$	$\ell_{23}^{(4)1} = 1$	$\ell_{24}^{(4)3} = -1$	$\ell_{34}^{(4)2} = 1$	1
$\ell_{12}^{(5)2} = 1$	$\ell_{13}^{(5)3} = 1$	$\ell_{14}^{(5)1} = 1$	$\ell_{23}^{(5)1} = 1$	$\ell_{24}^{(5)3} = -1$	$\ell_{34}^{(5)2} = 1$	1
$\tilde{\ell}_{12}^{(6)3} = 1$	$\tilde{\ell}_{13}^{(6)2} = 1$	$\tilde{\ell}_{14}^{(6)1} = 1$	$\tilde{\ell}_{23}^{(6)1} = -1$	$\tilde{\ell}_{24}^{(6)2} = 1$	$\tilde{\ell}_{34}^{(6)3} = -1$	-1
$\ell_{12}^{(7)2} = 1$	$\ell_{13}^{(7)3} = 1$	$\ell_{14}^{(7)1} = 1$	$\ell_{23}^{(7)1} = 1$	$\ell_{24}^{(7)3} = -1$	$\ell_{34}^{(7)2} = 1$	1
$\tilde{\ell}_{12}^{(8)3} = 1$	$\tilde{\ell}_{13}^{(8)2} = 1$	$\tilde{\ell}_{14}^{(8)1} = 1$	$\tilde{\ell}_{23}^{(8)1} = -1$	$\tilde{\ell}_{24}^{(8)2} = 1$	$\tilde{\ell}_{34}^{(8)3} = -1$	-1
$\tilde{\ell}_{12}^{(9)3} = 1$	$\tilde{\ell}_{13}^{(9)2} = 1$	$\tilde{\ell}_{14}^{(9)1} = 1$	$\tilde{\ell}_{23}^{(9)1} = -1$	$\tilde{\ell}_{24}^{(9)2} = 1$	$\tilde{\ell}_{34}^{(9)3} = -1$	-1
$\ell_{12}^{(10)2} = 1$	$\ell_{13}^{(10)3} = 1$	$\ell_{14}^{(10)1} = 1$	$\ell_{23}^{(10)1} = 1$	$\ell_{24}^{(10)3} = -1$	$\ell_{34}^{(10)2} = 1$	1
$\tilde{\ell}_{12}^{(11)3} = 1$	$\tilde{\ell}_{13}^{(11)2} = 1$	$\tilde{\ell}_{14}^{(11)1} = 1$	$\tilde{\ell}_{23}^{(11)1} = -1$	$\tilde{\ell}_{24}^{(11)2} = 1$	$\tilde{\ell}_{34}^{(11)3} = -1$	-1
$\ell_{12}^{(12)2} = 1$	$\ell_{13}^{(12)3} = 1$	$\ell_{14}^{(12)1} = 1$	$\ell_{23}^{(12)1} = 1$	$\ell_{24}^{(12)3} = -1$	$\ell_{34}^{(12)2} = 1$	1
$\ell_{12}^{(13)2} = 1$	$\ell_{13}^{(13)3} = 1$	$\ell_{14}^{(13)1} = 1$	$\ell_{23}^{(13)1} = 1$	$\ell_{24}^{(13)3} = -1$	$\ell_{34}^{(13)2} = 1$	1
$\tilde{\ell}_{12}^{(14)3} = 1$	$\tilde{\ell}_{13}^{(14)2} = 1$	$\tilde{\ell}_{14}^{(14)1} = 1$	$\tilde{\ell}_{23}^{(14)1} = -1$	$\tilde{\ell}_{24}^{(14)2} = 1$	$\tilde{\ell}_{34}^{(14)3} = -1$	-1
$\ell_{12}^{(15)2} = 1$	$\ell_{13}^{(15)3} = 1$	$\ell_{14}^{(15)1} = 1$	$\ell_{23}^{(15)1} = 1$	$\ell_{24}^{(15)3} = -1$	$\ell_{34}^{(15)2} = 1$	1
$\tilde{\ell}_{12}^{(16)3} = 1$	$\tilde{\ell}_{13}^{(16)2} = 1$	$\tilde{\ell}_{14}^{(16)1} = 1$	$\tilde{\ell}_{23}^{(16)1} = -1$	$\tilde{\ell}_{24}^{(16)2} = 1$	$\tilde{\ell}_{34}^{(16)3} = -1$	-1

Table 12. Non-vanishing ℓ , $\tilde{\ell}$, and χ_o values for representation $\mathcal{P}_{[2]}$.

$\mathcal{P}_{[3]} :$	χ_o					
$\tilde{\ell}_{12}^{(1)3} = -1$	$\tilde{\ell}_{13}^{(1)2} = 1$	$\tilde{\ell}_{14}^{(1)1} = -1$	$\tilde{\ell}_{23}^{(1)1} = 1$	$\tilde{\ell}_{24}^{(1)2} = 1$	$\tilde{\ell}_{34}^{(1)3} = 1$	-1
$\ell_{12}^{(2)2} = -1$	$\ell_{13}^{(2)3} = -1$	$\ell_{14}^{(2)1} = 1$	$\ell_{23}^{(2)1} = 1$	$\ell_{24}^{(2)3} = 1$	$\ell_{34}^{(2)2} = -1$	1
$\tilde{\ell}_{12}^{(3)3} = -1$	$\tilde{\ell}_{13}^{(3)2} = 1$	$\tilde{\ell}_{14}^{(3)1} = -1$	$\tilde{\ell}_{23}^{(3)1} = 1$	$\tilde{\ell}_{24}^{(3)2} = 1$	$\tilde{\ell}_{34}^{(3)3} = 1$	-1
$\ell_{12}^{(4)2} = -1$	$\ell_{13}^{(4)3} = -1$	$\ell_{14}^{(4)1} = 1$	$\ell_{23}^{(4)1} = 1$	$\ell_{24}^{(4)3} = 1$	$\ell_{34}^{(4)2} = -1$	1
$\tilde{\ell}_{12}^{(5)3} = -1$	$\tilde{\ell}_{13}^{(5)2} = 1$	$\tilde{\ell}_{14}^{(5)1} = -1$	$\tilde{\ell}_{23}^{(5)1} = 1$	$\tilde{\ell}_{24}^{(5)2} = 1$	$\tilde{\ell}_{34}^{(5)3} = 1$	-1
$\ell_{12}^{(6)2} = -1$	$\ell_{13}^{(6)3} = -1$	$\ell_{14}^{(6)1} = 1$	$\ell_{23}^{(6)1} = 1$	$\ell_{24}^{(6)3} = 1$	$\ell_{34}^{(6)2} = -1$	1
$\tilde{\ell}_{12}^{(7)3} = -1$	$\tilde{\ell}_{13}^{(7)2} = 1$	$\tilde{\ell}_{14}^{(7)1} = -1$	$\tilde{\ell}_{23}^{(7)1} = 1$	$\tilde{\ell}_{24}^{(7)2} = 1$	$\tilde{\ell}_{34}^{(7)3} = 1$	-1
$\ell_{12}^{(8)2} = -1$	$\ell_{13}^{(8)3} = -1$	$\ell_{14}^{(8)1} = 1$	$\ell_{23}^{(8)1} = 1$	$\ell_{24}^{(8)3} = 1$	$\ell_{34}^{(8)2} = -1$	1
$\ell_{12}^{(9)2} = -1$	$\ell_{13}^{(9)3} = -1$	$\ell_{14}^{(9)1} = 1$	$\ell_{23}^{(9)1} = 1$	$\ell_{24}^{(9)3} = 1$	$\ell_{34}^{(9)2} = -1$	1
$\tilde{\ell}_{12}^{(10)3} = -1$	$\tilde{\ell}_{13}^{(10)2} = 1$	$\tilde{\ell}_{14}^{(10)1} = -1$	$\tilde{\ell}_{23}^{(10)1} = 1$	$\tilde{\ell}_{24}^{(10)2} = 1$	$\tilde{\ell}_{34}^{(10)3} = 1$	-1
$\ell_{12}^{(11)2} = -1$	$\ell_{13}^{(11)3} = -1$	$\ell_{14}^{(11)1} = 1$	$\ell_{23}^{(11)1} = 1$	$\ell_{24}^{(11)3} = 1$	$\ell_{34}^{(11)2} = -1$	1
$\tilde{\ell}_{12}^{(12)3} = -1$	$\tilde{\ell}_{13}^{(12)2} = 1$	$\tilde{\ell}_{14}^{(12)1} = -1$	$\tilde{\ell}_{23}^{(12)1} = 1$	$\tilde{\ell}_{24}^{(12)2} = 1$	$\tilde{\ell}_{34}^{(12)3} = 1$	-1
$\ell_{12}^{(13)2} = -1$	$\ell_{13}^{(13)3} = -1$	$\ell_{14}^{(13)1} = 1$	$\ell_{23}^{(13)1} = 1$	$\ell_{24}^{(13)3} = 1$	$\ell_{34}^{(13)2} = -1$	1
$\tilde{\ell}_{12}^{(14)3} = -1$	$\tilde{\ell}_{13}^{(14)2} = 1$	$\tilde{\ell}_{14}^{(14)1} = -1$	$\tilde{\ell}_{23}^{(14)1} = 1$	$\tilde{\ell}_{24}^{(14)2} = 1$	$\tilde{\ell}_{34}^{(14)3} = 1$	-1
$\ell_{12}^{(15)2} = -1$	$\ell_{13}^{(15)3} = -1$	$\ell_{14}^{(15)1} = 1$	$\ell_{23}^{(15)1} = 1$	$\ell_{24}^{(15)3} = 1$	$\ell_{34}^{(15)2} = -1$	1
$\tilde{\ell}_{12}^{(16)3} = -1$	$\tilde{\ell}_{13}^{(16)2} = 1$	$\tilde{\ell}_{14}^{(16)1} = -1$	$\tilde{\ell}_{23}^{(16)1} = 1$	$\tilde{\ell}_{24}^{(16)2} = 1$	$\tilde{\ell}_{34}^{(16)3} = 1$	-1

Table 13. Non-vanishing ℓ , $\tilde{\ell}$, and χ_o values for representation $\mathcal{P}_{[3]}$.

$\mathcal{P}_{[4]} :$						χ_o
$\ell_{12}^{(1)2} = 1$	$\ell_{13}^{(1)3} = 1$	$\ell_{14}^{(1)1} = 1$	$\ell_{23}^{(1)1} = 1$	$\ell_{24}^{(1)3} = -1$	$\ell_{34}^{(1)2} = 1$	1
$\tilde{\ell}_{12}^{(2)3} = 1$	$\tilde{\ell}_{13}^{(2)2} = 1$	$\tilde{\ell}_{14}^{(2)1} = 1$	$\tilde{\ell}_{23}^{(2)1} = -1$	$\tilde{\ell}_{24}^{(2)2} = 1$	$\tilde{\ell}_{34}^{(2)3} = -1$	-1
$\ell_{12}^{(3)2} = 1$	$\ell_{13}^{(3)3} = 1$	$\ell_{14}^{(3)1} = 1$	$\ell_{23}^{(3)1} = 1$	$\ell_{24}^{(3)3} = -1$	$\ell_{34}^{(3)2} = 1$	1
$\tilde{\ell}_{12}^{(4)3} = 1$	$\tilde{\ell}_{13}^{(4)2} = 1$	$\tilde{\ell}_{14}^{(4)1} = 1$	$\tilde{\ell}_{23}^{(4)1} = -1$	$\tilde{\ell}_{24}^{(4)2} = 1$	$\tilde{\ell}_{34}^{(4)3} = -1$	-1
$\tilde{\ell}_{12}^{(5)3} = 1$	$\tilde{\ell}_{13}^{(5)2} = 1$	$\tilde{\ell}_{14}^{(5)1} = 1$	$\tilde{\ell}_{23}^{(5)1} = -1$	$\tilde{\ell}_{24}^{(5)2} = 1$	$\tilde{\ell}_{34}^{(5)3} = -1$	-1
$\ell_{12}^{(6)2} = 1$	$\ell_{13}^{(6)3} = 1$	$\ell_{14}^{(6)1} = 1$	$\ell_{23}^{(6)1} = 1$	$\ell_{24}^{(6)3} = -1$	$\ell_{34}^{(6)2} = 1$	1
$\tilde{\ell}_{12}^{(7)3} = 1$	$\tilde{\ell}_{13}^{(7)2} = 1$	$\tilde{\ell}_{14}^{(7)1} = 1$	$\tilde{\ell}_{23}^{(7)1} = -1$	$\tilde{\ell}_{24}^{(7)2} = 1$	$\tilde{\ell}_{34}^{(7)3} = -1$	-1
$\ell_{12}^{(8)2} = 1$	$\ell_{13}^{(8)3} = 1$	$\ell_{14}^{(8)1} = 1$	$\ell_{23}^{(8)1} = 1$	$\ell_{24}^{(8)3} = -1$	$\ell_{34}^{(8)2} = 1$	1
$\ell_{12}^{(9)2} = 1$	$\ell_{13}^{(9)3} = 1$	$\ell_{14}^{(9)1} = 1$	$\ell_{23}^{(9)1} = 1$	$\ell_{24}^{(9)3} = -1$	$\ell_{34}^{(9)2} = 1$	1
$\tilde{\ell}_{12}^{(10)3} = 1$	$\tilde{\ell}_{13}^{(10)2} = 1$	$\tilde{\ell}_{14}^{(10)1} = 1$	$\tilde{\ell}_{23}^{(10)1} = -1$	$\tilde{\ell}_{24}^{(10)2} = 1$	$\tilde{\ell}_{34}^{(10)3} = -1$	-1
$\ell_{12}^{(11)2} = 1$	$\ell_{13}^{(11)3} = 1$	$\ell_{14}^{(11)1} = 1$	$\ell_{23}^{(11)1} = 1$	$\ell_{24}^{(11)3} = -1$	$\ell_{34}^{(11)2} = 1$	1
$\tilde{\ell}_{12}^{(12)3} = 1$	$\tilde{\ell}_{13}^{(12)2} = 1$	$\tilde{\ell}_{14}^{(12)1} = 1$	$\tilde{\ell}_{23}^{(12)1} = -1$	$\tilde{\ell}_{24}^{(12)2} = 1$	$\tilde{\ell}_{34}^{(12)3} = -1$	-1
$\tilde{\ell}_{12}^{(13)3} = 1$	$\tilde{\ell}_{13}^{(13)2} = 1$	$\tilde{\ell}_{14}^{(13)1} = 1$	$\tilde{\ell}_{23}^{(13)1} = -1$	$\tilde{\ell}_{24}^{(13)2} = 1$	$\tilde{\ell}_{34}^{(13)3} = -1$	-1
$\ell_{12}^{(14)2} = 1$	$\ell_{13}^{(14)3} = 1$	$\ell_{14}^{(14)1} = 1$	$\ell_{23}^{(14)1} = 1$	$\ell_{24}^{(14)3} = -1$	$\ell_{34}^{(14)2} = 1$	1
$\tilde{\ell}_{12}^{(15)3} = 1$	$\tilde{\ell}_{13}^{(15)2} = 1$	$\tilde{\ell}_{14}^{(15)1} = 1$	$\tilde{\ell}_{23}^{(15)1} = -1$	$\tilde{\ell}_{24}^{(15)2} = 1$	$\tilde{\ell}_{34}^{(15)3} = -1$	-1
$\ell_{12}^{(16)2} = 1$	$\ell_{13}^{(16)3} = 1$	$\ell_{14}^{(16)1} = 1$	$\ell_{23}^{(16)1} = 1$	$\ell_{24}^{(16)3} = -1$	$\ell_{34}^{(16)2} = 1$	1

Table 14. Non-vanishing ℓ , $\tilde{\ell}$, and χ_o values for representation $\mathcal{P}_{[4]}$.

$\mathcal{P}_{[5]} :$						χ_o
$\ell_{12}^{(1)2} = 1$	$\ell_{13}^{(1)3} = 1$	$\ell_{14}^{(1)1} = 1$	$\ell_{23}^{(1)1} = 1$	$\ell_{24}^{(1)3} = -1$	$\ell_{34}^{(1)2} = 1$	1
$\tilde{\ell}_{12}^{(2)3} = 1$	$\tilde{\ell}_{13}^{(2)2} = 1$	$\tilde{\ell}_{14}^{(2)1} = 1$	$\tilde{\ell}_{23}^{(2)1} = -1$	$\tilde{\ell}_{24}^{(2)2} = 1$	$\tilde{\ell}_{34}^{(2)3} = -1$	-1
$\ell_{12}^{(3)2} = 1$	$\ell_{13}^{(3)3} = 1$	$\ell_{14}^{(3)1} = 1$	$\ell_{23}^{(3)1} = 1$	$\ell_{24}^{(3)3} = -1$	$\ell_{34}^{(3)2} = 1$	1
$\tilde{\ell}_{12}^{(4)3} = 1$	$\tilde{\ell}_{13}^{(4)2} = 1$	$\tilde{\ell}_{14}^{(4)1} = 1$	$\tilde{\ell}_{23}^{(4)1} = -1$	$\tilde{\ell}_{24}^{(4)2} = 1$	$\tilde{\ell}_{34}^{(4)3} = -1$	-1
$\ell_{12}^{(5)2} = 1$	$\ell_{13}^{(5)3} = 1$	$\ell_{14}^{(5)1} = 1$	$\ell_{23}^{(5)1} = 1$	$\ell_{24}^{(5)3} = -1$	$\ell_{34}^{(5)2} = 1$	1
$\tilde{\ell}_{12}^{(6)3} = 1$	$\tilde{\ell}_{13}^{(6)2} = 1$	$\tilde{\ell}_{14}^{(6)1} = 1$	$\tilde{\ell}_{23}^{(6)1} = -1$	$\tilde{\ell}_{24}^{(6)2} = 1$	$\tilde{\ell}_{34}^{(6)3} = -1$	-1
$\ell_{12}^{(7)2} = 1$	$\ell_{13}^{(7)3} = 1$	$\ell_{14}^{(7)1} = 1$	$\ell_{23}^{(7)1} = 1$	$\ell_{24}^{(7)3} = -1$	$\ell_{34}^{(7)2} = 1$	1
$\tilde{\ell}_{12}^{(8)3} = 1$	$\tilde{\ell}_{13}^{(8)2} = 1$	$\tilde{\ell}_{14}^{(8)1} = 1$	$\tilde{\ell}_{23}^{(8)1} = -1$	$\tilde{\ell}_{24}^{(8)2} = 1$	$\tilde{\ell}_{34}^{(8)3} = -1$	-1
$\tilde{\ell}_{12}^{(9)3} = 1$	$\tilde{\ell}_{13}^{(9)2} = 1$	$\tilde{\ell}_{14}^{(9)1} = 1$	$\tilde{\ell}_{23}^{(9)1} = -1$	$\tilde{\ell}_{24}^{(9)2} = 1$	$\tilde{\ell}_{34}^{(9)3} = -1$	-1
$\ell_{12}^{(10)2} = 1$	$\ell_{13}^{(10)3} = 1$	$\ell_{14}^{(10)1} = 1$	$\ell_{23}^{(10)1} = 1$	$\ell_{24}^{(10)3} = -1$	$\ell_{34}^{(10)2} = 1$	1
$\tilde{\ell}_{12}^{(11)3} = 1$	$\tilde{\ell}_{13}^{(11)2} = 1$	$\tilde{\ell}_{14}^{(11)1} = 1$	$\tilde{\ell}_{23}^{(11)1} = -1$	$\tilde{\ell}_{24}^{(11)2} = 1$	$\tilde{\ell}_{34}^{(11)3} = -1$	-1
$\ell_{12}^{(12)2} = 1$	$\ell_{13}^{(12)3} = 1$	$\ell_{14}^{(12)1} = 1$	$\ell_{23}^{(12)1} = 1$	$\ell_{24}^{(12)3} = -1$	$\ell_{34}^{(12)2} = 1$	1
$\tilde{\ell}_{12}^{(13)3} = 1$	$\tilde{\ell}_{13}^{(13)2} = 1$	$\tilde{\ell}_{14}^{(13)1} = 1$	$\tilde{\ell}_{23}^{(13)1} = -1$	$\tilde{\ell}_{24}^{(13)2} = 1$	$\tilde{\ell}_{34}^{(13)3} = -1$	-1
$\ell_{12}^{(14)2} = 1$	$\ell_{13}^{(14)3} = 1$	$\ell_{14}^{(14)1} = 1$	$\ell_{23}^{(14)1} = 1$	$\ell_{24}^{(14)3} = -1$	$\ell_{34}^{(14)2} = 1$	1
$\tilde{\ell}_{12}^{(15)3} = 1$	$\tilde{\ell}_{13}^{(15)2} = 1$	$\tilde{\ell}_{14}^{(15)1} = 1$	$\tilde{\ell}_{23}^{(15)1} = -1$	$\tilde{\ell}_{24}^{(15)2} = 1$	$\tilde{\ell}_{34}^{(15)3} = -1$	-1
$\ell_{12}^{(16)2} = 1$	$\ell_{13}^{(16)3} = 1$	$\ell_{14}^{(16)1} = 1$	$\ell_{23}^{(16)1} = 1$	$\ell_{24}^{(16)3} = -1$	$\ell_{34}^{(16)2} = 1$	1

Table 15. Non-vanishing ℓ , $\tilde{\ell}$, and χ_o Values For Representation $\mathcal{P}_{[5]}$.

$\mathcal{P}_{[6]} :$						χ_o
$\tilde{\ell}_{12}^{(1)3} = 1$	$\tilde{\ell}_{13}^{(1)2} = 1$	$\tilde{\ell}_{14}^{(1)1} = 1$	$\tilde{\ell}_{23}^{(1)1} = -1$	$\tilde{\ell}_{24}^{(1)2} = 1$	$\tilde{\ell}_{34}^{(1)3} = -1$	-1
$\ell_{12}^{(2)2} = 1$	$\ell_{13}^{(2)3} = 1$	$\ell_{14}^{(2)1} = 1$	$\ell_{23}^{(2)1} = 1$	$\ell_{24}^{(2)3} = -1$	$\ell_{34}^{(2)2} = 1$	1
$\tilde{\ell}_{12}^{(3)3} = 1$	$\tilde{\ell}_{13}^{(3)2} = 1$	$\tilde{\ell}_{14}^{(3)1} = 1$	$\tilde{\ell}_{23}^{(3)1} = -1$	$\tilde{\ell}_{24}^{(3)2} = 1$	$\tilde{\ell}_{34}^{(3)3} = -1$	-1
$\ell_{12}^{(4)2} = 1$	$\ell_{13}^{(4)3} = 1$	$\ell_{14}^{(4)1} = 1$	$\ell_{23}^{(4)1} = 1$	$\ell_{24}^{(4)3} = -1$	$\ell_{34}^{(4)2} = 1$	1
$\tilde{\ell}_{12}^{(5)3} = 1$	$\tilde{\ell}_{13}^{(5)2} = 1$	$\tilde{\ell}_{14}^{(5)1} = 1$	$\tilde{\ell}_{23}^{(5)1} = -1$	$\tilde{\ell}_{24}^{(5)2} = 1$	$\tilde{\ell}_{34}^{(5)3} = -1$	-1
$\ell_{12}^{(6)2} = 1$	$\ell_{13}^{(6)3} = 1$	$\ell_{14}^{(6)1} = 1$	$\ell_{23}^{(6)1} = 1$	$\ell_{24}^{(6)3} = -1$	$\ell_{34}^{(6)2} = 1$	1
$\tilde{\ell}_{12}^{(7)3} = 1$	$\tilde{\ell}_{13}^{(7)2} = 1$	$\tilde{\ell}_{14}^{(7)1} = 1$	$\tilde{\ell}_{23}^{(7)1} = -1$	$\tilde{\ell}_{24}^{(7)2} = 1$	$\tilde{\ell}_{34}^{(7)3} = -1$	-1
$\ell_{12}^{(8)2} = 1$	$\ell_{13}^{(8)3} = 1$	$\ell_{14}^{(8)1} = 1$	$\ell_{23}^{(8)1} = 1$	$\ell_{24}^{(8)3} = -1$	$\ell_{34}^{(8)2} = 1$	1
$\ell_{12}^{(9)2} = 1$	$\ell_{13}^{(9)3} = 1$	$\ell_{14}^{(9)1} = 1$	$\ell_{23}^{(9)1} = 1$	$\ell_{24}^{(9)3} = -1$	$\ell_{34}^{(9)2} = 1$	1
$\tilde{\ell}_{12}^{(10)3} = 1$	$\tilde{\ell}_{13}^{(10)2} = 1$	$\tilde{\ell}_{14}^{(10)1} = 1$	$\tilde{\ell}_{23}^{(10)1} = -1$	$\tilde{\ell}_{24}^{(10)2} = 1$	$\tilde{\ell}_{34}^{(10)3} = -1$	-1
$\ell_{12}^{(11)2} = 1$	$\ell_{13}^{(11)3} = 1$	$\ell_{14}^{(11)1} = 1$	$\ell_{23}^{(11)1} = 1$	$\ell_{24}^{(11)3} = -1$	$\ell_{34}^{(11)2} = 1$	1
$\tilde{\ell}_{12}^{(12)3} = 1$	$\tilde{\ell}_{13}^{(12)2} = 1$	$\tilde{\ell}_{14}^{(12)1} = 1$	$\tilde{\ell}_{23}^{(12)1} = -1$	$\tilde{\ell}_{24}^{(12)2} = 1$	$\tilde{\ell}_{34}^{(12)3} = -1$	-1
$\ell_{12}^{(13)2} = 1$	$\ell_{13}^{(13)3} = 1$	$\ell_{14}^{(13)1} = 1$	$\ell_{23}^{(13)1} = 1$	$\ell_{24}^{(13)3} = -1$	$\ell_{34}^{(13)2} = 1$	1
$\tilde{\ell}_{12}^{(14)3} = 1$	$\tilde{\ell}_{13}^{(14)2} = 1$	$\tilde{\ell}_{14}^{(14)1} = 1$	$\tilde{\ell}_{23}^{(14)1} = -1$	$\tilde{\ell}_{24}^{(14)2} = 1$	$\tilde{\ell}_{34}^{(14)3} = -1$	-1
$\ell_{12}^{(15)2} = 1$	$\ell_{13}^{(15)3} = 1$	$\ell_{14}^{(15)1} = 1$	$\ell_{23}^{(15)1} = 1$	$\ell_{24}^{(15)3} = -1$	$\ell_{34}^{(15)2} = 1$	1
$\tilde{\ell}_{12}^{(16)3} = 1$	$\tilde{\ell}_{13}^{(16)2} = 1$	$\tilde{\ell}_{14}^{(16)1} = 1$	$\tilde{\ell}_{23}^{(16)1} = -1$	$\tilde{\ell}_{24}^{(16)2} = 1$	$\tilde{\ell}_{34}^{(16)3} = -1$	-1

Table 16. Non-vanishing ℓ , $\tilde{\ell}$, and χ_o values for representation $\mathcal{P}_{[6]}$.

The value of the “Kye-Oh” function when expressed in terms of the ℓ and $\tilde{\ell}$ parameters of (2.7) takes the form

$$\begin{aligned}
 \chi_o(\mathcal{S}_{\mathcal{P}_{[\Lambda]}}[\alpha] \cdot \mathcal{P}_{[\Lambda]}) = & \frac{1}{3} \sum_{\hat{a}} \left[\ell_{12}^{(\mathcal{R})\hat{a}} \ell_{34}^{(\mathcal{R})\hat{a}} - \ell_{13}^{(\mathcal{R})\hat{a}} \ell_{24}^{(\mathcal{R})\hat{a}} + \ell_{14}^{(\mathcal{R})\hat{a}} \ell_{23}^{(\mathcal{R})\hat{a}} \right] + \\
 & \frac{1}{3} \sum_{\hat{a}} \left[\tilde{\ell}_{12}^{(\mathcal{R})\hat{a}} \tilde{\ell}_{34}^{(\mathcal{R})\hat{a}} - \tilde{\ell}_{13}^{(\mathcal{R})\hat{a}} \tilde{\ell}_{24}^{(\mathcal{R})\hat{a}} + \tilde{\ell}_{14}^{(\mathcal{R})\hat{a}} \tilde{\ell}_{23}^{(\mathcal{R})\hat{a}} \right]. \quad (\text{C.1})
 \end{aligned}$$

Here the representation label (\mathcal{R}) corresponds to a specification of $[\Lambda]$ and α .

D Adinkra Gadget values over the “small BC_4 library”

In this appendix, we give the values of the gadget between matrix elements over all 96 elements of the “small BC_4 library.”

S'	1	2	3	4	5	6	7	8	9	10	11	12	13	14	15	16
S																
1	1	0	1	0	1	0	1	0	0	1	0	1	0	1	0	1
2	0	1	0	1	0	1	0	1	1	0	1	0	1	0	1	0
3	1	0	1	0	1	0	1	0	0	1	0	1	0	1	0	1
4	0	1	0	1	0	1	0	1	1	0	1	0	1	0	1	0
5	1	0	1	0	1	0	1	0	0	1	0	1	0	1	0	1
6	0	1	0	1	0	1	0	1	1	0	1	0	1	0	1	0
7	1	0	1	0	1	0	1	0	0	1	0	1	0	1	0	1
8	0	1	0	1	0	1	0	1	1	0	1	0	1	0	1	0
9	0	1	0	1	0	1	0	1	1	0	1	0	1	0	1	0
10	1	0	1	0	1	0	1	0	0	1	0	1	0	1	0	1
11	0	1	0	1	0	1	0	1	1	0	1	0	1	0	1	0
12	1	0	1	0	1	0	1	0	0	1	0	1	0	1	0	1
13	0	1	0	1	0	1	0	1	1	0	1	0	1	0	1	0
14	1	0	1	0	1	0	1	0	0	1	0	1	0	1	0	1
15	0	1	0	1	0	1	0	1	1	0	1	0	1	0	1	0
16	1	0	1	0	1	0	1	0	0	1	0	1	0	1	0	1

Table 17. Gadget values for $\mathcal{P}_{[1]} \times \mathcal{P}_{[1]}$ with different boolean factors.

S'	1	2	3	4	5	6	7	8	9	10	11	12	13	14	15	16
S																
1	0	1	0	1	1	0	1	0	0	1	0	1	1	0	1	0
2	1	0	1	0	0	1	0	1	1	0	1	0	0	1	0	1
3	0	1	0	1	1	0	1	0	0	1	0	1	1	0	1	0
4	1	0	1	0	0	1	0	1	1	0	1	0	0	1	0	1
5	0	1	0	1	1	0	1	0	0	1	0	1	1	0	1	0
6	1	0	1	0	0	1	0	1	1	0	1	0	0	1	0	1
7	0	1	0	1	1	0	1	0	0	1	0	1	1	0	1	0
8	1	0	1	0	0	1	0	1	1	0	1	0	0	1	0	1
9	1	0	1	0	0	1	0	1	1	0	1	0	0	1	0	1
10	0	1	0	1	1	0	1	0	0	1	0	1	1	0	1	0
11	1	0	1	0	0	1	0	1	1	0	1	0	0	1	0	1
12	0	1	0	1	1	0	1	0	0	1	0	1	1	0	1	0
13	1	0	1	0	0	1	0	1	1	0	1	0	0	1	0	1
14	0	1	0	1	1	0	1	0	0	1	0	1	1	0	1	0
15	1	0	1	0	0	1	0	1	1	0	1	0	0	1	0	1
16	0	1	0	1	1	0	1	0	0	1	0	1	1	0	1	0

Table 18. Gadget values for $\mathcal{P}_{[1]} \times \mathcal{P}_{[2]}$ with different boolean factors.

S'	1	2	3	4	5	6	7	8	9	10	11	12	13	14	15	16
1	0	$-\frac{1}{3}$	0	$-\frac{1}{3}$	0	$-\frac{1}{3}$	0	$-\frac{1}{3}$	$-\frac{1}{3}$	0	$-\frac{1}{3}$	0	$-\frac{1}{3}$	0	$-\frac{1}{3}$	0
2	$-\frac{1}{3}$	0	$-\frac{1}{3}$	0	$-\frac{1}{3}$	0	$-\frac{1}{3}$	0	0	$-\frac{1}{3}$	0	$-\frac{1}{3}$	0	$-\frac{1}{3}$	0	$-\frac{1}{3}$
3	0	$-\frac{1}{3}$	0	$-\frac{1}{3}$	0	$-\frac{1}{3}$	0	$-\frac{1}{3}$	$-\frac{1}{3}$	0	$-\frac{1}{3}$	0	$-\frac{1}{3}$	0	$-\frac{1}{3}$	0
4	$-\frac{1}{3}$	0	$-\frac{1}{3}$	0	$-\frac{1}{3}$	0	$-\frac{1}{3}$	0	0	$-\frac{1}{3}$	0	$-\frac{1}{3}$	0	$-\frac{1}{3}$	0	$-\frac{1}{3}$
5	0	$-\frac{1}{3}$	0	$-\frac{1}{3}$	0	$-\frac{1}{3}$	0	$-\frac{1}{3}$	$-\frac{1}{3}$	0	$-\frac{1}{3}$	0	$-\frac{1}{3}$	0	$-\frac{1}{3}$	0
6	$-\frac{1}{3}$	0	$-\frac{1}{3}$	0	$-\frac{1}{3}$	0	$-\frac{1}{3}$	0	0	$-\frac{1}{3}$	0	$-\frac{1}{3}$	0	$-\frac{1}{3}$	0	$-\frac{1}{3}$
7	0	$-\frac{1}{3}$	0	$-\frac{1}{3}$	0	$-\frac{1}{3}$	0	$-\frac{1}{3}$	$-\frac{1}{3}$	0	$-\frac{1}{3}$	0	$-\frac{1}{3}$	0	$-\frac{1}{3}$	0
8	$-\frac{1}{3}$	0	$-\frac{1}{3}$	0	$-\frac{1}{3}$	0	$-\frac{1}{3}$	0	0	$-\frac{1}{3}$	0	$-\frac{1}{3}$	0	$-\frac{1}{3}$	0	$-\frac{1}{3}$
9	$-\frac{1}{3}$	0	$-\frac{1}{3}$	0	$-\frac{1}{3}$	0	$-\frac{1}{3}$	0	0	$-\frac{1}{3}$	0	$-\frac{1}{3}$	0	$-\frac{1}{3}$	0	$-\frac{1}{3}$
10	0	$-\frac{1}{3}$	0	$-\frac{1}{3}$	0	$-\frac{1}{3}$	0	$-\frac{1}{3}$	$-\frac{1}{3}$	0	$-\frac{1}{3}$	0	$-\frac{1}{3}$	0	$-\frac{1}{3}$	0
11	$-\frac{1}{3}$	0	$-\frac{1}{3}$	0	$-\frac{1}{3}$	0	$-\frac{1}{3}$	0	0	$-\frac{1}{3}$	0	$-\frac{1}{3}$	0	$-\frac{1}{3}$	0	$-\frac{1}{3}$
12	0	$-\frac{1}{3}$	0	$-\frac{1}{3}$	0	$-\frac{1}{3}$	0	$-\frac{1}{3}$	$-\frac{1}{3}$	0	$-\frac{1}{3}$	0	$-\frac{1}{3}$	0	$-\frac{1}{3}$	0
13	$-\frac{1}{3}$	0	$-\frac{1}{3}$	0	$-\frac{1}{3}$	0	$-\frac{1}{3}$	0	0	$-\frac{1}{3}$	0	$-\frac{1}{3}$	0	$-\frac{1}{3}$	0	$-\frac{1}{3}$
14	0	$-\frac{1}{3}$	0	$-\frac{1}{3}$	0	$-\frac{1}{3}$	0	$-\frac{1}{3}$	$-\frac{1}{3}$	0	$-\frac{1}{3}$	0	$-\frac{1}{3}$	0	$-\frac{1}{3}$	0
15	$-\frac{1}{3}$	0	$-\frac{1}{3}$	0	$-\frac{1}{3}$	0	$-\frac{1}{3}$	0	0	$-\frac{1}{3}$	0	$-\frac{1}{3}$	0	$-\frac{1}{3}$	0	$-\frac{1}{3}$
16	0	$-\frac{1}{3}$	0	$-\frac{1}{3}$	0	$-\frac{1}{3}$	0	$-\frac{1}{3}$	$-\frac{1}{3}$	0	$-\frac{1}{3}$	0	$-\frac{1}{3}$	0	$-\frac{1}{3}$	0

Table 19. Gadget values for $\mathcal{P}_{[1]} \times \mathcal{P}_{[3]}$ with different boolean factors.

S'	1	2	3	4	5	6	7	8	9	10	11	12	13	14	15	16
1	1	0	1	0	0	1	0	1	1	0	1	0	0	1	0	1
2	0	1	0	1	1	0	1	0	0	1	0	1	1	0	1	0
3	1	0	1	0	0	1	0	1	1	0	1	0	0	1	0	1
4	0	1	0	1	1	0	1	0	0	1	0	1	1	0	1	0
5	1	0	1	0	0	1	0	1	1	0	1	0	0	1	0	1
6	0	1	0	1	1	0	1	0	0	1	0	1	1	0	1	0
7	1	0	1	0	0	1	0	1	1	0	1	0	0	1	0	1
8	0	1	0	1	1	0	1	0	0	1	0	1	1	0	1	0
9	0	1	0	1	1	0	1	0	0	1	0	1	1	0	1	0
10	1	0	1	0	0	1	0	1	1	0	1	0	0	1	0	1
11	0	1	0	1	1	0	1	0	0	1	0	1	1	0	1	0
12	1	0	1	0	0	1	0	1	1	0	1	0	0	1	0	1
13	0	1	0	1	1	0	1	0	0	1	0	1	1	0	1	0
14	1	0	1	0	0	1	0	1	1	0	1	0	0	1	0	1
15	0	1	0	1	1	0	1	0	0	1	0	1	1	0	1	0
16	1	0	1	0	0	1	0	1	1	0	1	0	0	1	0	1

Table 20. Gadget values for $\mathcal{P}_{[1]} \times \mathcal{P}_{[4]}$ with different boolean factors.

\mathcal{S}'	1	2	3	4	5	6	7	8	9	10	11	12	13	14	15	16
\mathcal{S}																
1	1	0	1	0	1	0	1	0	0	1	0	1	0	1	0	1
2	0	1	0	1	0	1	0	1	1	0	1	0	1	0	1	0
3	1	0	1	0	1	0	1	0	0	1	0	1	0	1	0	1
4	0	1	0	1	0	1	0	1	1	0	1	0	1	0	1	0
5	1	0	1	0	1	0	1	0	0	1	0	1	0	1	0	1
6	0	1	0	1	0	1	0	1	1	0	1	0	1	0	1	0
7	1	0	1	0	1	0	1	0	0	1	0	1	0	1	0	1
8	0	1	0	1	0	1	0	1	1	0	1	0	1	0	1	0
9	0	1	0	1	0	1	0	1	1	0	1	0	1	0	1	0
10	1	0	1	0	1	0	1	0	0	1	0	1	0	1	0	1
11	0	1	0	1	0	1	0	1	1	0	1	0	1	0	1	0
12	1	0	1	0	1	0	1	0	0	1	0	1	0	1	0	1
13	0	1	0	1	0	1	0	1	1	0	1	0	1	0	1	0
14	1	0	1	0	1	0	1	0	0	1	0	1	0	1	0	1
15	0	1	0	1	0	1	0	1	1	0	1	0	1	0	1	0
16	1	0	1	0	1	0	1	0	0	1	0	1	0	1	0	1

Table 21. Gadget values for $\mathcal{P}_{[1]} \times \mathcal{P}_{[5]}$ with different boolean factors.

\mathcal{S}'	1	2	3	4	5	6	7	8	9	10	11	12	13	14	15	16
\mathcal{S}																
1	0	1	0	1	0	1	0	1	1	0	1	0	1	0	1	0
2	1	0	1	0	1	0	1	0	0	1	0	1	0	1	0	1
3	0	1	0	1	0	1	0	1	1	0	1	0	1	0	1	0
4	1	0	1	0	1	0	1	0	0	1	0	1	0	1	0	1
5	0	1	0	1	0	1	0	1	1	0	1	0	1	0	1	0
6	1	0	1	0	1	0	1	0	0	1	0	1	0	1	0	1
7	0	1	0	1	0	1	0	1	1	0	1	0	1	0	1	0
8	1	0	1	0	1	0	1	0	0	1	0	1	0	1	0	1
9	1	0	1	0	1	0	1	0	0	1	0	1	0	1	0	1
10	0	1	0	1	0	1	0	1	1	0	1	0	1	0	1	0
11	1	0	1	0	1	0	1	0	0	1	0	1	0	1	0	1
12	0	1	0	1	0	1	0	1	1	0	1	0	1	0	1	0
13	1	0	1	0	1	0	1	0	0	1	0	1	0	1	0	1
14	0	1	0	1	0	1	0	1	1	0	1	0	1	0	1	0
15	1	0	1	0	1	0	1	0	0	1	0	1	0	1	0	1
16	0	1	0	1	0	1	0	1	1	0	1	0	1	0	1	0

Table 22. Gadget values for $\mathcal{P}_{[1]} \times \mathcal{P}_{[6]}$ with different boolean factors.

S'	1	2	3	4	5	6	7	8	9	10	11	12	13	14	15	16
S																
1	1	0	1	0	0	1	0	1	1	0	1	0	0	1	0	1
2	0	1	0	1	1	0	1	0	0	1	0	1	1	0	1	0
3	1	0	1	0	0	1	0	1	1	0	1	0	0	1	0	1
4	0	1	0	1	1	0	1	0	0	1	0	1	1	0	1	0
5	0	1	0	1	1	0	1	0	0	1	0	1	1	0	1	0
6	1	0	1	0	0	1	0	1	1	0	1	0	0	1	0	1
7	0	1	0	1	1	0	1	0	0	1	0	1	1	0	1	0
8	1	0	1	0	0	1	0	1	1	0	1	0	0	1	0	1
9	1	0	1	0	0	1	0	1	1	0	1	0	0	1	0	1
10	0	1	0	1	1	0	1	0	0	1	0	1	1	0	1	0
11	1	0	1	0	0	1	0	1	1	0	1	0	0	1	0	1
12	0	1	0	1	1	0	1	0	0	1	0	1	1	0	1	0
13	0	1	0	1	1	0	1	0	0	1	0	1	1	0	1	0
14	1	0	1	0	0	1	0	1	1	0	1	0	0	1	0	1
15	0	1	0	1	1	0	1	0	0	1	0	1	1	0	1	0
16	1	0	1	0	0	1	0	1	1	0	1	0	0	1	0	1

Table 23. Gadget values for $\mathcal{P}_{[2]} \times \mathcal{P}_{[2]}$ with different boolean factors.

S'	1	2	3	4	5	6	7	8	9	10	11	12	13	14	15	16
S																
1	$-\frac{1}{3}$	0	$-\frac{1}{3}$	0	$-\frac{1}{3}$	0	$-\frac{1}{3}$	0	0	$-\frac{1}{3}$	0	$-\frac{1}{3}$	0	$-\frac{1}{3}$	0	$-\frac{1}{3}$
2	0	$-\frac{1}{3}$	0	$-\frac{1}{3}$	0	$-\frac{1}{3}$	0	$-\frac{1}{3}$	$-\frac{1}{3}$	0	$-\frac{1}{3}$	0	$-\frac{1}{3}$	0	$-\frac{1}{3}$	0
3	$-\frac{1}{3}$	0	$-\frac{1}{3}$	0	$-\frac{1}{3}$	0	$-\frac{1}{3}$	0	0	$-\frac{1}{3}$	0	$-\frac{1}{3}$	0	$-\frac{1}{3}$	0	$-\frac{1}{3}$
4	0	$-\frac{1}{3}$	0	$-\frac{1}{3}$	0	$-\frac{1}{3}$	0	$-\frac{1}{3}$	$-\frac{1}{3}$	0	$-\frac{1}{3}$	0	$-\frac{1}{3}$	0	$-\frac{1}{3}$	0
5	0	$-\frac{1}{3}$	0	$-\frac{1}{3}$	0	$-\frac{1}{3}$	0	$-\frac{1}{3}$	$-\frac{1}{3}$	0	$-\frac{1}{3}$	0	$-\frac{1}{3}$	0	$-\frac{1}{3}$	0
6	$-\frac{1}{3}$	0	$-\frac{1}{3}$	0	$-\frac{1}{3}$	0	$-\frac{1}{3}$	0	0	$-\frac{1}{3}$	0	$-\frac{1}{3}$	0	$-\frac{1}{3}$	0	$-\frac{1}{3}$
7	0	$-\frac{1}{3}$	0	$-\frac{1}{3}$	0	$-\frac{1}{3}$	0	$-\frac{1}{3}$	$-\frac{1}{3}$	0	$-\frac{1}{3}$	0	$-\frac{1}{3}$	0	$-\frac{1}{3}$	0
8	$-\frac{1}{3}$	0	$-\frac{1}{3}$	0	$-\frac{1}{3}$	0	$-\frac{1}{3}$	0	0	$-\frac{1}{3}$	0	$-\frac{1}{3}$	0	$-\frac{1}{3}$	0	$-\frac{1}{3}$
9	$-\frac{1}{3}$	0	$-\frac{1}{3}$	0	$-\frac{1}{3}$	0	$-\frac{1}{3}$	0	0	$-\frac{1}{3}$	0	$-\frac{1}{3}$	0	$-\frac{1}{3}$	0	$-\frac{1}{3}$
10	0	$-\frac{1}{3}$	0	$-\frac{1}{3}$	0	$-\frac{1}{3}$	0	$-\frac{1}{3}$	$-\frac{1}{3}$	0	$-\frac{1}{3}$	0	$-\frac{1}{3}$	0	$-\frac{1}{3}$	0
11	$-\frac{1}{3}$	0	$-\frac{1}{3}$	0	$-\frac{1}{3}$	0	$-\frac{1}{3}$	0	0	$-\frac{1}{3}$	0	$-\frac{1}{3}$	0	$-\frac{1}{3}$	0	$-\frac{1}{3}$
12	0	$-\frac{1}{3}$	0	$-\frac{1}{3}$	0	$-\frac{1}{3}$	0	$-\frac{1}{3}$	$-\frac{1}{3}$	0	$-\frac{1}{3}$	0	$-\frac{1}{3}$	0	$-\frac{1}{3}$	0
13	0	$-\frac{1}{3}$	0	$-\frac{1}{3}$	0	$-\frac{1}{3}$	0	$-\frac{1}{3}$	$-\frac{1}{3}$	0	$-\frac{1}{3}$	0	$-\frac{1}{3}$	0	$-\frac{1}{3}$	0
14	$-\frac{1}{3}$	0	$-\frac{1}{3}$	0	$-\frac{1}{3}$	0	$-\frac{1}{3}$	0	0	$-\frac{1}{3}$	0	$-\frac{1}{3}$	0	$-\frac{1}{3}$	0	$-\frac{1}{3}$
15	0	$-\frac{1}{3}$	0	$-\frac{1}{3}$	0	$-\frac{1}{3}$	0	$-\frac{1}{3}$	$-\frac{1}{3}$	0	$-\frac{1}{3}$	0	$-\frac{1}{3}$	0	$-\frac{1}{3}$	0
16	$-\frac{1}{3}$	0	$-\frac{1}{3}$	0	$-\frac{1}{3}$	0	$-\frac{1}{3}$	0	0	$-\frac{1}{3}$	0	$-\frac{1}{3}$	0	$-\frac{1}{3}$	0	$-\frac{1}{3}$

Table 24. Gadget values for $\mathcal{P}_{[2]} \times \mathcal{P}_{[3]}$ with different boolean factors.

\mathcal{S}'	1	2	3	4	5	6	7	8	9	10	11	12	13	14	15	16
\mathcal{S}																
1	0	1	0	1	1	0	1	0	0	1	0	1	1	0	1	0
2	1	0	1	0	0	1	0	1	1	0	1	0	0	1	0	1
3	0	1	0	1	1	0	1	0	0	1	0	1	1	0	1	0
4	1	0	1	0	0	1	0	1	1	0	1	0	0	1	0	1
5	1	0	1	0	0	1	0	1	1	0	1	0	0	1	0	1
6	0	1	0	1	1	0	1	0	0	1	0	1	1	0	1	0
7	1	0	1	0	0	1	0	1	1	0	1	0	0	1	0	1
8	0	1	0	1	1	0	1	0	0	1	0	1	1	0	1	0
9	0	1	0	1	1	0	1	0	0	1	0	1	1	0	1	0
10	1	0	1	0	0	1	0	1	1	0	1	0	0	1	0	1
11	0	1	0	1	1	0	1	0	0	1	0	1	1	0	1	0
12	1	0	1	0	0	1	0	1	1	0	1	0	0	1	0	1
13	1	0	1	0	0	1	0	1	1	0	1	0	0	1	0	1
14	0	1	0	1	1	0	1	0	0	1	0	1	1	0	1	0
15	1	0	1	0	0	1	0	1	1	0	1	0	0	1	0	1
16	0	1	0	1	1	0	1	0	0	1	0	1	1	0	1	0

Table 25. Gadget values for $\mathcal{P}_{[2]} \times \mathcal{P}_{[4]}$ with different boolean factors.

\mathcal{S}'	1	2	3	4	5	6	7	8	9	10	11	12	13	14	15	16
\mathcal{S}																
1	0	1	0	1	0	1	0	1	1	0	1	0	1	0	1	0
2	1	0	1	0	1	0	1	0	0	1	0	1	0	1	0	1
3	0	1	0	1	0	1	0	1	1	0	1	0	1	0	1	0
4	1	0	1	0	1	0	1	0	0	1	0	1	0	1	0	1
5	1	0	1	0	1	0	1	0	0	1	0	1	0	1	0	1
6	0	1	0	1	0	1	0	1	1	0	1	0	1	0	1	0
7	1	0	1	0	1	0	1	0	0	1	0	1	0	1	0	1
8	0	1	0	1	0	1	0	1	1	0	1	0	1	0	1	0
9	0	1	0	1	0	1	0	1	1	0	1	0	1	0	1	0
10	1	0	1	0	1	0	1	0	0	1	0	1	0	1	0	1
11	0	1	0	1	0	1	0	1	1	0	1	0	1	0	1	0
12	1	0	1	0	1	0	1	0	0	1	0	1	0	1	0	1
13	1	0	1	0	1	0	1	0	0	1	0	1	0	1	0	1
14	0	1	0	1	0	1	0	1	1	0	1	0	1	0	1	0
15	1	0	1	0	1	0	1	0	0	1	0	1	0	1	0	1
16	0	1	0	1	0	1	0	1	1	0	1	0	1	0	1	0

Table 26. Gadget values for $\mathcal{P}_{[2]} \times \mathcal{P}_{[5]}$ with different boolean factors.

\mathcal{S}'	1	2	3	4	5	6	7	8	9	10	11	12	13	14	15	16
\mathcal{S}																
1	1	0	1	0	1	0	1	0	0	1	0	1	0	1	0	1
2	0	1	0	1	0	1	0	1	1	0	1	0	1	0	1	0
3	1	0	1	0	1	0	1	0	0	1	0	1	0	1	0	1
4	0	1	0	1	0	1	0	1	1	0	1	0	1	0	1	0
5	0	1	0	1	0	1	0	1	1	0	1	0	1	0	1	0
6	1	0	1	0	1	0	1	0	0	1	0	1	0	1	0	1
7	0	1	0	1	0	1	0	1	1	0	1	0	1	0	1	0
8	1	0	1	0	1	0	1	0	0	1	0	1	0	1	0	1
9	1	0	1	0	1	0	1	0	0	1	0	1	0	1	0	1
10	0	1	0	1	0	1	0	1	1	0	1	0	1	0	1	0
11	1	0	1	0	1	0	1	0	0	1	0	1	0	1	0	1
12	0	1	0	1	0	1	0	1	1	0	1	0	1	0	1	0
13	0	1	0	1	0	1	0	1	1	0	1	0	1	0	1	0
14	1	0	1	0	1	0	1	0	0	1	0	1	0	1	0	1
15	0	1	0	1	0	1	0	1	1	0	1	0	1	0	1	0
16	1	0	1	0	1	0	1	0	0	1	0	1	0	1	0	1

Table 27. Gadget values for $\mathcal{P}_{[2]} \times \mathcal{P}_{[6]}$ with different boolean factors.

\mathcal{S}'	1	2	3	4	5	6	7	8	9	10	11	12	13	14	15	16
\mathcal{S}																
1	1	0	1	0	1	0	1	0	0	1	0	1	0	1	0	1
2	0	1	0	1	0	1	0	1	1	0	1	0	1	0	1	0
3	1	0	1	0	1	0	1	0	0	1	0	1	0	1	0	1
4	0	1	0	1	0	1	0	1	1	0	1	0	1	0	1	0
5	1	0	1	0	1	0	1	0	0	1	0	1	0	1	0	1
6	0	1	0	1	0	1	0	1	1	0	1	0	1	0	1	0
7	1	0	1	0	1	0	1	0	0	1	0	1	0	1	0	1
8	0	1	0	1	0	1	0	1	1	0	1	0	1	0	1	0
9	0	1	0	1	0	1	0	1	1	0	1	0	1	0	1	0
10	1	0	1	0	1	0	1	0	0	1	0	1	0	1	0	1
11	0	1	0	1	0	1	0	1	1	0	1	0	1	0	1	0
12	1	0	1	0	1	0	1	0	0	1	0	1	0	1	0	1
13	0	1	0	1	0	1	0	1	1	0	1	0	1	0	1	0
14	1	0	1	0	1	0	1	0	0	1	0	1	0	1	0	1
15	0	1	0	1	0	1	0	1	1	0	1	0	1	0	1	0
16	1	0	1	0	1	0	1	0	0	1	0	1	0	1	0	1

Table 28. Gadget values for $\mathcal{P}_{[3]} \times \mathcal{P}_{[3]}$ with different boolean factors.

S'	1	2	3	4	5	6	7	8	9	10	11	12	13	14	15	16
1	$-\frac{1}{3}$	0	$-\frac{1}{3}$	0	$-\frac{1}{3}$	0	$-\frac{1}{3}$	0	0	$-\frac{1}{3}$	0	$-\frac{1}{3}$	0	$-\frac{1}{3}$	0	$-\frac{1}{3}$
2	0	$-\frac{1}{3}$	0	$-\frac{1}{3}$	0	$-\frac{1}{3}$	0	$-\frac{1}{3}$	$-\frac{1}{3}$	0	$-\frac{1}{3}$	0	$-\frac{1}{3}$	0	$-\frac{1}{3}$	0
3	$-\frac{1}{3}$	0	$-\frac{1}{3}$	0	$-\frac{1}{3}$	0	$-\frac{1}{3}$	0	0	$-\frac{1}{3}$	0	$-\frac{1}{3}$	0	$-\frac{1}{3}$	0	$-\frac{1}{3}$
4	0	$-\frac{1}{3}$	0	$-\frac{1}{3}$	0	$-\frac{1}{3}$	0	$-\frac{1}{3}$	$-\frac{1}{3}$	0	$-\frac{1}{3}$	0	$-\frac{1}{3}$	0	$-\frac{1}{3}$	0
5	$-\frac{1}{3}$	0	$-\frac{1}{3}$	0	$-\frac{1}{3}$	0	$-\frac{1}{3}$	0	0	$-\frac{1}{3}$	0	$-\frac{1}{3}$	0	$-\frac{1}{3}$	0	$-\frac{1}{3}$
6	0	$-\frac{1}{3}$	0	$-\frac{1}{3}$	0	$-\frac{1}{3}$	0	$-\frac{1}{3}$	$-\frac{1}{3}$	0	$-\frac{1}{3}$	0	$-\frac{1}{3}$	0	$-\frac{1}{3}$	0
7	$-\frac{1}{3}$	0	$-\frac{1}{3}$	0	$-\frac{1}{3}$	0	$-\frac{1}{3}$	0	0	$-\frac{1}{3}$	0	$-\frac{1}{3}$	0	$-\frac{1}{3}$	0	$-\frac{1}{3}$
8	0	$-\frac{1}{3}$	0	$-\frac{1}{3}$	0	$-\frac{1}{3}$	0	$-\frac{1}{3}$	$-\frac{1}{3}$	0	$-\frac{1}{3}$	0	$-\frac{1}{3}$	0	$-\frac{1}{3}$	0
9	0	$-\frac{1}{3}$	0	$-\frac{1}{3}$	0	$-\frac{1}{3}$	0	$-\frac{1}{3}$	$-\frac{1}{3}$	0	$-\frac{1}{3}$	0	$-\frac{1}{3}$	0	$-\frac{1}{3}$	0
10	$-\frac{1}{3}$	0	$-\frac{1}{3}$	0	$-\frac{1}{3}$	0	$-\frac{1}{3}$	0	0	$-\frac{1}{3}$	0	$-\frac{1}{3}$	0	$-\frac{1}{3}$	0	$-\frac{1}{3}$
11	0	$-\frac{1}{3}$	0	$-\frac{1}{3}$	0	$-\frac{1}{3}$	0	$-\frac{1}{3}$	$-\frac{1}{3}$	0	$-\frac{1}{3}$	0	$-\frac{1}{3}$	0	$-\frac{1}{3}$	0
12	$-\frac{1}{3}$	0	$-\frac{1}{3}$	0	$-\frac{1}{3}$	0	$-\frac{1}{3}$	0	0	$-\frac{1}{3}$	0	$-\frac{1}{3}$	0	$-\frac{1}{3}$	0	$-\frac{1}{3}$
13	0	$-\frac{1}{3}$	0	$-\frac{1}{3}$	0	$-\frac{1}{3}$	0	$-\frac{1}{3}$	$-\frac{1}{3}$	0	$-\frac{1}{3}$	0	$-\frac{1}{3}$	0	$-\frac{1}{3}$	0
14	$-\frac{1}{3}$	0	$-\frac{1}{3}$	0	$-\frac{1}{3}$	0	$-\frac{1}{3}$	0	0	$-\frac{1}{3}$	0	$-\frac{1}{3}$	0	$-\frac{1}{3}$	0	$-\frac{1}{3}$
15	0	$-\frac{1}{3}$	0	$-\frac{1}{3}$	0	$-\frac{1}{3}$	0	$-\frac{1}{3}$	$-\frac{1}{3}$	0	$-\frac{1}{3}$	0	$-\frac{1}{3}$	0	$-\frac{1}{3}$	0
16	$-\frac{1}{3}$	0	$-\frac{1}{3}$	0	$-\frac{1}{3}$	0	$-\frac{1}{3}$	0	0	$-\frac{1}{3}$	0	$-\frac{1}{3}$	0	$-\frac{1}{3}$	0	$-\frac{1}{3}$

Table 31. Gadget values for $\mathcal{P}_{[3]} \times \mathcal{P}_{[6]}$ with different boolean factors.

S'	1	2	3	4	5	6	7	8	9	10	11	12	13	14	15	16
1	1	0	1	0	0	1	0	1	1	0	1	0	0	1	0	1
2	0	1	0	1	1	0	1	0	0	1	0	1	1	0	1	0
3	1	0	1	0	0	1	0	1	1	0	1	0	0	1	0	1
4	0	1	0	1	1	0	1	0	0	1	0	1	1	0	1	0
5	0	1	0	1	1	0	1	0	0	1	0	1	1	0	1	0
6	1	0	1	0	0	1	0	1	1	0	1	0	0	1	0	1
7	0	1	0	1	1	0	1	0	0	1	0	1	1	0	1	0
8	1	0	1	0	0	1	0	1	1	0	1	0	0	1	0	1
9	1	0	1	0	0	1	0	1	1	0	1	0	0	1	0	1
10	0	1	0	1	1	0	1	0	0	1	0	1	1	0	1	0
11	1	0	1	0	0	1	0	1	1	0	1	0	0	1	0	1
12	0	1	0	1	1	0	1	0	0	1	0	1	1	0	1	0
13	0	1	0	1	1	0	1	0	0	1	0	1	1	0	1	0
14	1	0	1	0	0	1	0	1	1	0	1	0	0	1	0	1
15	0	1	0	1	1	0	1	0	0	1	0	1	1	0	1	0
16	1	0	1	0	0	1	0	1	1	0	1	0	0	1	0	1

Table 32. Gadget values for $\mathcal{P}_{[4]} \times \mathcal{P}_{[4]}$ with different boolean factors.

S'	1	2	3	4	5	6	7	8	9	10	11	12	13	14	15	16
S																
1	1	0	1	0	1	0	1	0	0	1	0	1	0	1	0	1
2	0	1	0	1	0	1	0	1	1	0	1	0	1	0	1	0
3	1	0	1	0	1	0	1	0	0	1	0	1	0	1	0	1
4	0	1	0	1	0	1	0	1	1	0	1	0	1	0	1	0
5	0	1	0	1	0	1	0	1	1	0	1	0	1	0	1	0
6	1	0	1	0	1	0	1	0	0	1	0	1	0	1	0	1
7	0	1	0	1	0	1	0	1	1	0	1	0	1	0	1	0
8	1	0	1	0	1	0	1	0	0	1	0	1	0	1	0	1
9	1	0	1	0	1	0	1	0	0	1	0	1	0	1	0	1
10	0	1	0	1	0	1	0	1	1	0	1	0	1	0	1	0
11	1	0	1	0	1	0	1	0	0	1	0	1	0	1	0	1
12	0	1	0	1	0	1	0	1	1	0	1	0	1	0	1	0
13	0	1	0	1	0	1	0	1	1	0	1	0	1	0	1	0
14	1	0	1	0	1	0	1	0	0	1	0	1	0	1	0	1
15	0	1	0	1	0	1	0	1	1	0	1	0	1	0	1	0
16	1	0	1	0	1	0	1	0	0	1	0	1	0	1	0	1

Table 33. Gadget values for $\mathcal{P}_{[4]} \times \mathcal{P}_{[5]}$ with different boolean factors.

S'	1	2	3	4	5	6	7	8	9	10	11	12	13	14	15	16
S																
1	0	1	0	1	0	1	0	1	1	0	1	0	1	0	1	0
2	1	0	1	0	1	0	1	0	0	1	0	1	0	1	0	1
3	0	1	0	1	0	1	0	1	1	0	1	0	1	0	1	0
4	1	0	1	0	1	0	1	0	0	1	0	1	0	1	0	1
5	1	0	1	0	1	0	1	0	0	1	0	1	0	1	0	1
6	0	1	0	1	0	1	0	1	1	0	1	0	1	0	1	0
7	1	0	1	0	1	0	1	0	0	1	0	1	0	1	0	1
8	0	1	0	1	0	1	0	1	1	0	1	0	1	0	1	0
9	0	1	0	1	0	1	0	1	1	0	1	0	1	0	1	0
10	1	0	1	0	1	0	1	0	0	1	0	1	0	1	0	1
11	0	1	0	1	0	1	0	1	1	0	1	0	1	0	1	0
12	1	0	1	0	1	0	1	0	0	1	0	1	0	1	0	1
13	1	0	1	0	1	0	1	0	0	1	0	1	0	1	0	1
14	0	1	0	1	0	1	0	1	1	0	1	0	1	0	1	0
15	1	0	1	0	1	0	1	0	0	1	0	1	0	1	0	1
16	0	1	0	1	0	1	0	1	1	0	1	0	1	0	1	0

Table 34. Gadget values for $\mathcal{P}_{[4]} \times \mathcal{P}_{[6]}$ with different boolean factors.

\mathcal{S}'	1	2	3	4	5	6	7	8	9	10	11	12	13	14	15	16
\mathcal{S}																
1	1	0	1	0	1	0	1	0	0	1	0	1	0	1	0	1
2	0	1	0	1	0	1	0	1	1	0	1	0	1	0	1	0
3	1	0	1	0	1	0	1	0	0	1	0	1	0	1	0	1
4	0	1	0	1	0	1	0	1	1	0	1	0	1	0	1	0
5	1	0	1	0	1	0	1	0	0	1	0	1	0	1	0	1
6	0	1	0	1	0	1	0	1	1	0	1	0	1	0	1	0
7	1	0	1	0	1	0	1	0	0	1	0	1	0	1	0	1
8	0	1	0	1	0	1	0	1	1	0	1	0	1	0	1	0
9	0	1	0	1	0	1	0	1	1	0	1	0	1	0	1	0
10	1	0	1	0	1	0	1	0	0	1	0	1	0	1	0	1
11	0	1	0	1	0	1	0	1	1	0	1	0	1	0	1	0
12	1	0	1	0	1	0	1	0	0	1	0	1	0	1	0	1
13	0	1	0	1	0	1	0	1	1	0	1	0	1	0	1	0
14	1	0	1	0	1	0	1	0	0	1	0	1	0	1	0	1
15	0	1	0	1	0	1	0	1	1	0	1	0	1	0	1	0
16	1	0	1	0	1	0	1	0	0	1	0	1	0	1	0	1

Table 35. Gadget values for $\mathcal{P}_{[5]} \times \mathcal{P}_{[5]}$ with different boolean factors.

\mathcal{S}'	1	2	3	4	5	6	7	8	9	10	11	12	13	14	15	16
\mathcal{S}																
1	0	1	0	1	0	1	0	1	1	0	1	0	1	0	1	0
2	1	0	1	0	1	0	1	0	0	1	0	1	0	1	0	1
3	0	1	0	1	0	1	0	1	1	0	1	0	1	0	1	0
4	1	0	1	0	1	0	1	0	0	1	0	1	0	1	0	1
5	0	1	0	1	0	1	0	1	1	0	1	0	1	0	1	0
6	1	0	1	0	1	0	1	0	0	1	0	1	0	1	0	1
7	0	1	0	1	0	1	0	1	1	0	1	0	1	0	1	0
8	1	0	1	0	1	0	1	0	0	1	0	1	0	1	0	1
9	1	0	1	0	1	0	1	0	0	1	0	1	0	1	0	1
10	0	1	0	1	0	1	0	1	1	0	1	0	1	0	1	0
11	1	0	1	0	1	0	1	0	0	1	0	1	0	1	0	1
12	0	1	0	1	0	1	0	1	1	0	1	0	1	0	1	0
13	1	0	1	0	1	0	1	0	0	1	0	1	0	1	0	1
14	0	1	0	1	0	1	0	1	1	0	1	0	1	0	1	0
15	1	0	1	0	1	0	1	0	0	1	0	1	0	1	0	1
16	0	1	0	1	0	1	0	1	1	0	1	0	1	0	1	0

Table 36. Gadget values for $\mathcal{P}_{[5]} \times \mathcal{P}_{[6]}$ with different boolean factors.

\mathcal{S}'	1	2	3	4	5	6	7	8	9	10	11	12	13	14	15	16
\mathcal{S}																
1	1	0	1	0	1	0	1	0	0	1	0	1	0	1	0	1
2	0	1	0	1	0	1	0	1	1	0	1	0	1	0	1	0
3	1	0	1	0	1	0	1	0	0	1	0	1	0	1	0	1
4	0	1	0	1	0	1	0	1	1	0	1	0	1	0	1	0
5	1	0	1	0	1	0	1	0	0	1	0	1	0	1	0	1
6	0	1	0	1	0	1	0	1	1	0	1	0	1	0	1	0
7	1	0	1	0	1	0	1	0	0	1	0	1	0	1	0	1
8	0	1	0	1	0	1	0	1	1	0	1	0	1	0	1	0
9	0	1	0	1	0	1	0	1	1	0	1	0	1	0	1	0
10	1	0	1	0	1	0	1	0	0	1	0	1	0	1	0	1
11	0	1	0	1	0	1	0	1	1	0	1	0	1	0	1	0
12	1	0	1	0	1	0	1	0	0	1	0	1	0	1	0	1
13	0	1	0	1	0	1	0	1	1	0	1	0	1	0	1	0
14	1	0	1	0	1	0	1	0	0	1	0	1	0	1	0	1
15	0	1	0	1	0	1	0	1	1	0	1	0	1	0	1	0
16	1	0	1	0	1	0	1	0	0	1	0	1	0	1	0	1

Table 37. Gadget values for $\mathcal{P}_{[6]} \times \mathcal{P}_{[6]}$ with different boolean factors.

E Cycle labelling conventions

In this appendix we wish to discuss a point about using cycle notation to describe permutation matrices. There is an ambiguity in notation that we need to address in view of some of our past works.

Let us begin by writing a permutation in the form of a matrix. For the purposes of our discussion we will concentrate on \mathbf{M} and \mathbf{N} where

$$\mathbf{M} = \begin{bmatrix} 1 & 0 & 0 & 0 \\ 0 & 0 & 0 & 1 \\ 0 & 1 & 0 & 0 \\ 0 & 0 & 1 & 0 \end{bmatrix}, \quad \mathbf{N} = \begin{bmatrix} 0 & 1 & 0 & 0 \\ 0 & 0 & 0 & 1 \\ 1 & 0 & 0 & 0 \\ 0 & 0 & 1 & 0 \end{bmatrix}, \quad \mathbf{O} = \begin{bmatrix} 1 & 0 & 0 & 0 \\ 0 & 0 & 1 & 0 \\ 0 & 1 & 0 & 0 \\ 0 & 0 & 0 & 1 \end{bmatrix}. \quad (\text{E.1})$$

If we use the convention the numbers to appear in the cycle should denote the presence of the non-vanishing entries as read from an upward to downward direction along each column from the top, but which does not appear as a diagonal entry. We can refer to this as “the read down convention.”

Applying this rule to \mathbf{M} we see that the second column has a non-vanishing entry in the third row, the third column has a non-vanishing entry in the fourth row and the fourth column has a non-vanishing entry in the second row. This suggests a notation for the matrices \mathbf{M} in the form of (234) as we take each column from left to right. We can apply the same logic to \mathbf{N} to suggest a notation name (1342) and for \mathbf{O} notation name (23).

However, there is another possible convention.

We could use the convention the numbers to appear in the cycle should denote the presence of the non-vanishing entries as read from left side to right side along each row from the left, but which does not appear as a diagonal entry. We can refer to this as “the read across convention.”

Applying this rule to \mathbf{M} we see that the second row has a non-vanishing entry in the fourth column, the fourth row has a non-vanishing entry in the third column, and third row has a non-vanishing entry in the second column. This suggests a notation for the matrix \mathbf{M} in the form of (243) as we take each column from top to bottom. We can apply the same logic to \mathbf{N} to suggest a notation name (1243) and for \mathbf{O} notation name (23).

This discussion illustrates that for 2-cycles like \mathbf{O} , either convention leads to the same name. However, for 3-cycles and 4-cycles, the notational names are different for the same matrix depending on the convention used. However, there is a simply “translation” between the two conventions. If the notation of a permutation is given by one expression in the read down convention, the notation for the same permutation can be found by reading in a “backward ordering” for the notation in the other convention. When (234) is read backward it becomes (432) or (using cyclicity) (243). Similarly, when (1342) is read backward, it becomes (2431) or (using cyclicity) (1243). For 2-cycles both conventions lead to the same expression.

The L-matrices for each of the respective representations (CM), (TM), and (VM) are given by

$$\begin{aligned}
 \mathbf{L}_1^{(CM)} &= \begin{bmatrix} 1 & 0 & 0 & 0 \\ 0 & 0 & 0 & -1 \\ 0 & 1 & 0 & 0 \\ 0 & 0 & -1 & 0 \end{bmatrix}, & \mathbf{L}_2^{(CM)} &= \begin{bmatrix} 0 & 1 & 0 & 0 \\ 0 & 0 & 1 & 0 \\ -1 & 0 & 0 & 0 \\ 0 & 0 & 0 & -1 \end{bmatrix}, \\
 \mathbf{L}_3^{(CM)} &= \begin{bmatrix} 0 & 0 & 1 & 0 \\ 0 & -1 & 0 & 0 \\ 0 & 0 & 0 & -1 \\ 1 & 0 & 0 & 0 \end{bmatrix}, & \mathbf{L}_4^{(CM)} &= \begin{bmatrix} 0 & 0 & 0 & 1 \\ 1 & 0 & 0 & 0 \\ 0 & 0 & 1 & 0 \\ 0 & 1 & 0 & 0 \end{bmatrix}. \\
 \mathbf{L}_1^{(TM)} &= \begin{bmatrix} 1 & 0 & 0 & 0 \\ 0 & 0 & -1 & 0 \\ 0 & 0 & 0 & -1 \\ 0 & -1 & 0 & 0 \end{bmatrix}, & \mathbf{L}_2^{(TM)} &= \begin{bmatrix} 0 & 1 & 0 & 0 \\ 0 & 0 & 0 & 1 \\ 0 & 0 & -1 & 0 \\ 1 & 0 & 0 & 0 \end{bmatrix}, \\
 \mathbf{L}_3^{(TM)} &= \begin{bmatrix} 0 & 0 & 1 & 0 \\ 1 & 0 & 0 & 0 \\ 0 & 1 & 0 & 0 \\ 0 & 0 & 0 & -1 \end{bmatrix}, & \mathbf{L}_4^{(TM)} &= \begin{bmatrix} 0 & 0 & 0 & 1 \\ 0 & -1 & 0 & 0 \\ 1 & 0 & 0 & 0 \\ 0 & 0 & 1 & 0 \end{bmatrix}, \\
 \mathbf{L}_1^{(VM)} &= \begin{bmatrix} 0 & 1 & 0 & 0 \\ 0 & 0 & 0 & -1 \\ 1 & 0 & 0 & 0 \\ 0 & 0 & -1 & 0 \end{bmatrix}, & \mathbf{L}_2^{(VM)} &= \begin{bmatrix} 1 & 0 & 0 & 0 \\ 0 & 0 & 1 & 0 \\ 0 & -1 & 0 & 0 \\ 0 & 0 & 0 & -1 \end{bmatrix}, \\
 \mathbf{L}_3^{(VM)} &= \begin{bmatrix} 0 & 0 & 0 & 1 \\ 0 & 1 & 0 & 0 \\ 0 & 0 & 1 & 0 \\ 1 & 0 & 0 & 0 \end{bmatrix}, & \mathbf{L}_4^{(VM)} &= \begin{bmatrix} 0 & 0 & 1 & 0 \\ -1 & 0 & 0 & 0 \\ 0 & 0 & 0 & -1 \\ 0 & 1 & 0 & 0 \end{bmatrix}. \tag{E.2}
 \end{aligned}$$

Using the “read down convention” these matrices in (E.2) become the expressions given in (E.3).

$$\begin{aligned}
 \mathbf{L}_1^{(CM)} &= (10)_b(234), & \mathbf{L}_2^{(CM)} &= (12)_b(132), & \mathbf{L}_3^{(CM)} &= (6)_b(143), & \mathbf{L}_4^{(CM)} &= (0)_b(124), \\
 \mathbf{L}_1^{(TM)} &= (14)_b(243), & \mathbf{L}_2^{(TM)} &= (4)_b(142), & \mathbf{L}_3^{(TM)} &= (8)_b(123), & \mathbf{L}_4^{(TM)} &= (2)_b(134), \\
 \mathbf{L}_1^{(VM)} &= (10)_b(1342), & \mathbf{L}_2^{(VM)} &= (4)_b(23), & \mathbf{L}_3^{(VM)} &= (0)_b(14), & \mathbf{L}_4^{(VM)} &= (6)_b(1243).
 \end{aligned}
 \tag{E.3}$$

Using the “read across convention” these matrices in (E.2) become the expressions given in (E.4).

$$\begin{aligned}
 \mathbf{L}_1^{(CM)} &= (10)_b(243), & \mathbf{L}_2^{(CM)} &= (12)_b(123), & \mathbf{L}_3^{(CM)} &= (6)_b(134), & \mathbf{L}_4^{(CM)} &= (0)_b(142), \\
 \mathbf{L}_1^{(TM)} &= (14)_b(234), & \mathbf{L}_2^{(TM)} &= (4)_b(124), & \mathbf{L}_3^{(TM)} &= (8)_b(132), & \mathbf{L}_4^{(TM)} &= (2)_b(143), \\
 \mathbf{L}_1^{(VM)} &= (10)_b(1243), & \mathbf{L}_2^{(VM)} &= (4)_b(23), & \mathbf{L}_3^{(VM)} &= (0)_b(14), & \mathbf{L}_4^{(VM)} &= (6)_b(1342).
 \end{aligned}
 \tag{E.4}$$

All the expressions, tables, etc. in this work are written in the read across convention.

Open Access. This article is distributed under the terms of the Creative Commons Attribution License ([CC-BY 4.0](https://creativecommons.org/licenses/by/4.0/)), which permits any use, distribution and reproduction in any medium, provided the original author(s) and source are credited.

References

- [1] S.J. Gates, Jr. and L. Rana, *A theory of spinning particles for large- N extended supersymmetry*, *Phys. Lett. B* **352** (1995) 50 [[hep-th/9504025](#)] [[INSPIRE](#)].
- [2] S.J. Gates, Jr. and L. Rana, *A theory of spinning particles for large- N extended supersymmetry. 2.*, *Phys. Lett. B* **369** (1996) 262 [[hep-th/9510151](#)] [[INSPIRE](#)].
- [3] S.J. Gates, Jr., W.D. Linch, III, J. Phillips and L. Rana, *The Fundamental supersymmetry challenge remains*, *Grav. Cosmol.* **8** (2002) 96 [[hep-th/0109109](#)] [[INSPIRE](#)].
- [4] S.J. Gates, Jr., W.D. Linch, III and J. Phillips, *When Superspace Is Not Enough*, Caltech Preprint #CALT-68-2387 [[hep-th/0211034](#)] [[INSPIRE](#)].
- [5] C. Doran, K. Iga, J. Kostiuk, G. Landweber and S. Mendez-Diez, *Geometrization of N -extended 1-dimensional supersymmetry algebras, I*, *Adv. Theor. Math. Phys.* **19** (2015) 1043 [[arXiv:1311.3736](#)] [[INSPIRE](#)].
- [6] C. Doran, K. Iga, J. Kostiuk and S. Méndez-Diez, *Geometrization of N -Extended 1-Dimensional Supersymmetry Algebras, II*, [arXiv:1610.09983](#) [[INSPIRE](#)].
- [7] M. Faux and S.J. Gates, Jr., *Adinkras: A Graphical technology for supersymmetric representation theory*, *Phys. Rev. D* **71** (2005) 065002 [[hep-th/0408004](#)] [[INSPIRE](#)].
- [8] B. Bollobás, *Modern Graph Theory*, Springer, Berlin Germany (1998).
- [9] S.J. Gates, Jr et al., *4D, $N = 1$ Supersymmetry Genomics (I)*, *JHEP* **12** (2009) 008 [[arXiv:0902.3830](#)] [[INSPIRE](#)].

- [10] S. Bellucci, S. Krivonos, A. Marrani and E. Orazi, 'Root' action for $N = 4$ supersymmetric mechanics theories, *Phys. Rev. D* **73** (2006) 025011 [[hep-th/0511249](#)] [[INSPIRE](#)].
- [11] A. Pashnev and F. Toppan, On the classification of N extended supersymmetric quantum mechanical systems, *J. Math. Phys.* **42** (2001) 5257 [[hep-th/0010135](#)] [[INSPIRE](#)].
- [12] E. Ivanov and O. Lechtenfeld, $N = 4$ supersymmetric mechanics in harmonic superspace, *JHEP* **09** (2003) 073 [[hep-th/0307111](#)] [[INSPIRE](#)].
- [13] E. Ivanov, S. Krivonos and O. Lechtenfeld, $N = 4$, $D = 1$ supermultiplets from nonlinear realizations of $D(2, 1; \alpha)$, *Class. Quant. Grav.* **21** (2004) 1031 [[hep-th/0310299](#)] [[INSPIRE](#)].
- [14] F. Delduc and E. Ivanov, Gauging $N = 4$ Supersymmetric Mechanics, *Nucl. Phys. B* **753** (2006) 211 [[hep-th/0605211](#)] [[INSPIRE](#)].
- [15] F. Delduc and E. Ivanov, $N = 4$ mechanics of general $(4, 4, 0)$ multiplets, *Nucl. Phys. B* **855** (2012) 815 [[arXiv:1107.1429](#)] [[INSPIRE](#)].
- [16] F. Delduc and E. Ivanov, Gauging $N = 4$ supersymmetric mechanics II: $(1, 4, 3)$ models from the $(4, 4, 0)$ ones, *Nucl. Phys. B* **770** (2007) 179 [[hep-th/0611247](#)] [[INSPIRE](#)].
- [17] L. Zhao, What is an Adinkra, Shanghai Jiao Tong University on-line presentation, <http://math.sjtu.edu.cn/conference/Bannai/2014/data/20141213B/slides.pdf>.
- [18] H.S.M. Coxeter, Discrete groups generated by reflections, *Ann. Math.* **35** (1934) 588.
- [19] N. Bourbaki, *Elements of Mathematics*, in *Lie Groups and Lie Algebras* Springer, Berlin Germany (2002), chapters 4–6 [ISBN:978-3-540-42650-9].
- [20] F. Klein, *Vorlesungen ueber das Ikosaeder und die Aufloesung der Gleichungen vom fuenften*, Leipzig B.G. Teubner, Leipzig Germany (1884). Reprinted as *Lectures on the Icosahedron and the Solution of Equations of the Fifth Degree*, second reviewed edition, Dover, New York U.S.A. (1956).
- [21] G. Arfken, *Mathematical Methods for Physicists*, third edition, Academic Press, Orlando U.S.A. (1985), pp. 184–185 and 239–240.
- [22] M. Marcolli and N. Zolman, Adinkras, Dessins, Origami and Supersymmetry Spectral Triples, [arXiv:1606.04463](#) [[INSPIRE](#)].
- [23] Y.X. Zhang, Adinkras for Mathematicians, *Trans. Am. Math. Soc.* **366** (2014) 3325 [[arXiv:1111.6055](#)] [[INSPIRE](#)].
- [24] C. Doran, K. Iga and G. Landweber, An application of Cubical Cohomology to Adinkras and Supersymmetry Representations, [arXiv:1207.6806](#) [[INSPIRE](#)].
- [25] C.F. Doran, M.G. Faux, S.J. Gates, Jr., T. Hubsch, K.M. Iga and G.D. Landweber, On graph-theoretic identifications of Adinkras, supersymmetry representations and superfields, *Int. J. Mod. Phys. A* **22** (2007) 869 [[math-ph/0512016](#)] [[INSPIRE](#)].
- [26] C.F. Doran et al., Topology Types of Adinkras and the Corresponding Representations of N -Extended Supersymmetry, [arXiv:0806.0050](#) [[INSPIRE](#)].
- [27] C.F. Doran et al., Relating Doubly-Even Error-Correcting Codes, Graphs and Irreducible Representations of N -Extended Supersymmetry, [arXiv:0806.0051](#) [[INSPIRE](#)].
- [28] C.F. Doran et al., Codes and Supersymmetry in One Dimension, *Adv. Theor. Math. Phys.* **15** (2011) 1909 [[arXiv:1108.4124](#)] [[INSPIRE](#)].

- [29] S.J. Gates, Jr. and T. Hübsch, *On Dimensional Extension of Supersymmetry: From Worldlines to Worldsheets*, *Adv. Theor. Math. Phys.* **16** (2012) 1619 [[arXiv:1104.0722](#)] [[INSPIRE](#)].
- [30] C.F. Doran et al., *On the matter of $N = 2$ matter*, *Phys. Lett. B* **659** (2008) 441 [[arXiv:0710.5245](#)] [[INSPIRE](#)].
- [31] M. Faux, *The Conformal Hyperplet*, [arXiv:1610.07822](#) [[INSPIRE](#)].
- [32] M.G. Faux and G.D. Landweber, *Spin Holography via Dimensional Enhancement*, *Phys. Lett. B* **681** (2009) 161 [[arXiv:0907.4543](#)] [[INSPIRE](#)].
- [33] M.G. Faux, K.M. Iga and G.D. Landweber, *Dimensional Enhancement via Supersymmetry*, *Adv. Math. Phys.* **2011** (2011) 259089 [[arXiv:0907.3605](#)] [[INSPIRE](#)].
- [34] S.J. Gates and T. Hübsch, *On Dimensional Extension of Supersymmetry: From Worldlines to Worldsheets*, *Adv. Theor. Math. Phys.* **16** (2012) 1619 [[arXiv:1104.0722](#)] [[INSPIRE](#)].
- [35] K. Iga and Y.X. Zhang, *Structural Theory and Classification of 2D Adinkras*, *Adv. High Energy Phys.* **2016** (2016) 3980613 [[arXiv:1508.00491](#)] [[INSPIRE](#)].
- [36] S.J. Gates, Jr., *The Search for Elementarity Among Off-Shell SUSY Representations*, in *Korea Institute for Advanced Study (KIAS) Newsletter. Vol. 5*, KIAS, Seoul South Korea (2012), pg. 19.
- [37] S.J. Gates, Jr., T. Hübsch and K. Stiffler, *Adinkras and SUSY Holography: Some explicit examples*, *Int. J. Mod. Phys. A* **29** (2014) 1450041 [[arXiv:1208.5999](#)] [[INSPIRE](#)].
- [38] S.J. Gates, T. Hübsch and K. Stiffler, *On Clifford-algebraic dimensional extension and SUSY holography*, *Int. J. Mod. Phys. A* **30** (2015) 1550042 [[arXiv:1409.4445](#)] [[INSPIRE](#)].
- [39] M. Calkins, D.E.A. Gates, S.J. Gates and K. Stiffler, *Adinkras, 0-branes, Holoraumy and the SUSY QFT/QM Correspondence*, *Int. J. Mod. Phys. A* **30** (2015) 1550050 [[arXiv:1501.00101](#)] [[INSPIRE](#)].
- [40] S.J. Gates et al., *A Lorentz covariant holoraumy-induced “gadget” from minimal off-shell $4D$, $\mathcal{N} = 1$ supermultiplets*, *JHEP* **11** (2015) 113 [[arXiv:1508.07546](#)] [[INSPIRE](#)].
- [41] D.E.A. Gates, S.J. Gates, Jr. and K. Stiffler, *A proposal on culling & filtering a coxeter group for $4D$, $\mathcal{N} = 1$ spacetime SUSY representations*, [arXiv:1601.00725](#) [[INSPIRE](#)].
- [42] D.E.A. Gates, S.J. Gates and K. Stiffler, *A proposal on culling & filtering a coxeter group for $4D$, $\mathcal{N} = 1$ spacetime SUSY representations: revised*, *JHEP* **08** (2016) 076 [[INSPIRE](#)].
- [43] R. Jackiw and C. Rebbi, *Spin from Isospin in a Gauge Theory*, *Phys. Rev. Lett.* **36** (1976) 1116.
- [44] I. Chappell, II, S.J. Gates and T. Hübsch, *Adinkra (in)equivalence from Coxeter group representations: A case study*, *Int. J. Mod. Phys. A* **29** (2014) 1450029 [[arXiv:1210.0478](#)] [[INSPIRE](#)].
- [45] T. Hübsch, *Linear and chiral superfields are usefully inequivalent*, *Class. Quant. Grav.* **16** (1999) L51 [[hep-th/9903175](#)] [[INSPIRE](#)].
- [46] S.J. Gates, Jr., *Superspace Formulation of New Nonlinear σ -models*, *Nucl. Phys. B* **238** (1984) 349 [[INSPIRE](#)].
- [47] S.J. Gates, Jr., C.M. Hull and M. Roček, *Twisted Multiplets and New Supersymmetric Nonlinear σ -models*, *Nucl. Phys. B* **248** (1984) 157 [[INSPIRE](#)].

- [48] https://en.wikipedia.org/wiki/Platonic_solid.
- [49] https://en.wikipedia.org/wiki/Mysterium_Cosmographicum.
- [50] http://scgp.stonybrook.edu/video_portal/video.php?id=2873 and http://scgp.stonybrook.edu/video_portal/video.php?id=3021.
- [51] N.A. Nekrasov, *Seiberg-Witten Prepotential From Instanton Counting*, *Adv.Theor. Math. Phys.* **7** (2004) 831 [[hep-th/0206161v1](#)].
- [52] N.A. Nekrasov and S.L. Shatashvili, *Bethe/Gauge correspondence on curved spaces*, *JHEP* **01** (2015) 100 [[arXiv:1405.6046](#)] [[INSPIRE](#)].
- [53] N.A. Nekrasov, *Non-Perturbative Schwinger-Dyson Equations: From BPS/CFT Correspondence to the Novel Symmetries of Quantum Field Theory*, in *Proceedings of 100th Anniversary of the Birth of I.Ya. Pomeranchuk*, Moscow Russia (2013) [*Phys. Usp.* **57** (2014) 152].
- [54] N. Nekrasov, *BPS/CFT correspondence: non-perturbative Dyson-Schwinger equations and qq-characters*, *JHEP* **03** (2016) 181 [[arXiv:1512.05388](#)] [[INSPIRE](#)].
- [55] N. Nekrasov, *BPS/CFT correspondence II: Instantons at crossroads, Moduli and Compactness Theorem*, [arXiv:1608.07272](#) [[INSPIRE](#)].
- [56] N. Nekrasov, *BPS/CFT Correspondence III: Gauge Origami partition function and qq-characters*, [arXiv:1701.00189](#) [[INSPIRE](#)].